Relevance of the Activation and Migration Patterns of CD8 T cells for the Development of Immune-Mediated Liver Injury

Dissertation

zur Erlangung des akademischen Grades
doctor rerum naturalium
(Dr. rer. nat.)
im Fach Biologie
eingereicht an der

Mathematisch-Naturwissenschaftlichen Fakultät I
der Humboldt-Universität zu Berlin

von

Diplom-Biologin Ira Eickmeier

Präsident der Humboldt-Universität zu Berlin
Prof. Dr. Jan-Hendrik Olbertz
Dekan der Mathematisch-Naturwissenschaftlichen Fakultät I
Prof. Stefan Hecht, Ph.D.

Gutachter/innen: 1. Prof. Dr. Alf Hamann

2. Prof. Dr. Eckart Schott

3. Dr. Michal Or-Guil

Eingereicht am: 17.10.2013
Tag der mündlichen Prüfung: 19.05.14

Contents

List of Figures

List of Tables

List of Abbreviations

AIH	Autoimmune hepatitis
ALT	Alanine aminotransferase
APC	Antigen presenting cell
AST	Aspartate aminotransferase
CCL	CC Chemokine ligand
CCR	CC Chemokine receptor
CD	Cluster of differentiation
cDNA	Complementary DNA
CFSE	Carboxyfluorescein succinimidyl ester
Ci	Curie
CLA	Cutaneous lymphocyte-associated antigen
cRNA	Complementary RNA
CTL	Cytotoxic T lymphocyte
CXCL	CXC Chemokine ligand
CXCR	CXC Chemokine receptor
DAPI	Diamidino-phenylindole
DC	Dendritic cell
ddH_2O	Double distilled water
DNA	Deoxyribonucleic acid
DT	Diphtheria toxin
DTR	Diphtheria toxin receptor
FCS	Fetal calf serum
GALT	Gut-asociated lymphoid tissue
GCOS	GeneChip Operating Software
GFP	Green fluorescent protein
GVHD	Graft-versus-host disease
HE	Hematoxylin and eosin
HEV	High endothelial venule

HLA	Human leukocyte antigen
HPCDA	High Performance Chip Data Analysis
HSC	Hepatic stellate cell
IBD	Inflammatory bowel disease
ICAM-1	Intercellular adhesion molecule 1
ID	Probe set identifier
iFABP	Intestinal fatty acid-binding protein promoter
IFN-γ	Interferon-γ
IL	Interleukin
i.p.	Intraperitonal
KC	Kupffer cell
LSEC	Liver sinusoidal endothelial cell
MAdCAM-1	Mucosal addressin cell adhesion molecule 1
mDC	Myeloid dendritic cell
MHC-I, MHC-II	Major histocompatibility complex class I or II
NK	Natural killer cell
NKT	Natural killer T cell
NPC	Non-parenchymal cell
OVA	Ovalbumin
PBC	Primary biliary cirrhosis
PBS	Phospate-buffered saline
pDC	Plasmacytoid dendritic cell
PD-1	Programmed cell death 1
PD-L1	Programmed cell death 1 ligand 1
pLN	Peripheral lymph node
PMA	Phorbol 12-myristate 13-acetate
PSC	Primary sclerosing cholangitis
qRT-PCR	Real-time reverse-transcription PCR
RNA	Ribonuclein
RPL4	Ribosomal protein L4
rpm	Rotation per minute
RPMI	Roswell Park Memorial Institute medium
RT	Room temperature
SD	Standard deviation

List of Abbreviations

SLO	Secondary lymphoid organ
TCR	T-cell receptor
TF	Transferrin
$T_H$cell	T helper cell
TNF-α	Tumor necrosis factor-α
T_{reg}	Regulatory T cell
U/l	International units/liter
VCAM-1	Vascular cell adhesion molecule 1

Zusammenfassung

Die initialen immunologischen Prozesse, die zur Entwicklung autoimmuner Lebererkrankungen führen, sind weitgehend unbekannt. Deshalb wurden in dieser Arbeit die Antigenpräsentation, die Migration sowie der Phänotyp *in vivo* aktivierter CD8 T-Zellen in der Leber anhand eines Mausmodells der autoimmunen Hepatitis untersucht.

Es ist bekannt, dass nicht-professionelle antigenpräsentierende Zellen, wie sinusoidale Leber-Endothelzellen aber auch Hepatozyten, naïve CD8 T-Zellen aktivieren und so zu ihrer Toleranz oder Deletion beitragen können. In dieser Arbeit konnte jedoch gezeigt werden, dass hepatische dendritische Zellen an der Entstehung von CD8 Effektor-T-Zellen und an der Inflammation der Leber beteiligt sind. Kupffer-Zellen dagegen nehmen im autoimmunen Kontext in der Leber eine tolerogene Funktion ein.

Die *in vivo* in der Leber aktivierten CD8 T-Zellen zeigten spezifische Oberflächenmarker und ein ungewöhnliches Migrationsverhalten. So wurde zum einen mit Neuropilin-1 ein weitgehend unbekannter Oberflächenmarker identifiziert, zum anderen spricht die Expression von bekannten Markern, die den Aktivierungstatus der CD8 T-Zellen definieren, für einen hybriden Phänotyp. Sie besitzen sowohl Charakteristika von naïven CD8 T-Zellen als auch von Effektorzellen, eine Eigenschaft, die auch bei zentralen Gedächtniszellen gefunden wird. In der Leber aktivierte CD8 T-Zellen können nicht nur proinflammatorische Zytokine ausschütten und somit eine Inflammation in der Leber auslösen, sondern sind außerdem in der Lage durch Lymphknoten zu zirkulieren. Dagegen ist ihnen der Zugang zum Darm verwehrt, womit eine direkte regulatorische Funktion im Darm ausgeschlossen werden kann. Obwohl auf in der Leber aktivierten CD8 T-Zellen spezifische Adhäsionsmoleküle identifiziert wurden, existiert keine exklusive gewebespezifische Migration in die Leber, wie sie etwa für im Darm aktivierte CD8 T-Zellen nachgewiesen wurde.

Zusammenfassung

Im darmassoziierten lymphatischen Gewebe aktivierte CD8 T-Zellen akkumulieren in der Leber und tragen möglicherweise zur Schädigung der Leber im Rahmen chronisch entzündlicher Darmerkrankungen bei.
Diese Arbeit trägt somit zum besseren Verständnis der Entstehung autoimmuner Prozesse in der Leber bei.

Summary

Initial immunological processes leading to autoimmune liver diseases are largely unknown. Therefore this thesis analyzed the antigen presentation, the migration as well as the phenotype of *in vivo* activated CD8 T cells in the liver by employing a mouse model for autoimmune hepatitis.

It is known that non-professional antigen-presenting cells, such as liver sinusoidal endothelial cells as well as hepatocytes activate naïve CD8 T cells, which leads to their tolerance or deletion. However, this thesis provides evidence that hepatic dendritic cells are effective antigen-presenting cells, which contribute to the induction of functional effector CD8 T cells in the liver and hepatitis. In contrast, Kupffer cells have a tolerogenic role during autoimmune processes in the liver.

CD8 T cells that were *in vivo* activated in the liver display specific surface markers and unusual migration patterns. On the one hand an unknown surface molecule Neuropilin-1 was identified, on the other hand expression of well-known markers defining the activation-status of CD8 T cells suggests a hybrid phenotype. They display characteristics of naïve and effector T cells, but also aspects of central memory T cells. Liver-primed CD8 T cells do not only produce pro-inflammatory cytokines leading to hepatitis, but they also retain their ability to circulate through lymph nodes. However, they have no access to the gut, which suggests that a direct regulatory function in the gut can be excluded. Although specific adhesion molecules on CD8 T cells activated in the liver were identified, no exclusive tissue-specific migration into the liver exists, as was shown for CD8 T cells primed in the gut. CD8 T cells activated in the gut-associated lymphoid tissue accumulate in the liver, in principle enabling them to induce liver pathology in the context of inflammatory bowel disease. Thus, the here described findings contribute to the understanding of initial immunological processes in autoimmune liver diseases.

1 Introduction

1.1 The liver, its anatomy and function

The liver is the largest internal organ of the body and is essential for survival. It has numerous functions including blood detoxification, bile production, metabolism of nutrients, protein synthesis, and hormone excretion as well as storage of vitamins, glycogen and minerals, to name only the most important.

Liver tissue is predominantly composed of parenchymal cells called hepatocytes. These cells are arranged as interconnected plates in hexagonal structures that form the hepatic lobule. A lobule is defined by the central vein in the center, and the portal tract – consisting of portal vein, hepatic artery, and bile duct – located at the lobule periphery. The hepatocytes are separated by a special capillary system – the sinusoids – lined by liver sinusoidal endothelial cells.

The liver receives dual blood supply. Gut-derived blood, enriched in nutrients, but also toxins and microbial products enter the sinusoids through the portal vein, whereas oxygenated blood enters the liver through the hepatic artery. From the portal tract, nutrient-rich and oxygenated blood is mixed within the liver lobules and percolates through the sinusoids, where nutrients are exchanged between blood and liver cells. The blood finally passes into the central veins and returns to the body circulation (Abdel-Misih and Bloomston, 2010).

Hepatocytes account for the largest cell population in the liver. Other non-parenchymal cell populations include liver sinusoidal endothelial cells (LSECs), Kupffer cells (KCs), dendritic cells (DCs), hepatic stellate cells (HSCs) as well as lymphocytes (Racanelli and Rehermann, 2006). Within the hepatic lymphocyte population $\gamma\delta$-T cells, natural killer (NK) cells, and natural killer T (NKT) cells are highly enriched.

Whereas CD4 T cells are more abundant within blood lymphocytes, more CD8 T cells are present in the liver (Norris et al., 1998; Tu et al., 2007).

All cells in the liver are continuously exposed to antigens from intestinal-derived blood. A large number of these antigens are tolerated to avoid permanent immune reactions, while other antigens, possibly pathogenic, are eliminated. As a result, the liver has a unique local immune environment that maintains self-tolerance while also responding to pathogens.

A remarkable feature of the liver is the spontaneous tolerance of transplanted liver allografts. In animals, the liver may be tolerated without immunosupression (Calne et al., 1969; Houssin et al., 1980; Sugioka et al., 2001). Transplantation of the liver can improve the tolerance and survival of a simultaneously transplanted kidney in humans (Rasmussen et al., 1995; Lang et al., 1998). In addition, liver-transplantation reverses the allograft rejection of pancreas and skin in rodents (Wang et al., 1998; Kamada et al., 1981).

In summary, the liver is tolerant towards antigens itself, but also transfers tolerance to other organs. Although the liver's immunologic environment is generally tolerogenic, some pathogens cause chronic inflammation. Autoimmune liver diseases occur when the liver's tolerance capabilities fail.

1.2 Breaking tolerance leads to autoimmunity

Central and peripheral tolerance

The immune system has developed several mechanisms to initiate an immune response when attacked by pathogens while ignoring the body's own cells and harmless antigens. The latter mechanism is generally referred to as "tolerance".

The first regulatory mechanism is named central tolerance and occurs during lymphocyte development. T cells mature in the thymus and undergo several positive and negative selection processes. Such selected T cells are tolerant to self-antigens, but recognize foreign antigens bound to major histocompatibility complex proteins (MHC) (Gallegos and Bevan, 2006). B cells, developing in the bone marrow, also undergo negative selection and are deleted if their receptors bind to self-antigens (Cornall et al., 1995).

Some lymphocytes escape central selection and have the potential to react to

self-antigens in the periphery (Liu et al., 1995). Such self-reactive lymphocytes are controlled by peripheral tolerance mechanisms. These include antigen ignorance, T-cell anergy, peripheral deletion of autoreactive T cells, and suppression by CD4 T_{reg} (regulatory CD4 T cells).

For instance, constant high-level antigen exposure of self-antigens leads to deletion of lymphocytes (Miller et al., 1998). The absence of pro-inflammatory cytokines or co-stimulatory signals during antigen presentation causes anergy (Mondino et al., 1996). In addition, an anti-inflammatory cytokine milieu can induce CD4 T_{reg}, which are able to suppress activated lymphocytes or antigen-presenting cells (APCs) by production of anti-inflammatory cytokines (Shevach, 2009). Furthermore, inhibitory molecules expressed by lymphocytes and APCs lead to inactivation, apoptosis, and elimination of autoreactive lymphocytes (Probst et al., 2005).

Autoimmunity

Tolerance mechanisms normally protect the body from immune reactions against itself. However, self-reactive lymphocytes are found in the periphery in all healthy individuals (Lohse et al., 1996). In some cases activation of these cells, followed by reactions against self-antigens causes autoimmune diseases. Autoreactive T cells and/or autoantibodies are involved in cellular damage (Shlomchik, 2009). They recognize target-structures, destroy cells by cytolysis or induce an inflammatory response.

In general, autoimmune diseases are divided into two categories: organ-specific and systemic disorders. In organ-specific autoimmune diseases the immune response is directed against a specific organ, such as the liver in autoimmune hepatitis. A typical example of systemic autoimmunity is lupus erythematosus, characterized by inflammation of multiple tissues due to reactions against autoantigens found in every cell of the organism (Kotzin, 1996).

Autoimmune diseases develop spontaneously and their triggers are not known. A combination of dysregulated immune response, genetic predisposition, and environmental factors may promote autoimmunity. Genetic predisposition is often associated with genes located in the human leukocyte antigen (HLA)

locus, also known as major histocompatibility complex (MHC) (Thorsby and Lie, 2005). MHC molecules present small peptides from foreign antigens and self-antigens to T cells. Certain HLA alleles may influence the susceptibility to autoimmune diseases, by promoting binding of specific peptide antigens. Insufficient presentation of self-antigens by HLA molecules to developing lymphocytes in the thymus leads to the release of self-reactive lymphocytes into the periphery. In addition, enhanced presentation of self-antigens may increase lymphocyte activation in tissues (Simmonds and Gough, 2004). However, identical twins demonstrate that genetic predisposition does not induce autoimmunity alone and other factors have to be involved (Cooper et al., 1999). For example, environmental factors, such as pathogens or drugs may trigger autoimmune diseases. The immune system reacts to infections by releasing pro-inflammatory cytokines. These cytokines can promote the activation of autoreactive T cells or enhance the antigen presentation of self-antigens to lymphocytes, known as bystander-activation (Wucherpfennig, 2001). "Molecular mimicry" is discussed as a possible trigger for autoimmune diseases. Pathogens invading an organism may present antigens with similarity to self-antigens. Production of autoantibodies or autoreactive lymphocytes that cross-react with these self-antigens may be the result of reactions against self (Wucherpfennig and Strominger, 1995).

1.3 Autoimmune liver diseases

Autoimmune diseases affecting the liver include autoimmune hepatitis (AIH), primary biliary cirrhosis (PBC), and primary sclerosing cholangitis (PSC). Neither cause nor pathogenesis of any of these diseases are known. As in other autoimmune disorders, a combination of genetic background, gender, and environmental factors are thought to trigger autoimmune liver disease. The detection of specific autoantibodies as well as histological analyses are essential to distinguish these disorders, which partially overlap (Rust and Beuers, 2008). Autoimmune liver diseases are often accompanied by other disorders, such as thyroid diseases, celiac disease, psoriasis, and rheumatoid arthritis (Efe et al., 2012).

1.3.1 Autoimmune hepatitis

AIH is a chronic liver disease characterized by an immunological reaction against hepatocytes. Untreated, AIH can cause fibrosis and cirrhosis, resulting in liver failure and death. Humans of all ages are affected, predominantly women. Patients responding to immunosuppressive treatment have a good prognosis and normal life expectancy. However, when diagnosis is delayed in patients displaying progressive liver damage and who are unresponsive to therapy may require liver transplantation (Manns and Vergani, 2009). The risk of developing AIH depends on genetic predisposition. HLA alleles are strongly associated with the disease, and other genes outside the HLA locus are discussed (Tang et al., 2012). A typical histological finding in liver biopsies are infiltrates of mononuclear cells, containing lymphocytes, plasma cells, and macrophages (Krawitt, 2006). These inflammatory cells spread from the portal areas, between and around hepatocytes into the periportal regions, thereby destroying hepatocytes, leaving the characteristic "interface hepatitis" (Vergani and Mieli-Vergani, 2008). Serological findings include elevated transaminases (ALT, AST), IgG, and autoantibodies. Based on detection of autoantibodies two types of AIH are distinguished. The autoantibodies ANA (antinuclear antibody), SMA (smooth muscle actin), and SLA (soluble liver antigen) are found in AIH type 1. The presence of the autoantibodies LKM (liver kidney microsomal antigen) and LC 1 (liver cytosol type 1) are characteristic for AIH type 2, occurring mostly in children (Gossard and Lindor, 2012). The target structures of LKM-1 and LC 1 and the fact that cross-reaction occurs with certain viruses, implies that molecular mimicry may trigger AIH type 2 (Manns et al., 1991; Kerkar et al., 2003). Because autoantibodies are absent in 20% of patients and are found also in other diseases, a pathogenic role is not assumed.

1.3.2 Primary biliary cirrhosis

PBC is a chronic liver disease that destroys the small intrahepatic bile ducts resulting in defective bile flow (cholestasis), fibrosis, and cirrhosis. Women are affected predominantly (Smyk et al., 2012). PBC frequently occurs in first-degree relatives, and shows a high concordance rate in twins, which suggests a genetic predisposition (Bogdanos et al., 2012). Patients diagnosed early

who respond to ursodeoxycholic acid (UDCA) treatment, one of the secondary bile acids, have an excellent prognosis. In contrast, patients with progressive PBC usually require liver transplantation (Ishibashi et al., 2011). Genome-wide association studies implicate that various alleles within the HLA locus, but also genes involved in the regulation of immune responses, for instance in interleukin-12 signaling, increase the susceptibility for PBC (Hirschfield et al., 2009). Liver biopsies exhibit loss of bile ducts (ductupenia) as well as infiltration of lymphocytes and macrophages. Serological findings include elevated gamma-glutamyl transferase (γ-GT), elevated alkaline phosphatase (ALP) and the detection of AMA (anti-mitochondrial antibody) (Hirschfield and Gershwin, 2011). AMAs in PBC are directed against the E2 subunits of the pyruvate dehydrogenase complex (PDC-E2) (Fussey et al., 1988). Regions within this target antigen are also recognized by CD4 T cells and CD8 T cells (Kita et al., 2002; Shimoda et al., 1998). Infectious organisms, for instance *Escherichia coli* or *Novosphingobium aromativorans* are suggested to trigger PBC through molecular mimicry (Fussey et al., 1990; Selmi et al., 2003).

1.3.3 Primary sclerosing cholangitis

PSC is a progressive liver disease of unknown cause, characterized by inflammation and destruction of large intrahepatic and extrahepatic bile ducts. The disease causes fibrosis, cirrhosis and acute liver failure. In contrast to other autoimmune disorders, PSC affects men predominantly. Death or the decision for liver transplantation occurs between 12 to 17 years after diagnosis (LaRusso et al., 2006). PSC patients have a high risk of developing cholangiocarcinoma and colorectal carcinoma (Saich and Chapman, 2008). Endoscopic retrograde cholangiopancreatography (ERCP) is used to identify structural changes of the bile ducts. Strictures can be dilated by endoscopy, but liver transplantation remains the only life-extending treatment (Michaels and Levy, 2008). p-ANCA autoantibodies (perinuclear antineutrophil cytoplasmic antibodies) are found in 80% of PSC patients. Genetic susceptibility to PSC is conferred by specific HLA-genes and non-HLA genes involved in bile homeostasis and inflammatory pathways (Karlsen et al., 2010; Eri et al., 2004; Hov et al., 2010).

Up to 80% of PSC patients have inflammatory bowel disease (IBD) as the

underlying condition (Broomé and Bergquist, 2006). In conjunction with PSC the most often classified IBD is ulcerative colitis, but there is also an association with Crohn's disease (Loftus et al., 2005; Fausa et al., 1991). PSC can occur years after colectomy, and colectomy before or during liver-transplantation prevents the recurrence of PSC (Chapman et al., 1980; Alabraba et al., 2009).

In livers of PSC patients, atypical T cells are detected which express molecules usually found on gut-derived T cells (Hillan et al., 1999; Eksteen et al., 2009). These findings led to the theory that these anatomically distinct diseases are linked by the recruitment of gut-activated lymphocytes to the liver, where they trigger an inflammatory response (Grant et al., 2001).

1.4 How T cells travel through the body

Mature naïve T cells patrol the body through blood vessels, lymphatic vessels and secondary lymphoid organs (SLOs), including the spleen, peripheral lymph nodes (pLN), and the gut-associated lymphoid tissue (GALT). Naïve as well as activated lymphocytes leave the blood and extravasate into the lymph nodes or into inflamed non-lymphoid tissues.

A process called "multistep adhesion cascade" involves rolling and tethering of T cells, mediated by interactions between selectins and addressins (Butcher, 1991). Equipped with chemokine receptors, T cells detect immobilized chemokines on endothelial cells leading to their arrest (Cyster, 1999). After signal transduction through the G-protein coupled chemokine receptors integrins are activated and form high-affinity conformations. Binding of integrins to adhesion molecules mediates the firm adhesion of lymphocytes before they transmigrate into tissues (Luo et al., 2007).

1.4.1 Naïve T cells constantly patrol the secondary lymphoid organs

Naïve T cells enter the lymph nodes *via* specialized high endothelial venules (HEV). They express L-selectin (CD62L) that binds to ligands, collectively called peripheral node addressins (PNAds), such as GLyCAM-1 and CD34 (Ley and Kansas, 2004). This interaction enables T cells to roll along endothelial cells and enhances the probability of encountering the chemokines CCL19 and

CCL21 displayed by the HEV. CCL19 and CCL21 interact with CCR7, a G protein-coupled receptor, which mediates intracellular signaling, leading to activation and conformational changes of nearby integrins (Förster et al., 2008). Firm adhesion of lymphocytes in the pLN is mediated by binding of lymphocyte function-associated antigen 1 (LFA-1; αLβ2) on T cells to intercellular adhesion molecule 1 (ICAM-1). Low expression of α4β7 on naïve T cells and interaction with mucosal addressin cell adhesion molecule (MAdCAM-1) promotes the entry into the GALT (Bargatze et al., 1995). Lymphocytes transmigrate into lymph nodes either taking a paracellular route through open junctions or a transcellular route directly through endothelial cells (Cernuda-Morollon et al., 2010). Lymphocytes not meeting their cognate antigen, leave the lymph node *via* efferent lymphatics and return to the blood circulation.

1.4.2 Tissue-tropic T cells migrate into specific sites

Within the lymph nodes dendritic cells display antigens, sampled from inflamed sites, to naïve T cells. Once they recognize their cognate antigen, naïve T cells differentiate into effector cells and acquire a new repertoire of surface molecules, which promote entry into inflamed sites. Effector T cells leave the lymph nodes, return to the blood stream, and migrate preferentially into tissues that are associated with the secondary lymphoid organs, in which they first encountered their antigen. This process is known as tissue tropism (Kantele et al., 1999).

T cells that enter the gut or the skin are the best described examples of tissue-specific migration of T cells. Lymphocytes activated by DCs in the GALT upregulate the integrin α4β7 and the chemokine receptor CCR9 (Stagg et al., 2002; Johansson-Lindbom et al., 2005). Retinoic acid, a metabolite of vitamin A produced by intestinal DCs, is essential to induce the expression of α4β7 and CCR9 on T cells (Iwata et al., 2004). CCR9 recognizes its ligand CCL25, secreted by epithelial cells and lamina propria venules in the small intestine (Wurbel et al., 2000; Kunkel et al., 2000). α4β7 binds to MAdCAM-1 expressed in the gut lamina propria venules (Berlin et al., 1993; Briskin et al., 1997). Interactions between these molecules are required for T cells to enter the small intestine, but it remains controversial if CCL25 and CCR9 are necessary for migration into the colon (Papadakis et al., 2000; Wurbel et al., 2011).

T cells activated by skin-derived DCs express cutaneous lymphocyte-associated antigen (CLA), CCR10 and CCR4. Vitamin D3 or its metabolites induce the expression of the chemokine receptor CCR10 (Sigmundsdottir et al., 2007). Rolling of T cells on dermal endothelium is mediated by CLA binding to E-selectin (CD62E) (Picker et al., 1991). CCL17 and CCL27, the ligands for CCR4 and CCR10, are expressed by skin venules and keratinocytes, respectively (Campbell et al., 1999; Homey et al., 2002). Interaction of these receptors and molecules mediate the migration of tissue-tropic T cells to sites of cutaneous inflammation.

The expression of tissue-specific molecules on T cells is not stable. Skin- and gut-derived T cells can be reprogrammed to express alternative homing receptors by restimulation with DCs from the reciprocal organ *in vitro* (Mora et al., 2005).

1.5 T-cell migration into the liver differs from the multistep paradigm

The liver contains a special microvasculature – the sinusoids – where lymphocyte adhesion takes place (Wong et al., 1997). In contrast to other capillaries, the discontinuous endothelial monolayer is fenestrated and lacks a basal membrane (Wisse et al., 1996), allowing direct contact of T cells with the underlying hepatocytes (Warren et al., 2006). Naïve and memory T cells frequently migrate through the healthy liver, whereas the majority of activated T cells are retained (Luettig et al., 1999; Mehal et al., 1999). The unique architecture of the liver contributes to T-cell migration, which differs from the multistep paradigm observed in lymphoid tissues and other organs.

Selectins and appropriate ligands are required for T cells to roll along endothelial cells. In contrast, leukocyte rolling in the liver is independent of E-, P-selectin, and L-selectin (Wong et al., 1997) and may not be required at all given the small diameter of 5-7 µm and the slow blood flow in the sinusoids (MacPhee et al., 1995).

Effector T cells infiltrating the inflamed human and murine liver in viral hepatitis and autoimmune liver diseases express CXCR3 (Shields et al., 1999; Curbishley et al., 2005; Kakimi et al., 2001; Zhang et al., 2011). Likewise, the ligands for CXCR3, namely CXCL9, CXCL10 and CXCL11, are upregulated and displayed by LSECs in the inflamed liver (Curbishley et al., 2005; Narumi et al., 1997). Blocking CXCL9 and CXCL10 reduces the infiltration of T cells into the liver in a murine model of hepatitis B (Kakimi et al., 2001). The development of primary biliary cirrhosis (PBC) is delayed in CXCR3-deficient mice, but infiltration of T cells into the liver is not entirely absent (Zhang et al., 2011). Another chemokine receptor expressed by T cells in the inflamed liver is CXCR6 (Boisvert et al., 2003; Sato et al., 2005). Its ligand CXCL16, produced by hepatocytes, LSECs and biliary epithelial cells in healthy and inflamed human liver, promotes activation of β1-integrin and binding to VCAM-1 (Heydtmann et al., 2005). Murine graft-versus-host disease (GVHD) is reduced when CXCR6-deficient CD8 T cells are transferred (Sato et al., 2005). Yet another chemokine receptor CCR5 and its ligands CCL3 and CCL4 are expressed in the inflamed murine and human liver (Murai et al., 1999; Shields et al., 1999; Larrubia et al., 2007). Blocking CCR5 reduces the infiltration of T cells in the liver in GVHD (Murai et al., 1999). In contrast, T cell-mediated hepatitis in CCR5-deficient mice leads to enriched T-cell infiltration and hepatitis that makes CCR5 an unlikely candidate for migration into the liver (Moreno et al., 2005).

After T cells slow down and arrest, integrins and their ligands promote the firm adhesion to endothelial cells. The adhesion molecules ICAM-1, ICAM-2 and VCAM-1 are constitutively expressed in the liver, and expression of ICAM-1 and VCAM-1 increase upon inflammation (Steinhoff et al., 1993; van Oosten et al., 1995). αLβ2 (LFA-1), the binding partner of ICAM-1, mediates adhesion of naïve and effector CD8 T cells to the liver (Bertolino et al., 2005; John and Crispe, 2004; Sato et al., 2006). ICAM-1-mediated adhesion has been proposed to be dependent on antigen presentation, because TCR-ligation regulates LFA-1 (John and Crispe, 2004; Bertolino et al., 2005). Antigen-independent adhesion of activated CD8 T cells to the liver occurs *via* VCAM-1/α4-integrin (John and Crispe, 2004), although α4-integrin is dispensable for the recruitment of naïve T cells to the liver (Bertolino et al., 2005).

Lymphocytes activated in the GALT express the integrin α4β7 and the chemokine receptor CCR9, recognizing MAdCAM-1 and CCL25 in the intestinal tract. MAdCAM-1, a typical gut-addressin, is upregulated in the liver in various liver diseases, such as AIH, PSC, and PBC (Hillan et al., 1999). Both α4β7/CCR9-positive T cells as well as CCL25 are detected in the inflamed liver of patients suffering from PSC (Grant et al., 2001; Eksteen et al., 2004). These T cells must be gut-derived, since neither dendritic cells nor stellate cells derived from the liver are capable of imprinting the gut-specific phenotype (Grant et al., 2001; Eksteen et al., 2009). However, it remains possible that LSECs induce this phenotype (Neumann et al., 2012).

The vascular adhesion protein-1 (VAP-1) has enzymatic activity and may play a role in the induction of MAdCAM-1 in the liver. Activation of VAP-1 by deamination of methylamine, present in the portal venous blood, induces the expression of MAdCAM-1 on LSECs (Liaskou et al., 2011).

In summary, chemokine receptors and integrins play a role in T-cell infiltration into the liver, but it is unknown whether they are regulated in the liver or required for migration into the liver. A liver-specific adhesion molecule has yet to be reported.

1.6 Antigen presentation and activation of T cells

Antigen presentation, a short overview

Adaptive immunity requires activation of T cells by antigen-presenting cells (APCs). The antigen-specific T cell receptor recognizes antigens displayed by major histocompatibility complex (MHC) molecules.

MHC class I (MHC-I) molecules, expressed by almost all nucleated cells, present self-proteins but also exogenous intracellular antigens derived from viral or bacterial infections to CD8 T cells. Antigens are degraded by cytosolic and nuclear proteasomes. The resulting short peptides are translocated into the endoplasmatic reticulum (ER) by transporter associated with antigen presentation (TAP). In the ER peptides are loaded onto MHC-I and transported *via* the Golgi complex to the cell surface, where the antigens are displayed to CD8 T cells (Neefjes et al., 2011).

In contrast to MHC-I molecules, MHC class II (MHC-II) molecules are mainly expressed by professional APCs, such as DCs, macrophages, and B cells. MHC-II expression can be induced by inflammatory stimuli in non-professional APCs, including endothelial cells, epithelial cells and others. Ingested exogenous antigens are taken up into phagosomal compartments that fuse with lysosomes. In the resulting phagolysosomes, MHC-II molecules interact with peptides, and the peptide-loaded MHC-II molecules are transported to the cell surface, where antigens are displayed to CD4 T cells (Neefjes et al., 2011).

However, the general paradigm of presentation of endogenous and extracellular antigens by MHC molecules has expanded in recent years. CD8 T cells are usually activated by professional APCs. When APCs are not infected by pathogens, an appropriate immunogenic answer would fail. Therefore professional APCs also load exogenous antigens onto MHC-I molecules, displayed to CD8 T cells, a process called cross-presentation (Bevan, 1976; Kurts et al., 2001). The theory that endogenous antigens are presented by MHC-I molecules only, can be extended as well. Through autophagy, a process by which cells remove damaged organelles, endogenous antigens are also delivered to MHC-II molecules and displayed to CD4 T cells (Schmid et al., 2007; Nimmerjahn et al., 2003).

Activation of T cells

The interaction of an MHC/antigen complex and the TCR is not sufficient to differentiate T cells into effector cells. Co-stimulatory molecules, such as molecules of the B7-family expressed by APCs, but also cytokines and adhesion molecules are involved in enhancing TCR-mediated responses. A well described example is CD28 expressed by T cells, which interacts with the B7 members CD80 and CD86. Binding of these molecules results in stimulation of T-cell activation (Chen, 2004). In addition, co-inhibitory molecules, such as CTLA-4 (cytotoxic T lymphocyte antigen 4) and PD-1 (programmed cell death 1), bind the same B7 members, down-modulating the T-cell response (Probst et al., 2005).

Activation of naïve CD8 T cells leads to differentiation into cytotoxic effector cells (CTL). By secreting granzyme and perforin they specifically lyse self-

infected target cells. Binding of Fas molecules to the target cell *via* Fas ligand on the CTL leads to apoptosis of the infected cell. The secretion of IFN-γ enhances the expression of MHC molecules on others cells, thereby enhancing antigen presentation and the removal of pathogens (Zhang and Bevan, 2011).

CD4 T cells differentiate into various subsets of CD4 T helper cells (T_H), depending on the cytokine milieu and the strength of the interaction of the TCR with antigen. They regulate the adaptive immune responses by secreting cytokines, which activate or recruit target cells. T_H1 cells are involved in elimination of intracellular pathogens and secrete pro-inflammatory cytokines, which enhance phagocytic activity, promote CD8 T-cell activation, and help to generate memory T cells (Zhu et al., 2010). T_H2 cells mediate host defense against extracellular parasites and support the humoral response. By secreting a battery of pro- and anti-inflammatory cytokines, they stimulate B-cell proliferation and antibody production, but also dampen strong immune responses (Zhu and Paul, 2010). CD4 T_{reg} maintain the immunologic tolerance to self and foreign antigens. They negatively regulate a variety of immune responses, such as allergy or pathogen-induced inflammation (Sakaguchi et al., 2006). Numerous other subsets, such as T_H17 cells or T_H9 cells are described and reviewed in (Luckheeram et al., 2012).

1.7 T-cell activation within the liver

In general T cells are activated by professional APCs in the lymph nodes or spleen and then migrate into non-lymphoid tissues. The liver is an exception to this rule insofar as it is a site at which naïve T cells can be activated (Bertolino et al., 2001). Animal models extended the understanding of immunological processes in the liver, from which the most significant examples are introduced in the following section.

One of the first studies of liver inflammation was based on repeated immunization of mice with liver-proteins in Freund's adjuvant leading to hepatitis. The induced hepatitis could be transferred to healthy mice by injecting lymphocytes from diseased mice, providing evidence that T cells play a major role in immune-mediated liver disease (Mori et al., 1985).

The injection of the leptin concanavalin (Con) A into mice leads to acute liver damage driven by CD4 T cells, KCs, and NKT cells, all of which produce pro-inflammatory cytokines such as TNF-α and IFN-γ (Tiegs et al., 1992; Schumann et al., 2000; Kaneko et al., 2000; Küsters et al., 1996). However, this model represents a cytokine-mediated model for acute liver injury rather than antigen-driven hepatitis.

Transgenic models of autoimmune hepatitis are based on the expression of model antigens in the liver. Expression of allogenic MHC-I molecules on hepatocytes and transfer of TCR-transgenic T cells results in activation of naïve CD8 T cells within the liver, but these T cells have a shortened life-span and are soon deleted (Bertolino et al., 2001; Limmer et al., 1998). In contrast, the expression of the same alloantigen in the liver and in lymph nodes results in effector CD8 T cells mediating hepatitis, suggesting that efficient T-cell activation only occurs outside of the liver (Bowen et al., 2004). However, a limitation of these models is that the antigen is not presented by professional APCs within the liver. Another mouse model expressing the glycoprotein 33 in the liver, an epitope of the lymphocytic choriomeningitis virus (LCMV), is ignored by transferred antigen-specific T cells and tolerance could be broken only by additional LCMV-infection (Voehringer et al., 2000). TF-OVA mice, a model established in our laboratory, express the antigen ovalbumin in hepatocytes (Derkow et al., 2007). Adoptive transfer of antigen-specific naïve CD8 T cells induces transient hepatitis, a result confirmed by other groups using different promoters or antigens (Buxbaum et al., 2008; Zierden et al., 2010). In addition Zierden et al. crossed mice expressing the influenza virus hemagglutinin (HA) in the liver with mice with expressing HA-specific CD8 T cells. These mice developed spontaneous chronic liver inflammation (Zierden et al., 2010).

Other animal models are based on the theory of "molecular mimicry". For example, infection of wild-type mice with an adenovirus expressing the human cytochrome P450 2D6 (Ad-2D6) (an autoantigen in human AIH type 2) results in chronic autoimmune-mediated liver damage (Holdener et al., 2008).

T cells in the portal tracts and in the sinusoids have contact to a variety of

non-professional and professional APCs. Although various cell types in the liver have the potential to activate T cells, the fate of these T cells depends on the type of APC on which they were activated.

1.7.1 T-cell activation by non-professional hepatic APCs

Hepatocytes

The majority of cells in the liver are hepatocytes. They express MHC-I and under inflammatory conditions upregulate MHC-II as well as the co-stimulatory molecules CD80, CD86, and CD40. (Franco et al., 1988; Sacher et al., 2002). T cells interact with hepatocytes through fenestrations of LSECs (Warren et al., 2006). Hepatocytes activate naïve CD4 T cells and CD8 T cells *in vitro*, leading to premature death or to T_H2-polarization (Bertolino et al., 1999; Herkel et al., 2003). The transgenic expression of allogenic MHC-I molecules on hepatocytes results in activation of naïve CD8 T cells *in vivo* (Bertolino et al., 2001). These T cells are dysfunctional, undergo apoptosis and die by a process that depends upon expression of pro-apoptotic protein Bim and caspase 3 (Holz et al., 2008). In contrast, the injection of an adeno-associated virus (AAV-OVA) vector into mice, that localizes in hepatocytes, leads to functional CD8 T-cell activation, but fails to activate CD4 T cells (Wuensch et al., 2006, 2010).

The majority of reports indicate that hepatocytes act as APCs, activate naïve CD8 T cells, but induce tolerance rather than immunity. Maintaining tolerance induction by hepatocytes has been recently proposed, by a process called "suicidal emperipolesis". Thereby autoreactive T cells invade hepatocytes and are degraded by lysosomal proteolytic enzymes (Benseler et al., 2011).

Liver sinusoidal endothelial cells

LSECs are scavenger cells, clearing the blood from foreign molecules and antigens (Smedsrod et al., 1990). They express low levels of MHC-II, CD80, and CD86, all of which are downregulated by IL-10 (Knolle et al., 1998). LSECs cross-present soluble antigens to naïve CD8 T cells *in vitro* and *in vivo* (Limmer et al., 2000; Oppen et al., 2009). Such primed T cells fail to induce a cytotoxic response and are tolerized, correlating with the expression

of inhibitory molecule PD-L1 (programmed cell death 1 ligand 1) expressed by LSECs (Limmer et al., 2000; Diehl et al., 2008). CD8 T-cell activation by potent APCs is inhibited when co-cultured with LSECs (Schildberg et al., 2008). CD4 T cells activated by LSECs *in vitro* fail to develop a T_H1-phenotype, but differentiate into CD4 T cells with regulatory function (Knolle et al., 1999; Kruse et al., 2009). Contradictory to these results, LSECs were also reported to be poor in stimulating T cells, to lack MHC-II as well as co-stimulatory molecules (Katz et al., 2004), and to fail to activate antigen-specific CD4 T cells *in vitro* (Derkow et al., 2011).

Overall, LSEC represent a population of non-professional APCs, which contribute to liver tolerance.

Hepatic stellate cells

HSCs are located in the space of Dissé and store the majority of vitamin A (Li and Friedman, 1999). Following liver injury they differentiate into myofibroblasts, which induce liver fibrosis (Gressner and Weiskirchen, 2006). Reports about HSCs acting as APCs are contradictory. Whereas HSCs were shown to express MHC-I, MHC-II, and co-stimulatory molecules, other reports found that they lack these molecules (Vinas et al., 2003; Ichikawa et al., 2011). They activate antigen-specific CD4 and CD8 T cells as well as NKT cells, leading to IFN-γ-secretion (Winau et al., 2007). In contrast, co-cultures of HSCs with allogenic T cells induce CD4 T_{reg} (Jiang et al., 2008; Wu et al., 2012). Additionally, HSCs fail to activate T cells (Ichikawa et al., 2011). Instead they act as bystander cells for DC-T-cell activation in generating CD4 T_{reg}, depending on retinoic acid (Dunham et al., 2013). In liver transplantation HSCs contribute to immune tolerance by induction of T-cell apoptosis (Jiang et al., 2013).

In summary, only a few reports support that HSCs act as APCs for T cells. More likely they represent a cell population that mediates tolerance.

1.7.2 T-cell activation by professional hepatic APCs

Kupffer cells

KCs are liver-resident macrophages located in the sinusoids (Wisse et al., 1996). They phagocytose cell remnants and pathogens, eliminate toxic agents, and play a vital role in liver-regeneration (Hirakata et al., 1991; Eipel et al., 2007; Abshagen et al., 2008). The majority of KCs express F4/80 and different levels of CD11b and CD68 (Lloyd et al., 2008; Kinoshita et al., 2010). In addition, the expression of MHC-II and the co-stimulatory molecules CD80 and CD86 render KCs potential APCs (You et al., 2008).

In response to low concentrations of lipopolysaccaride (LPS), they secrete IL-10 leading to reduced T-cell proliferation (Knolle et al., 1995). KCs are weak stimulators of CD4 T cells. They inhibit proliferation of T cells initially activated by DCs and interact with CD4 T_{reg} thereby enhancing T-cell tolerance (You et al., 2008; Breous et al., 2009).

However, in response to microbial signals, KCs antagonize the suppressive activity of CD4 T_{reg} and produce pro-inflammatory cytokines such as TNF-α and IL-18 (Wiegard et al., 2005; Okamura et al., 1995; Lichtman et al., 1998). IL-18 leads to activation of NK cells and NKT cells in the liver, while TNF-α contributes to concanavalin A-mediated hepatitis in mice (Schumann et al., 2000; Dao et al., 1998).

Overall, KCs have tolerogenic but also immunogenic properties, depending on signals present in the liver.

Hepatic dendritic cells

Hepatic DCs are located in the periportal areas and in the sinusoids (Watanabe et al., 2007). Multiple populations of DCs exist in the murine and human liver. Depending on their origin, myeloid (mDC) and plasmacytoid (pDCs) DCs are distinguished by expression of different levels of CD11c (Lian et al., 2003).

mDCs in the murine liver express CD11c and CD11b, while human mDCs are additionally defined by BDCA-1 expression. They secrete anti-inflammatory cytokines mediating the expansion of CD4 T_{reg} and T_H2 cells (Chen et al., 2009; Goddard et al., 2004; Bamboat et al., 2009).

Murine hepatic pDCs are B220-positive, express low levels of CD11c, and secrete anti-inflammatory cytokines, mediating antigen-specific T-cell suppression and induction of CD4 T_{reg} (Lian et al., 2003; Goubier et al., 2008; Matta et al., 2012). In contrast, when being activated, pDCs are effective APCs and activate NK cells, NKT cells as well as antigen-specific CD8 T cells (Kingham et al., 2007). Little is known about human hepatic pDCs and their potential to activate T cells, but they may contribute to liver transplant tolerance (Gupta et al., 2009).

The murine liver contains two subpopulations of DCs not found in the human liver. CD11cCD8α-positive DCs are strong T-cell activators and produce pro-inflammatory cytokines (O'Connell et al., 2000, 2003). Another subset, called "natural killer DCs," characterized by markers of DCs and NK cells (CD11c, NK1.1), secrete IFN-γ, lyse tumor cells, and induce antigen-specific T-cell activation (Pillarisetty et al., 2005).

Taken together, the liver contains heterogeneous populations of DCs. The majority of liver DCs are weak activators of T cells, but some subsets may induce immunity. It remains unclear whether hepatic DCs contribute to T-cell activation in the liver, mediating hepatitis.

1.8 Aims of the Study

Studies of T-cell priming in the liver have led investigators to assume that non-professional APCs such as LSECs, but also hepatocytes induce tolerance and possibly apoptosis and deletion of T cells. However, professional APCs such as DCs and macrophages may influence the differentiation and the fate of T cells in the liver. Therefore, we hypothesized that hepatic DCs and KCs, the liver-resident macrophages, play a pivotal role in T-cell activation in the liver. To test this hypothesis, liver inflammation was induced in a mouse model of autoimmune hepatitis, in which a model antigen is expressed in the liver. In addition, DCs and KCs were selectively depleted, and it was analyzed whether they are capable of activating autoreactive naïve CD8 T cells mediating liver inflammation *in vivo*.

The liver is a site of T-cell activation, but little is known about the migratory properties of liver-primed T cells. Activated T cells that enter the liver may originate from other organs such as the gut. Therefore, several questions arise regarding the migration of liver-activated and gut-activated T cells. Do liver-primed T cells display tissue-tropic migration as known for gut-derived T cells? Do they migrate to other organs such as the gut? Conversely, do T cells initially activated in the gut-associated lymphoid tissue migrate to the liver where they are retained because they are activated? What happens if they encounter their cognate antigen in the liver? By employing an *in vivo* migration assay, this study intended to determine the migratory patterns of CD8 T cells primed by the same antigen in the small intestine or in the liver. In addition, differentially activated T cells were tested for their migration towards their cognate antigen expressed in the liver or small intestine.

Activation of T cells in the liver and gut likely induces different phenotypes, characterized by a distinct repertoire of surface molecules. A specific homing receptor for the liver has not been reported yet. Therefore, this study intended to compare the phenotype of liver-and gut-primed T cells. Of the two T-cell populations, activation markers, inhibitory molecules as well as adhesion molecules were characterized, with the aim of identifying markers that distinguish liver-primed T cells from T cells activated in other organs.

2 Materials and Methods

2.1 Mice

TF-OVA mice express the antigen $OVA_{139\text{-}385}$ fused to the transferrin-receptor under the transferrin-promoter (TF) in hepatocytes (Derkow et al., 2007).

iFABP-OVA mice express the antigen $OVA_{138\text{-}386}$ under control of the intestinal fatty acid-binding protein promoter (iFABP) in enterocytes. Mice were provided by Prof. Lefrançois (Vezys et al., 2000).

CD11cDTR mice express the simian DTR (diphtheria toxin receptor) fused to GFP (green fluorescent protein) under control of the murine CD11c promoter (Jung et al., 2002) and were provided by the German Rheumatism Research Center Berlin.

TF-OVA×CD11cDTR mice were generated by crossing TF-OVA mice to CD11cDTR mice. For experiments the F1 generation was employed.

OT-I mice express a transgenic TCR (Vα2Vβ5) specific for the H2-K^b-restricted peptide $OVA_{254\text{-}267}$ (Hogquist et al., 1994). Mice were provided by Prof.Blankenstein.

All lines were bred under specific pathogen free conditions in the Research Institute for Experimental Medicine, Charité (FEM). Wild-type mice (C57Bl6J) were purchased from the FEM. All animal experiments were approved by the State Office of Health and Social Affairs, Berlin.

2.2 Antibodies

Table 1: Antibodies for flow cytometry. All anti-mouse antibodies were purchased from the following companies: [1] eBioscience, San Diego, USA, [2] BioLegend, San Diego, USA, [3] BD Bioscience, Heidelberg, Germany, [4] R&D Systems, Minneapolis, USA.

Name	Clone	Isotype
αL [1]	M17/4	Rat IgG_{2a}, κ
α4 [2]	9C10 (MFR.B)	Rat IgG_{2a}, κ
α6 [2]	GoH3	Rat IgG_{2a}, κ
αV [2]	RMV-7	Rat IgG_1, κ
α4 β7 [2]	DATK32	Rat IgG_{2a}, κ
β1 [2]	HMβ 1-1	Armenian Hamster IgG
β2 [1]	M18/2	IgG_{2a}, κ
CD11b [1]	M1/70	Rat IgG_{2b}, κ
CD11c [1]	N418	Armenian Hamster IgG
CD16/CD32 [1]	93	Rat IgG_{2a}, λ
CD200 [2]	OX-90	Rat IgG_{2a}, κ
CD25 [1]	PLS 1.5	Rat IgG_1, λ
CD62 L[1]	MEL-14	Rat IgG_{2a}, κ
CD44 [1]	IM7	Rat IgG_{2b}, κ
CD69 [3]	H1.2F3	Armenian Hamster IgG
CD8a [3]	53-6.7	Rat IgG_{2a}, κ
CCR7 [1]	4B12	Rat IgG_{2a}, κ
CCR9 [2]	CW-1.2	Mouse IgG_{2a}, κ
CXCR3 [2]	CXCR-173	Rat IgG_{2a}
CXCR6 [4]	221002	Rat IgG_{2b}
F4/80 [1]	BM8	Rat IgG_{2a}, κ
GzmB [3]	GB11	Mouse IgG_1, κ
IFN-γ [1]	XMG 1.2	Rat IgG_1, λ
Ly-6C [2]	HK 1.4	Rat IgG_{2c}, κ
PD-1 [1]	J43	Armenian Hamster IgG
Vα2 TCR [3]	B20.1	Rat IgG_{2a}, κ

Table 2: Antibodies for immunohistochemistry. All antibodies were purchased from the following companies: [1] BioLegend, San Diego, USA; [2] Abcam, Cambridge, UK; [3] DAKO, Glostrup, Denmark; [4] eBioscience, San Diego, USA; [5] Invitrogen, Carlsbad, USA; [6] Dianova, Hamburg, Germany.

Primary antibodies	**Clone**	**Conjugate**
Rat anti-mouse ICAM-1 [1]	YN1/1.7.4	Alexa Fluor 488
Rat anti-mouse MadCam-1 [1]	Meca-367	purified
Rat anti-mouse VCAM-1 [1]	429 (MVCAM.A)	purified
Rabbit anti-mouse Laminin [2]	polyclonal	purified
Rabbit anti-human CD3 [3]	polyclonal	purified
Rat anti-mouse F4/80 [4]	BM8	purified
Secondary antibodies		
Donkey anti-rat IgG [5]	polyclonal	Alexa Fluor 488
Donkey anti-rat IgG [5]	polyclonal	Alexa Fluor 555
Donkey anti-rat IgG [6]	polyclonal	Biotin
Donkey anti-Rabbit IgG [6]	polyclonal	Biotin

2.3 Reagents and chemicals

Media, buffer & supplements	
β-mercaptoethanol	Sigma-Aldrich, Steinheim, Germany
Bovine serum albumin (BSA)	Sigma-Aldrich, St. Louis, Germany
Dulbecco's	PAA Laboratories, Pasching, Austria
Phospate-buffered saline (PBS)	
Fetal calf serum (FCS)	Biochrom AG, Berlin, Germany
L-glutamine	Life Technologies, Carlsbad, USA

continued on next page ...

Penicillin/streptomycin (10,000 U, 10 mg/ml)	Biochrom AG, Berlin, Germany
RPMI Media 1640	Life Technologies, Carlsbad, USA
Staining reagents	
Carboxyfluorescein succinimidyl ester (CFSE)	Life Technologies, Carlsbad, USA
4',6-diamidino-2-phenylindole (DAPI)	Roche Applied Science, Penzberg, Germany
Eosin	Merck, Darmstadt, Germany
Haematoxylin	Merck, Darmstadt, Germany
Propidium iodide (PI)	Sigma-Aldrich, Taufkirchen, Germany
Trypan blue	Biochrom AG, Berlin, Germany
Reagents for cell stimulation	
Brefeldin A	Sigma-Aldrich, Taufkirchen, Germany
Ionomycin	Sigma-Aldrich, Taufkirchen, Germany
Phorbol 12-myristate 13-acetate (PMA)	Sigma-Aldrich, Taufkirchen, Germany
Protein Transport Inhibitor Cocktail	eBioscience, San Diego, USA
Saponin	Sigma-Aldrich, Taufkirchen, Germany
SIINFEKL $OVA_{257\text{-}264}$	Institute Biochemistry, HU Berlin
Histology	
Formaldehyde solution 4% buffered (pH 6.9)	Herbeta Arzneimittel, Berlin, Germany
Kaisers glycerol gelatin	Merck, Darmstadt, Germany
ParaplastPlus	McCormick Scientific, St. Louis, USA
Pro Taqs Clear	Quartett, Berlin, Germany
Roti-Histol	Roth, Karlsruhe, Germany
Tissue-Tek Compound	Sakura Finetek, Torrence, USA
Liposome-preparation	
Cholesterol	Avanti Polar Lipids, Alabaster, USA

continued on next page ...

Clodronic acid salt	Gift from Roche Diagnostics, Mannheim, Germany
L-α-Phosphatidylcholine	Avanti Polar Lipids, Alabaster, USA
Enzymes	
Collagenase Type IV	Sigma-Aldrich, Taufkirchen, Germany
DNase I	Sigma-Aldrich, Taufkirchen, Germany
Proteinase K	Sigma-Aldrich, St.Louis, USA
Cell separation	
Easycoll (1.124 g/ml)	Biochrom AG, Berlin, Germany
Nycoprep	Axis-Shield, Oslo, Norway
Reagents for DNA & RNA	
Agarose	Serva, Electrophoresis GmbH, Heidelberg, Germany
Chloroform	Merck, Darmstadt, Germany
RNApro Solution	MP Biomedicals, Illkirch, France
TRIzol	Life Technologies, Carlsbad, USA
100bp Plus DNA ladder	Invitrogen, Karlsruhe, Germany
Other chemicals & reagents	
Acetic acid	Merck, Darmstadt, Germany
Ammonium chloride (NH_4Cl)	Merck, Darmstadt, Germany
Sodium [^{51}Cr] chromate	GE Healthcare, Munich, Germany
Dimethyl sulfoxide (DMSO)	IC-Biochemicals, Ohio, USA
Diphtheria toxin	Sigma-Aldrich, Taufkirchen, Germany
Ethanol	Avantor Performance Materials, Deventer, Netherlands
Ethylenediaminetetraacetic acid (EDTA)	Merck, Darmstadt, Germany
Glycerol	Sigma-Aldrich, St.Louis, USA
Potassium bicarbonate ($KHCO_3$)	Merck, Darmstadt, Germany
2-Propanol	Merck, Darmstadt, Germany
Sodium chloride (NaCl)	Merck, Darmstadt, Germany

continued on next page ...

Sodium dodecyl sulfate (SDS)	Roth, Karlsruhe, Germany
TRIS Base	Calbiochem, La Jolla, USA

2.4 Buffers, media and solutions

Name	**Ingredients**
Digestion medium	RPMI 1640 10 % FCS (v/v) 0.05 % Collagenase Type IV
Erylysis buffer, pH = 7.3	150 mM NH_4Cl 1 mM $KHCO_3$ 0.1 mM EDTA
PBS/BSA	PBS 0.5% BSA 2mM EDTA
PBS/FCS	PBS 1% FCS
RPMI complete	RPMI 1640 10 % FCS (v/v) 2 mM L-glutamine 100 U/ml penicillin/streptomycin 50 µM β-mercaptoethanol
TAE buffer, pH = 8	40 mM Tris 1 mM EDTA 20 mM acetic acid
Tail lysis buffer, pH = 8.5	100 mM Tris 10 mM EDTA 200 mM sodium chloride 0.2 % SDS

2.5 Kits

Product	Company
CD11b Micro Beads	Miltenyi, Bergisch Gladbach, Germany
CD11c Micro Beads	Miltenyi, Bergisch Gladbach, Germany
$CD8^+$ T Cell Isolation Kit	Miltenyi, Bergisch Gladbach, Germany
Dako Detection System, AP/Red	Dako, Glostrup, Denmark
ENZO RNA Transcript Labeling Kit	Affymetrix, Santa Clara, USA
FastRNA Pro Green Kit	MP Biomedicals, Illkirch, France
GeneChip 3´IVT Express Kit	Affymetrix, Santa Clara, USA
Pellet Paint Co-Precipitant	Novagen, Madison, USA
Red Load Taq Master	Jena Bioscience, Germany
RNeasy Mini Kit	Qiagen, Hilden, Germany
SsoFast EvaGreen Supermix	Bio-Rad Laboratories, Hercules, USA
SuperScript III Reverse Transcriptase KIT	Life Technologies, Carlsbad, USA

2.6 Equipment

Centrifuges	
Centrifuge 5415R	Eppendorf, Hamburg, Germany
Rotina 420R	Hettich, Tuttlingen, Germany
SIGMA 2K15	Braun Biotec, Melsungen, Germany
Incubators	
Incubator C2000	Labotect, Göttingen, Germany
Thermomixer compact	Eppendorf, Hamburg, Germany
Thermoshake	Gerhardt, Königswinter, Germany
Waterbath Julabo U3	Julabo, Seelbach, Germany

continued on next page ...

Flow cytometer & cell sorter	Becton Dickinson, Heidelberg, Germany
FACS Calibur flow cytometer	
FACS Canto II flow cytometer	
FACS Aria I cell sorter	
FACS Aria II cell sorter	
Equipment for histology	
Cryostat 2800 Frigocut E	Reichert-Jung, Nussloch, Germany
Embedding station	Microm, Walldorf, Germany
Hypercenter XP Tissue Processor	Shandon, Frankfurt, Germany
Microtome HM355S	Microm, Walldorf, Germany
Microscopes	Carl Zeiss, Jena, Germany
AxioImager Z1 microscope & AxioCam MRm	
Axiophot & AxioCamHRc	
Axiovert 25	
MACS Separation	Miltenyi, Bergisch Gladbach, Germany
MACS Multistand	
MidiMacs Separation Unit	
MiniMacs Separation Unit	
LS Column	
MS Column	
Equipment for DNA & RNA	
ABI Prism 7500 Sequence Detection System	Foster City, Applied Biosystems, USA
Agarose Gel Electrophoresis Systems	Bio-Rad Laboratories , München, Germany
Agilent 2100 Bioanalyzer	Agilent Technologies, Waldbronn, Germany
Electrophoresis power supply	Consort, Turnhout, Belgium
GeneChip Fluidics Station 450	Affymetrix, Santa Clara, USA
GeneChip Hybridization Oven 640	Affymetrix, Santa Clara, USA

continued on next page ...

GeneChip Scanner 3000	Affymetrix, Santa Clara, USA
NanoDrop ND-1000	NanoDrop Technologies, Wilmington, Germany
Robo Cycler Gradent 96	Stratagene, La Jolla, USA
Thermocycler GeneAmp PCR System 96000	PerkinElmer, Waltham, USA
UV-transilluminator	Bioblock Scientific, Illkirch, France
Benchtop homogenizer	MP Biomedicals, Santa Ana, USA
Other Equipment	
Clean bench LaminAir 2448	Heraeus Instruments, Hanau, Germany
Wizard γ-counter	Wallac, Turku, Finland
Sonorex sonicator	Bandelin, Berlin, Germany

2.7 General consumables

Tubes	
PCR-Softtubes	Biozym, Oldendorf, Germany
15 / 50 ml Polypropylene tubes	BD Falcon, Bedford, USA
5 ml Polystyrene tubes	BD Falcon, Bedford, USA
1.5 / 2 ml Reaction tubes	Eppendorf, Hamburg, Germany
1.5 / 2 ml Reaction tubes	Sarstedt, Nümbrecht, Germany
Filter	
Filter 70µm	BD Falcon, Bedford, USA
Pre-Separation Filter, 30 µm	Miltenyi, Bergisch Gladbach, Germany
Bottle-Top-Filter	Nalgene, Rochester, USA
Tips & pipets	
5 / 10 / 25 ml cell-culture pipets	BD Falcon, Bedford, USA
Sterilized Filter Tips	Biozym, Oldendorf Germany
Tips	Sarstedt, Nümbrecht, Germany
For histology	

continued on next page ...

Capillary Gap(microscope slide)	Dako, Glostrup, Dänemark
Coverslip (24 x 32 mm)	Menzel-Gläser, Braunschweig, Germany
Disposable Microtome Blades Typ R 35	Feather, Osaka, Japan
SuperFrost Plus Coverslip	Langenbrinck, Emmendingen, Germany
Tissue-Tek cassettes	Langenbrinck, Emmendingen, Germany
Other consumables	
Hematocrite-Capillaries	Hettich, Tuttlingen, Germany
Neubauer counting chamber	LO-Laboroptik GmbH, Friedrichsdorf
Set of instruments	Aesculab AG, Tuttlingen
Plasmatube (Lithium-Heparin)	Kabe Labortechnik, Nümbrecht, Germany
Syringes & cannulas, Discardit, Microlance	BD, Heidelberg, Germany
96-well plates	BD Falcon, Bedford, USA

2.8 Primer

Table 3: Primer for genotyping by PCR. Primer were generated by ABI Primer express 2.0 software and synthesized by TIP Molbiol company.

Name	Sequence	Fragment
TF-OVA	F: 5'-CAAGCACATCGCAACCA-3' R: 5'-GCAATTGCCTTGTCAGCAT-3'	480 bp
iFABP-OVA	F: 5'-GCCATCACACTTGACCCTAA-3' R: 5'-TCAGGCAACAGCACCAACAT-3'	608 bp
CD11cDTR	F: 5'-GCCACCATGAAGCTGCTGCCG-3' R: 5'-TCAGTGGGAATTAGTCATGCC-3'	625 bp

Table 4: Primer for qRT-PCR. Primer were generated by ABI Primer express 2.0 software and synthesized by TIP Molbiol company.

Name	Sequence
*Rpl*4	F: 5'-GTGGGCATGTGGGCCGTTTCT-3' R: 5'-GCGATGAATCTTCTTGCGTGGTGC-3'
Icam-1	F: 5'-AGCCTCCGGACTTTCGATCTT-3' R: 5'-AGAGGCAGGAAACAGGCCTT-3'
Madcam-1	F:5'-CCCTACCAGCTCAGCAGAGGACA-3' R: 5'-ACCCGGGCTACACCCTCGTC-3'
Vcam-1	F: 5'-GGGGGCCAAATCCACGCTTGT-3' R: 5'-AGGGAATGAGTAGACCTCCACCTGG-3'

2.9 Software

BD FACS Diva Software, BD FACS Cellquest Software, Microsoft Excel for Mac, ImageJ, Prism 5 for Mac, Photoshop CS6, Genes@work, Axio Vision, Latex, Citavi, DAVID (Database for Annotation, Visualization and Integrated Discovery).

2.10 Primary cell isolation from mouse tissue

2.10.1 Isolation of cells from lymph nodes and spleen

Lymph nodes (inguinal, superficial cervical, brachial, axillary, mesenteric, lumbar, caudal, hepatic) and spleen were collected and passed through a nylon cell strainer (70 µm) with PBS/1% FCS. After centrifugation at 500 x g, 5 min, erythrocytes were lysed using an erylysis buffer followed by an additional washing step (500 x g, 5 min, 4°C). Cells were kept at 4°C in PBS/1% FCS for further experiments.

2.10.2 Isolation of non-parenchymal cells from the liver

To isolate T cells from liver tissue for flow cytometry or to proceed with sections for microscopy, livers were perfused with PBS. After cannulation of the hepatic portal vein and perfusion with 10 ml PBS, the liver was dissected from the abdomen and the gallbladder removed.

In order to yield higher frequencies of T cells, or to isolate dendritic cells and Kupffer cells, livers were perfused with 10 ml digestion medium (RPMI, containing 0.05 % (w/v) collagenase IV). The liver was removed from the abdomen, sliced in 10 ml digestion medium and shaked in an incubation chamber (20 min, 200 rpm, 37 °C).

Livers were passed through a nylon mesh (70 µm), followed by centrifugation to remove hepatocytes and cell debris (50 x g, 3 min, 4°C). The supernatant was transferred into a new tube, pelleted (500 x g, 5 min, 4°C), and erythrocytes were lysed followed by an additional washing step (500 x g, 5 min, 4°C). Thereafter, cells diluted in 40 % Percoll were overlaid on a 70 % Percoll solution and centrifuged at 1,000 x g, 20 min, RT. Recovered cells from the interface were washed (500 x g, 5 min, 4°C), counted, and kept at 4°C in PBS/1 %FCS for further analysis.

2.11 Isolation of cell-subsets by magnetic cell separation (MACS)

2.11.1 Isolation of naïve OT-I CD8 T cells

T cells were purified from the spleen and lymph nodes of OT-I mice as described (section 2.10.1). CD8 T cells were isolated by depletion of non-CD8$^+$T cells using the CD8α^+T Cell Isolation Kit (Miltenyi Biotec) according to manufacturer's instructions. Naïve OT-I CD8 T cells were identified based on expression of the markers Vα2, CD8 and CD69, using flow cytometry. Naïve T cells with purity higher than 95% were used in further experiments.

2.11.2 Enrichment of dendritic cells and macrophages

Non-parenchymal cells from the liver and spleen were isolated as described (section 2.10.2). Dendritic cells were enriched by positive selection of CD11c$^+$ cells using CD11c MicroBeads (Miltenyi). In order to enrich macrophages, CD11b MicroBeads (Miltenyi) were used according to manufacturer's instructions.

2.12 Isolation of liver-activated and gut-activated OT-I CD8 T cells

Naïve OT-I CD8 T cells were isolated as described (section 2.11.1), labeled with the cell tracker CFSE and injected into TF-OVA and iFABP-OVA mice. After three days, proliferated CFSE$^+$CD8 T cells activated by liver-derived antigen were isolated from livers of TF-OVA mice (section 2.10.2) and purified by subsequent fluorescence activated cell sorting. OT-I CD8 T cells were referred to as "liver-activated T cells."

OT-I CD8 T cells activated by small intestine-derived antigen were isolated from mesenteric lymph nodes of iFABP-OVA mice (section 2.10.1) and sorted likewise for CFSE$^+$CD8 T cells. OT-I CD8 T cells were referred to as "gut-activated T cells."

2.13 Determination of cell numbers

10 µl of the cell suspension was diluted with trypan blue solution and transferred to a Neubauer counting chamber. Living cells (not stained blue) were counted in four outer quadrants and calculated as followed:

$$\frac{\text{cells}}{\text{ml}} = \frac{\text{counted cells}}{4} \times \text{dilution factor} \times 10^4$$

2.14 *In vivo* experiments

2.14.1 Adoptive transfer of T cells

Naïve OT-I CD8 T cells were isolated as described (section 2.11.1) and 8×10^6 T cells, diluted in 200 µl sterile PBS, were intravenously injected into the lateral tail vein of TF-OVA mice and TF-OVA×CD11cDTR mice, to induce hepatitis or into iFABP-OVA mice to induce gut-activated T cells.

2.14.2 Depletion of dendritic cells

In order to deplete dendritic cells, 4 ng diphtheria toxin (DT) per gram body weight was *i.p.* injected into TF-OVA×CD11cDTR mice. Control mice received PBS. CD11cDTR mice (Jung et al., 2002) express the simian DTR (diphtheria toxin receptor) fused to GFP (green fluorescent protein) under control of the murine CD11c promotor. Application of DT leads to systemic depletion of dendritic cells and can be followed by GFP expression, using flow cytomtry.

2.14.3 Depletion of macrophages by liposome-encapsulated clodronate

Liposome-encapsulated clodronate is used to deplete macrophages in rodents. Phagocytosis of these liposomes leads to degradation of phospholipidbilayers by lysosomal phospholipases, thereby releasing clodronate into the cytosol (van Rooijen et al., 1997). Clodronate is misleadingly recognized as cellular pyrophosphate and synthesized to a non-hydrolizable ATP (adenosine triphosphate) analog (Frith et al., 1997). The ATP analog inhibits the mitochondrial

ATP/ADP translocase, thereby initiates mitochondrial pore openings and release of molecular signals, which leads to cell death *via* apoptosis (Lehenkari et al., 2002).

Multilamellar clodronate-liposomes were prepared as described earlier (van Rooijen and Sanders, 1994) with minor modifications. A stock solution of phosphatidylcholine (100 mg/ml) and cholesterol (100 mg/ml) in chloroform was prepared. Subsequently a mixture of 860 µl phosphatidylcholine and 80 µl cholesterol was transferred into a glass vial and evaporated by nitrogen gas. The phospholipid-layer was dissolved in 10 ml clodronate (2.5 g dichloromethylene-bisphosphonate in ddH_2O) by gently shaking at room temperature and sonicated for five minutes till the solution became cloudy. After swelling the liposomes at 4°C, 1 h, they were centrifuged at 10,000 x g for 15 minutes. The clear lower phase (clodronate) was collected and kept for the next preparation. The cloudy upper phase (clodronate-encapsulated liposomes) was washed twice with sterile PBS at 25,000 x g for 30 minutes and dissolved in 4 ml PBS. Liposomes were kept for no longer than 14 days. Control-liposomes were produced in the same manner, but instead of adding clodronate sterile PBS was used. For systemic depletion of macrophages *in vivo*, 100 µl liposomes per mouse were injected intravenously into TF-OVA mice.

2.14.4 *In vivo* migration assay

To analyze T-cell trafficking *in vivo*, migration assays using radioactively labeled lymphocytes were performed (Siegmund and Hamann, 2006).

Naïve, liver-activated, and gut-activated OT-I CD8 T cells were isolated as described (section 2.11.1, 2.12) and incubated for one hour at 37°C in the presence of 20 µCi/mL ^{51}Cr (chromium) in complete RPMI. Following the exclusion of dead cells by gradient centrifugation (Nycoprep 17 %), cells were washed, and 0.8 to 1 x 10^6 T cells were injected intravenously into wild-type, TF-OVA, or iFABP-OVA mice. 20 hours after transfer, mice were sacrificed and the following organs were taken: blood, peripheral, hepatic and mesenteric lymph nodes, Peyer's patches, small and large intestine, lung, liver, and spleen. Radioactivity found within isolated tissue and the remaining body was measured using a γ-counter.

2.14.5 *In vitro* stimulation of T cells

To characterize cells for their potential to secrete cytokines, initially *in vivo* activated T cells were re-isolated from the liver, spleen or mesenteric lymph nodes and activated *in vitro*. T cells were cultured in complete RPMI at 37°C and activated in the presence of 20 nM PMA (phorbol 12-myristate 13-acetate), which is an intracellular stimulator and 1 µM ionomycin, which functions as ionophor to transport PMA into the cell. After incubation for one hour, brefeldin-A (5 µg/ml) was added to inhibit the secretion of synthesized cytokines. After an additional three hours, T cells were stained for surface markers and intracellular cytokines and analyzed by flow cytomtry.

2.14.6 *In vitro* cytolysis assay

Liver-and gut-activated OT-I CD8 T cells were isolated as described (section 2.12) and analyzed for their ability to lyse target cells. 2×10^5 activated T cells were incubated with 4×10^5 splenocytes, isolated from wild-type mice. One part of splenocytes was previously labeled with 5 µM CFSE (high) and pulsed with 1 µg/ml SIINFEKL (as target cells), whereas the other part of splenocytes was labeled with 0.5 µM CFSE (low) and left untreated for 1 h. SIINFEKL-pulsed splenocytes and control splenocytes were mixed in equal numbers and incubated with liver-and gut-activated T cells for five hours. As control, splenocytes were incubated without effector T cells. Target splenocytes were analyzed for CFSE staining and specific lysis was calculated:

$$\% \text{ specific lysis} = 100 \times \frac{\text{1-(CFSE}^{low}{}_{control}/\text{CFSE}^{high}{}_{control})}{(\text{CFSE}^{low}{}_{treated}/\text{CFSE}^{high}{}_{treated})}$$

2.15 ALT levels

The cytoplasmatic enzyme alanine aminotransferase (ALT) is mainly found in hepatocytes. An increase in ALT indicates hepatic tissue damage. To measure ALT in mice, blood was taken from the tail or submandibular vein, and transferred into plasma-collection tubes.

After centrifugation (6,000 x g, 10 min, RT) the supernatant (plasma) was stored at -20°C, until analyzed by a Roche Modular Analyzer. ALT is measured in international units/liter (U/L).

2.16 Flow cytometry

The flow cytometer is a tool to detect and count single cells passing in a stream through a laser beam. The detection of scattered light gives information about the cell size (Forward Scatter) and the granularity (Side Scatter). Further detection of the fluorescent emission of labeled antibodies is used to characterize individual cells in a mixed population. Cells were analyzed on BD FACS Calibur or FACS Canto II using the CellQuest and DIVA software.

Fluorescence-activated cell sorting (FACS) is a specialized form of flow cytometry whereby cells of particular interest are detected by their fluorescent labels and subsequently separated and sorted. Cells passing through a liquid stream are separated into single cells per droplet. Based on their fluorescent labels, cells pass an electrical charger. A subsequent opposite charge attracts charged (positive or negative) cells and diverts them into tubes. Cells were sorted on BD FACS Aria I or II Sorter.

2.16.1 Analysis of surface proteins using flow cytometry

Analysis of cells due to their expression of specific proteins was performed using fluorescently labeled antibodies. Cells were washed and dependent on experiments, 0.1 to 1×10^6 cells were labeled with fluorochrome-coupled antibodies in 100 µl PBS/1 %FCS for 20 minutes in the dark. Applied antibodies were used according to manufacturer's instructions or titrated before proceeding. When biotinylated antibodies were used, cells were additionally stained with a secondary fluorochrome-coupled streptavidin antibody, for 20 minutes. Cells were washed (500 x g, 4°C, 5 min), dissolved in 300 µl PBS/1 %FCS, and analyzed by flow cytometry.

2.16.2 Detection of intracellular proteins

After surface staining of cells, intracellular proteins may be labeled and analyzed. T cells were washed (500 x g, 4°C, 5 min), fixed and permeabilized using IC-Fixationbuffer and permeabilization buffer according to manufacturer's instructions (eBioscience). For intracellular detection cells were stained with GzmB- or IFN-γ-antibodies in permeabilization buffer (20 min, RT). After washing (500 x g, 4°C, 5 min) cells were analyzed by flow cytometry.

2.16.3 CFSE-staining

CFSE is a fluorescent dye used as cell tracker but also in proliferation assays, due to an equal inheritance of the dye to daughter cells. CFDA-SE (carboxyfluorescein diacetate succinimidyl ester) is a non-fluorescent compound, which passively diffuses into the cytoplasm of cells. When acetate groups are cleaved by intracellular esterases, the fluorescent carboxyfluorescein succinimidyl ester (CFSE) is generated, which remain intracellular. For *in vivo* proliferation assays, tracking and re-isolation of T cells, 1×10^7 T cells were labeled with 15µM CFSE (10 min, 37°C). The reaction was stopped by adding RPMI/5% FCS and centrifugation (500 x g, 4°C, 5 min).

2.17 Molecular biology techniques

2.17.1 Screening of transgenic mice by PCR

Tail biopsies were digested in 200 µl tail lysis buffer for one hour at 55°C. The reaction was stopped by incubating samples at 95°C for five minutes and diluted 1:5 with ddH_2O. The PCR was prepared in a total volume of 25 µl, containing 1µl sample, Red Load Taq Master Mix, and 10 µM primer (Tab. 3). PCR protocol:

	Temperature	Time	
Initialization	94°C	2 min	
Denaturation	94°C	30 sec	
Annealing	55°C (OVA) 62°C (DTR)	30 sec	30 cycles
Elongation	72°C	1 min	
Final elongation	72°C	10 min	
Final hold	4°C		

PCR products were separated by 1.5 % agarosis gel electrophoresis at 100 V. Pictures were taken from ethidium bromide-stained gels, visualized using UV (ultraviolet) transillumination.

2.17.2 qRT-PCR

Liver tissue was mixed with Trizol and shredded with beads in a bench-top homogenizer. After chloroform extraction, RNA was precipitated with 100 % ethanol, diluted in ddH_2O and RNA content was measured by a NanoDrop spectrophotometer. After digestion of 10 µg RNA with DNase I, cDNA was synthesized from 2 µg RNA using the SuperScript III First-Strand Synthesis System, and real-time PCR was performed with the SsoFast EVAGreen Supermix using an ABI Prism 7500 Sequence Detection System with primers (Tab. 4). Ratios of mRNA levels were normalized to the housekeeping gene *Rpl*4.

2.17.3 Microarray

Naïve, liver-activated, and gut-activated OT-I CD8 T cells were isolated as described (section 2.11.1, 2.12) and used for transcriptome analysis. RNA-Isolation, cDNA-synthesis, and *in vitro* transcription in biotinylated cRNA were performed using the GeneChip 3'IVT Express Kit (Affymetrix). DNA was removed by on-column digestion (Qiagen). The quality of RNA was determined using the Agilent 2100 Bioanalyzer, and RNA content was checked with a Nano Drop spectrophotometer. cDNA was synthesized from 300 ng RNA. cRNA was synthesized using the Enzo RNA Transcript Labeling Kit (Affymetrix). 15 µg of fragmented biotinylated cRNA was hybridized to a mouse genome 430 2.0 GeneChip (Affymetrix) in two biological replicates for each of the three groups.

Chips were washed and stained with streptavidin-phycoerythrin, and hybridized microarrays were scanned with the GeneChip Scanner 3000, using the GCOS (GeneChip Operating Software) software (both Affymetrix). Microarrays were performed with the help of Dr. Andreas Grützkau and Heidi Schliemann.

2.17.4 Microarray analysis

All relevant GCOS data plus additional t tests were uploaded to the Bioretis database (http://www.bioretis-analysis.de) and used for High Performance Chip Data Analysis (HPCDA) to filter differentially expressed probe-sets with the default query parameters (Menssen et al., 2009). The default parameters use a signal threshold and the present call rate to detect the present genes and a Bonferroni corrected Welch t test with the log 2 of fold changes (SLR; signal log ratio) and/or the increase/decrease change call rate, calculated by GCOS software with non-parametrical tests to obtain the significantly regulated genes. These parameters were validated with the Affymetrix Latin Square dataset (Menssen et al., 2009). High standard-deviations of some genes from the two chips with liver-activated T cells were noted. Due to probable contamination with RNA from liver tissue, genes were excluded using the following query conditions:

$$\frac{\text{Mean signal (liver chip 1 \& 2)}}{\text{SD}} < 2 \text{ AND}$$

$$\frac{\text{Mean signal (liver chip 1 \& 2)}}{\text{Mean signal (chip 3, 4, 5, 6)}} > 10 \text{ AND}$$

$$\text{signal of contaminated liver chip 2} > 200 \text{ AND}$$

$$\text{(signal liver chip 1 (x 3))} < \text{(signal liver chip 2) OR}$$

$$\text{(signal liver chip 2–signal liver chip 1)} > 1,000$$

With this query, 67 probe sets were excluded from the list of HPCDA significant genes. For hierarchical cluster analysis, Genes@Work (Lepre et al., 2004) was used with gene vectors for normalization, along with Pearson w/mean for similarity measure and center of mass as cluster type. For functional annotations a subset of 2,537 differentially regulated IDs was uploaded to

DAVID (Database for Annotation, Visualization and Integrated Discovery) (Huang et al., 2009). The data analysis was performed with the help of Dr. Joachim Grün.

2.18 Histological methods

2.18.1 Frozen histological sections

Perfused liver biopsies were frozen in liquid nitrogen, and stored at -80°C.Liver biopsies were embedded in Tissue-Tek and cut into 5µm frozen tissue sections using a cryotome.

2.18.2 PFA-fixed histological sections

Perfused liver biopsies were fixed in 4% PFA for 24 hours and stored in 100 % EtOH. Liver biopsies were dehydrated in a Hypercenter Tissue Processor. After paraffin-embedding, tissue was cut into 3 µm sections using a microtome, followed by deparaffinization and re-hydration using Roti-Histol and decreased alcohol concentrations.

2.18.3 Hematoxylin and eosin staining (H & E)

Hematoxylin and eosin stains are used to recognize various tissue types and morphologic changes in tissue. Liver tissue sections were incubated in haematoxylin that stains nuclei blue and eosin that colors the cytoplasm red. After rinsing in water, sections were embedded in Kaiser's glycerol gelatin.

2.18.4 Immunohistochemistry

PFA-fixed liver sections were incubated with unconjugated primary CD3, laminin and F4/80 antibodies, followed by biotinylated secondary antibodies. After incubation of streptavidin alkaline phosphatase, the target antigen is visualized by an enzyme-substrate reaction with chromogen Fast Red. Nuclei were counter stained with haematoxylin.

2.18.5 Immunofluorescence

5µm sections of cryo-preserved liver tissue were incubated with monoclonal rat antibodies against MAdCAM-1, ICAM-1, or VCAM-1, followed by incubation with donkey anti-rat Alexa488-labeled or Alexa555-labeled antibody. Nuclei were counter stained with DAPI. Negative controls were performed by omitting the primary antibodies. Immunohistochemical staining was performed with the help of Prof. Dr. Loddenkemper, Dr. Anja Kühl and, Simone Spieckermann.

2.18.6 Microscopy and analysis

Images were acquired using microscopes equipped with a camera and processed with AxioVision software (Carl Zeiss, Jena, Germany). To calculate cells or quantify the area percentage of immunohistochemical staining on liver sections, ImageJ was used. Three visual fields of $0.6\,mm^2$ of each liver section were converted into grayscale and split into red, green and blue channels. The red-stained channel was used for thresholding and percentage of thresholded area or particles were measured.

2.19 Statistical analysis

Statistical analysis was performed using GraphPad Prism software. The non-parametric two-tailed Mann-Whitney U-test was used (*$p<0.05$; **$p<0.01$; ***$p<0.001$ were considered as significant). In the case of multiple comparisons the Bonferonni-corrected Mann-Whitney U-test was used.

3 Results

3.1 Activation of CD8 T cells by antigen-presenting cells in the liver of TF-OVA mice

TF-OVA mice express the antigen ovalbumin in hepatocytes and adoptive transfer of antigen-specific naïve OT-I CD8 T cells induces hepatitis. Reconstitution of TF-OVA mice with MHC class I-deficient bone marrow revealed that professional APCs are incapable of presenting ovalbumin to naïve CD8 T cells. Accordingly, cells not derived from bone marrow, such as hepatocytes and LSECs, failed to induce effector T cells and indicating that professional APCs are essential to induce effector CD8 T cells in the liver (Derkow et al., 2007).

Several professional and non-professional APCs, such as liver DCs, KCs, and LSECs are capable of phagocytosis of cell debris from hepatocytes. These cells ingest liver-derived ovalbumin, process it and cross-present it to naïve OT-I CD8 T cells, leading to their proliferation *in vitro* (Derkow et al., 2011).

It remains to be determined, which professional APC in the liver is required for efficient activation of naïve CD8 T cells *in vivo*. Therefore, experiments that analyzed the role of KCs and hepatic DCs are described in the following chapters.

3.1.1 TF-OVA×CD11cDTR mice as a model to study the influence of dendritic cells in liver inflammation

TF-OVA mice were crossed to CD11cDTR mice (Jung et al., 2002) to analyze the role of DCs during liver inflammation. CD11cDTR mice express the primate DTR (diphtheria toxin receptor) fused to GFP (green fluorescent protein) under control of the murine CD11c promotor. Intraperitoneal injection of DT (diphtheria toxin) systemically depletes $CD11c^{+}GFP^{+}$DCs.

To estimate the extent and duration of DC depletion in the liver and spleen, TF-OVA×CD11cDTR mice received a single injection of DT. Within 24 hours

the administration of DT led to rapid depletion of $CD11c^+GFP^+$DCs in the liver as well as in the spleen (Fig. 1 A). The absence persisted for 48 hours, after which liver and splenic DCs rejuvenated to original numbers (Fig. 1 B).

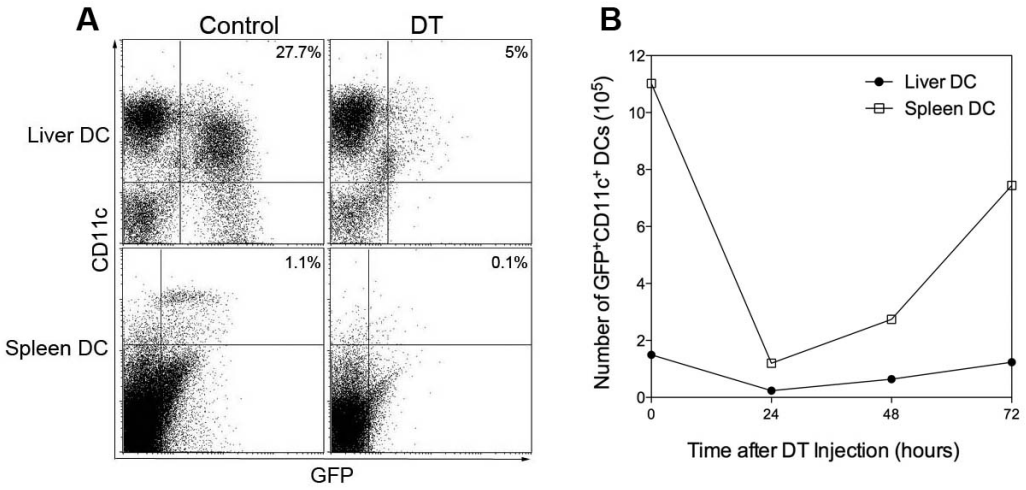

Figure 1: Depletion of dendritic cells in the liver and spleen. TF-OVA×CD11cDTR mice received a single injection of diphtheria toxin (DT). A) Spleen cells and CD11c-enriched liver cells were stained with anti-CD11c antibody followed by flow cytometric analysis. Shown are dot plots of GFP^+CD11c^+cells in the liver and spleen, 24 hours after DC depletion compared to untreated control. B) Spleen and liver cells were isolated 24, 48, and 72 hours after DC depletion, counted and stained with anti-CD11c antibody. Numbers of GFP^+CD11c^+DCs in the liver and spleen are depicted. Each value at each time point represents an individual mouse.

In summary, TF-OVA×CD11cDTR mice provide a useful model to study liver inflammation in the absence of DCs. However, as previously reported, multiple injections of DT leads to the lethality of these mice (Jung et al., 2002; Zaft et al., 2005). Therefore, DCs were depleted every two days and hepatitis was analyzed for four days, in further experiments.

3.1.2 Dendritic cells are required for the activation of self-reactive CD8 T cells in the liver

To analyze whether absence of DCs influences liver inflammation, OT-I CD8 T cells were transferred into TF-OVA×CD11cDTR mice to induce hepatitis. Dendritic cells were depleted one day before and two days after T-cell transfer.

The absence of DCs ameliorated the hepatitis, indicated by reduced alanine aminotransferases (ALT levels), an enzyme that is released into the serum when

hepatocytes are destroyed. This reduction was not significant possibly due to increased background ALT levels in mice that were DC-depleted only (Fig. 2 A). In addition, the absence of DCs led to decreased numbers of IFN-γ-producing OT-I CD8 T cells in the liver and spleen compared with non-depleted mice (Fig. 2 B).

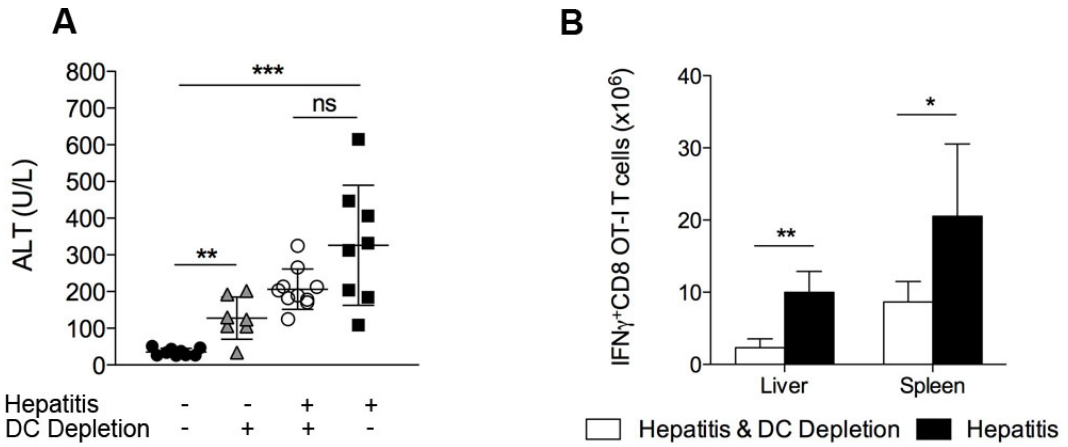

Figure 2: The absence of DCs ameliorates hepatitis. Transfer of naïve OT-I CD8 T cells into TF-OVA×CD11cDTR mice induced hepatitis. Diphtheria toxin was injected *i.p.* one day before and two days after the induction of hepatitis. The degree of liver inflammation and T-cell activation was analyzed on day four. A) Dot Plot depicts ALT levels ± SD (alanin aminotransferase levels) measured in serum from n≥7 mice in three separate experiments. ** p≤0.003, *** p≤0.0003, ns = not significant; Bonferroni-corrected Mann-Whitney test. B) The number of interferon-γ producing OT-I CD8 T cells in the liver and spleen were identified by *ex vivo* stimulation with PMA/ionomycin. Two pooled experiments (n = 6, mean ± SD) are shown. * p≤0.05, ** p≤0.01; Mann-Whitney test.

In conclusion, the absence of DCs led to ameliorated hepatitis and reduced effector function of OT-I CD8 T cells in the liver and spleen. That implies that the liver-derived ovalbumin is cross-presented by hepatic and splenic dendritic cells, which leads to efficient activation of naïve OT-I CD8 T cells, in early stages of hepatitis.

3.1.3 Livers of DC-depleted mice display diminished infiltration of T cells

Liver sections were analyzed to determine tissue damage and hepatic infiltration of inflammatory cells in DC-depleted TF-OVA×CD11cDTR mice.

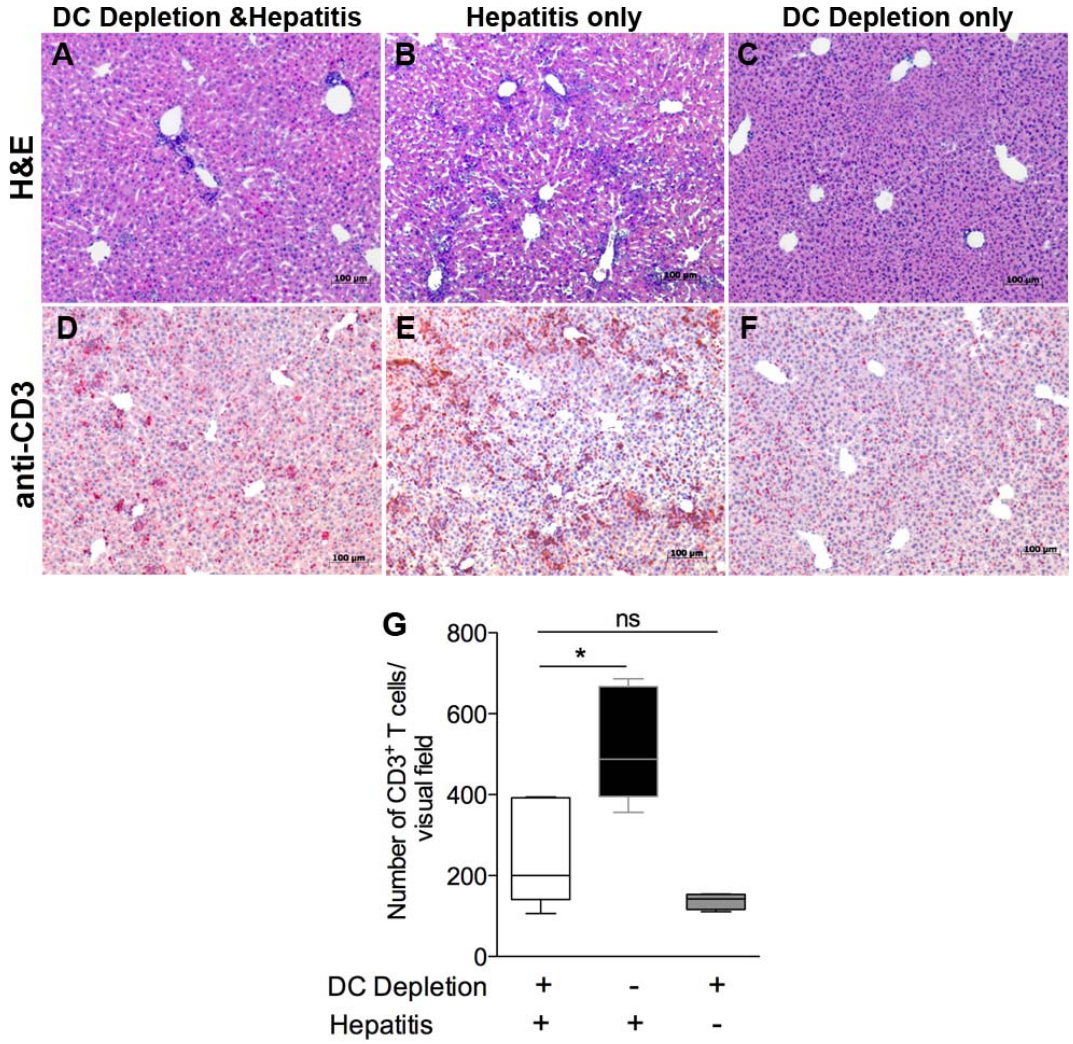

Figure 3: Histological analysis of liver sections in TF-OVA×CD11cDTR mice. Experiments were performed as described in figure 2). Liver sections were stained with H&E (haematoxylin and eosin) (A, B, C). To identify T cells, immunohistochemical stainings with anti-CD3 were performed (D, E, F). Representative images of six mice per group are shown (scale bar = 100 µm, magnification 100×). G) Box Plot depicts the number of $CD3^+$T cells in liver sections quantified by counting three visual fields (0.6 mm^2) of each liver section using the software ImageJ of n = 6 mice. * $p \leq 0.025$, ns = not significant; Bonferroni-corrected Mann-Whitney test.

The induction of hepatitis led to portal, periportal and lobular infiltration of immune cells into the liver (Fig. 3 B). Depletion of DCs led to decreased infiltration of immune cells (Fig. 3 A) as compared with untreated mice (Fig. 3 C). To estimate T cells within the repertoire of immune cells in the liver, anti-CD3 staining was performed (Fig. 3 D, E, F). Reduced numbers of $CD3^+$T cells were detected and quantified in DC-depleted mice suffering from hepatitis, compared

with non-depleted mice (Fig. 3 G).

Thus, liver inflammation is diminished in the absence of dendritic cells, characterized by reduced T-cell numbers.

3.1.4 Depletion of macrophages by clodronate liposomes

Clodronate encapsulated liposomes provide a tool to deplete macrophages in mice. To determine the efficiency of macrophage depletion, TF-OVA mice received a single injection of clodronate liposomes. Liver and spleen were analyzed for the presence of $CD11b^+F4/80^+$macrophages for three consecutive days.

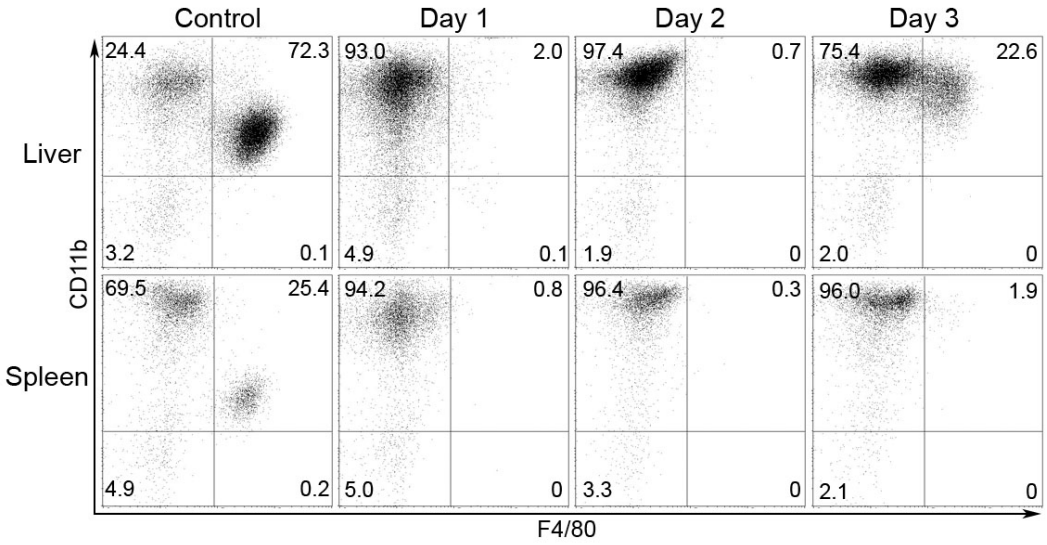

Figure 4: Depletion of macrophages in the liver and spleen by administration of clodronate liposomes. TF-OVA mice received a single intravenous injection of clodronate encapsulated liposomes. On day 1, 2, and 3, liver cells and spleen cells were isolated from macrophage-depleted and untreated mice. Liver cells were additionally enriched by anti-CD11b magnetic beads, as described in methods. Depicted are representative dot plots and percentage of liver and spleen cells, positive for F4/80 and CD11b, analyzed by flow cytometry (n = 2).

Figure 4 shows efficient depletion of $CD11b^+F4/80^+$macrophages in the liver and spleen for two days, compared with the untreated control. After three days macrophage-population recovered in the liver, whereas splenic macrophages remained depleted.

In summary, the absence of Kupffer cells in the liver, after a single depletion, lasted for two days. After that time, $F4/80^+$ macrophages, evolving from a

$CD11b^+$cell population, repopulated the liver. Accordingly, in further experiments, clodronate liposomes were administered every two days to ensure the depletion of Kupffer cells.

3.1.5 The intensity of hepatitis is increased after Kupffer cell depletion

To study the effect of KC depletion on liver inflammation, naïve OT-I CD8 T cells were transferred into TF-OVA mice. In addition, macrophages were depleted by clodronate liposome-injections every two days.

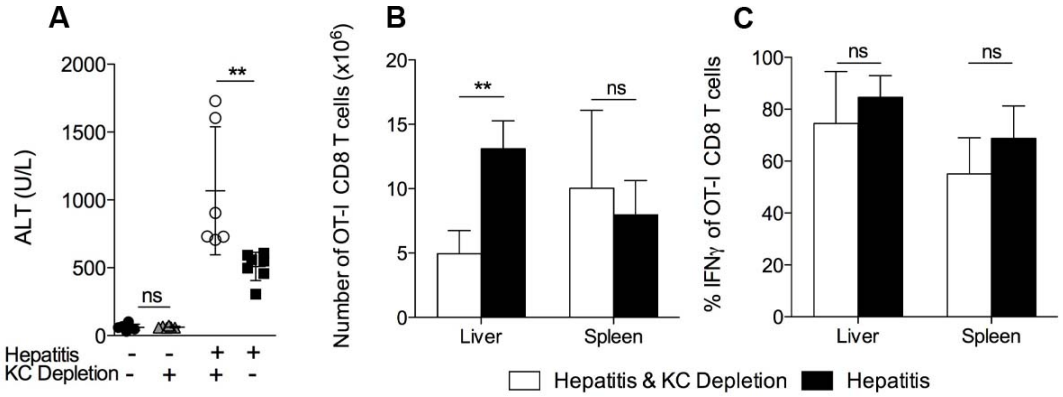

Figure 5: The intensity of hepatitis was increased in the absence of Kupffer cells. Hepatitis was induced by transfer of naïve OT-I CD8 T cells into TF-OVA mice. Clodronate liposomes were injected at day 0 and 3. A) Dot plot depicts ALT levels ± SD in the serum of mice determined on day five. ** $p \leq 0.005$, ns = not significant; Bonferroni-corrected Mann-Whitney test. B) The number of antigen-specific OT-I CD8 T cells in the liver and spleen were determined by flow cytometry and cell count. C) The effector function of CD8 T cells in the liver and spleen was measured by their ability to produce IFN-γ after *in vitro* stimulation with PMA/ionomycin. Results are shown from two independent experiments (n = 6, mean ± SD). ** $p \leq 0.01$, ns = not significant; Mann-Whitney test.

Within five days, the induction of hepatitis led to liver damage, as indicated by increased serum ALT levels. The additional depletion of KCs increased the severity of hepatitis, whereas the depletion of KCs alone did not alter the ALT levels (Fig. 5 A). Decreased numbers of antigen-specific OT-I CD8 T cells were detected in the liver of KC-depleted mice. However, T-cell numbers in the spleen remained similar (Fig. 5 B). By measuring the pro-inflammatory cytokine interferon-γ it was determined whether KC depletion influences the generation of effector CD8 T cells. Independent of the presence of KCs, the ability of OT-I CD8 T cells to produce this cytokine remained similar in liver

and spleen (Fig. 5 C).

Thus, Kupffer cell depletion led to more severe hepatitis, although less antigen-specific CD8 T cells were recovered from liver. The data suggest that Kupffer cells may play a role in priming tolerogenic T cells.

3.1.6 Kupffer cell-depleted mice display reduced numbers of CD3$^+$T cells in the liver

Hepatitis was induced in TF-OVA mice and Kupffer cells were depleted as described (section 2.14.3). Liver sections were analyzed for the presence of tissue damage, inflammatory cells, and Kupffer cells.

The induction of hepatitis led to similar portal, periportal, and lobular infiltration of leukocytes into the liver, independent of the absence of KCs (Fig. 6 A, B). Infiltrating cells observed in the liver of KC-depleted mice did not consist primarily of T cells. In fact, decreased CD3$^+$T-cell infiltration was observed in KC-depleted mice (Fig. 6 D, J), as compared with control mice (Fig. 6 E, J). The absence of Kupffer cells in livers of clodronate liposome-treated mice was confirmed by anti-F4/80 staining, a marker for macrophages (Fig. 6 G, I). No leukocyte infiltration or tissue damage has been observed in livers of mice that were KC-depleted only, suggesting that clodronate liposomes do not harm the liver (Fig. 6 C, F, J).

In summary, the absence of Kupffer cells in mice suffering from hepatitis led to reduced infiltration of CD3$^+$T cells.

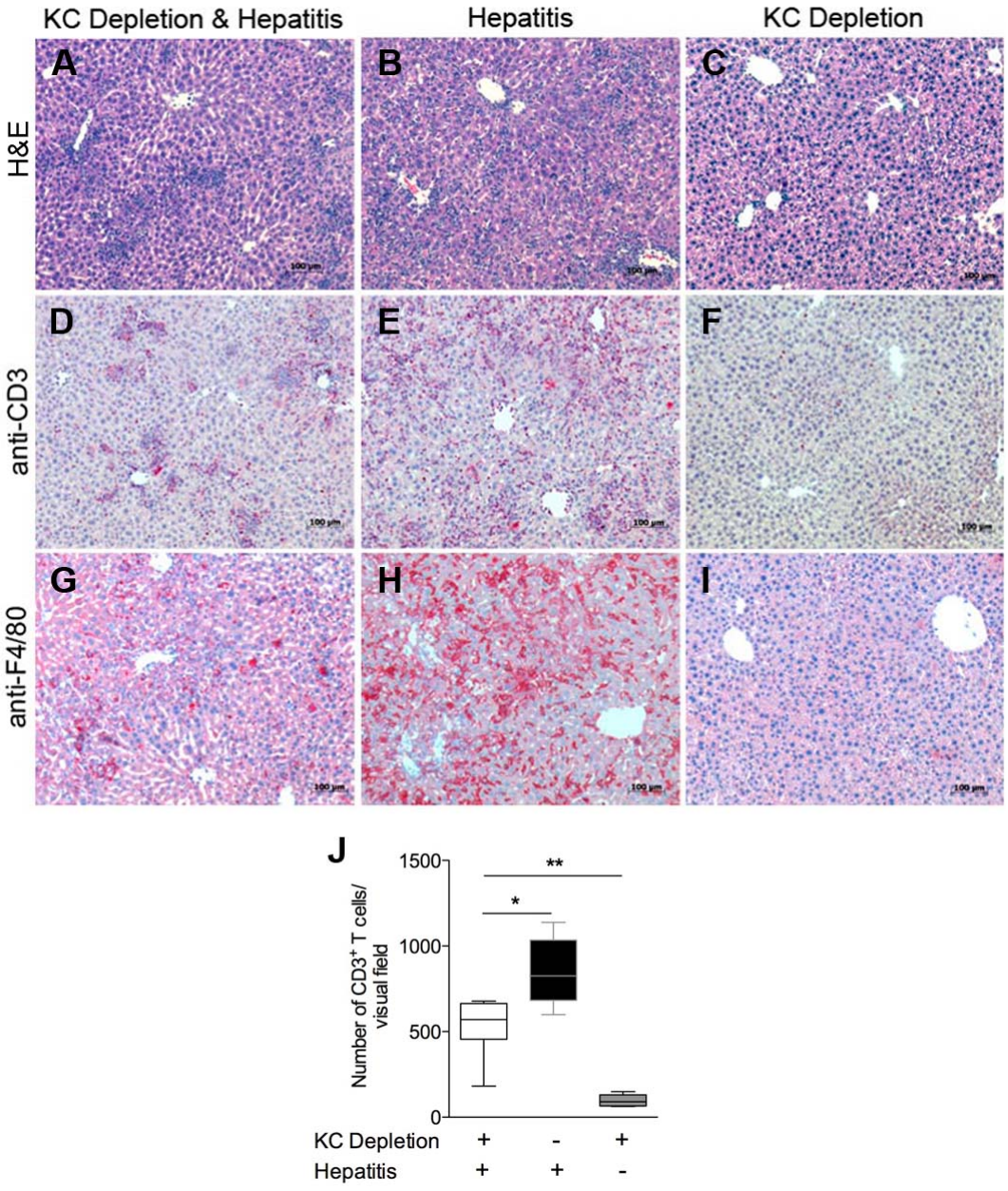

Figure 6: Histological analysis of liver sections in Kupffer cell-depleted TF-OVA mice. The experiment was performed as described in figure 5. A, B, C) Livers sections were stained with H&E (haematoxylin and eosin). D, E, F) Immunohistochemical stainings with anti-CD3 antibody were performed to indicate T cells or G, H, I) stainings with anti-F4/80 antibody to confirm the absence of KCs. Depicted are representative images of six mice per group (scale bar = 100µm, magnification 100×). J) Box plot depicts the number of $CD3^+$T cells quantified by counting three visual fields (0.6 mm^2) per section of two independent experiments (n = 6), using ImageJ. * $p \leq 0.025$, ** $p \leq 0.005$; Bonferroni-corrected Mann-Whitney test.

3.2 Migration patterns of liver-activated CD8 T cells compared to naïve and gut-activated T cells

Naïve T cells circulate through blood and secondary lymphoid organs. Once they encounter their specific antigen, they become activated and migrate into tissues towards the site of inflammation. Gut-specific migration requires tissue-specific adhesion molecules as well as appropriate receptors on the T-cell surface. Little is known about T-cell migration into the liver, or the migration behavior of T cells activated by liver-derived antigen. Therefore, *in vivo* migration-assays with naïve, liver-activated, and gut-activated OT-I CD8 T cells were performed.

In the following sections the terms "liver-activated" and "gut-activated" T cells are used. TF-OVA mice express the antigen ovalbumin in hepatocytes (liver). OT-I CD8 T cells injected into TF-OVA mice were activated in the liver and re-isolated from livers (liver-activated). iFABP-OVA mice express the antigen ovalbumin in enterocytes of the small intestine and OT-I CD8 T-cell transfer leads to their activation in the GALT (gut-associated lymphoid tissue). Gut-activated T cells were re-isolated from mesenteric lymph nodes of iFABP-OVA mice.

3.2.1 Migration of naïve OT-I CD8 T cells in mice expressing ovalbumin in the liver or in the small intestine

To analyze how the presence of the antigen ovalbumin influences the migration of naïve T cells, radioactively labeled naïve OT-I CD8 T cells were transferred into TF-OVA, iFABP-OVA, or wild-type mice. The amount of radioactivity recovered from a specific organ correlates with the number of T cells found to have migrated into this organ.

Naïve OT-I CD8 T cells migrated mainly to the secondary lymphoid organs in wild-type mice. In contrast, the vast majority of OT-I CD8 T cells migrated into the liver in TF-OVA mice in which the antigen was expressed in hepatocytes. OT-I CD8 T cells transferred into iFABP-OVA mice displayed similar migration patterns to the ones seen in wild-type mice and no preferential migration to the site of antigen expression – neither in the small intestine nor in the associated lymphoid structures – was observed (Fig. 7).

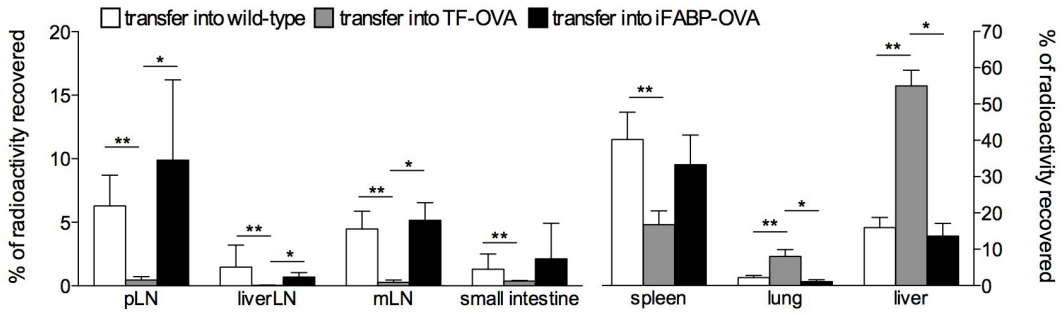

Figure 7: Migration of naïve OT-I CD8 T cells in mice expressing ovalbumin in the liver or in the small intestine. Naïve OT-I CD8 T cells were labeled with ^{51}Chromium and injected intravenously into wild-type, TF-OVA, and iFABP-OVA mice. Radioactivity was measured in the indicated organs 20 hours after transfer (mLN, mesenteric lymph node; pLN, peripheral lymph node). The percentage of recovered radioactivity is shown from three pooled experiments ($n \geq 5$, mean $\pm$ SD). * $p \leq 0.016$, ** $p \leq 0.003$; Bonferroni-corrected Mann-Whitney test. Note the different scales for large and small organs.

Thus, presence of the antigen in the liver but not in the small intestine, leads to accumulation of naïve OT-I CD8 T cells at the site of antigen presentation. This suggests that the antigen is accessible to naïve T cells in the liver but not in the gut.

3.2.2 Migration of liver-activated OT-I CD8 T cells compared to naïve and gut-activated T cells in wild-type mice

It is known that T cells primed in the GALT preferentially migrate to the gut. Whether T cells activated in the liver display organ-specific migration behavior was analyzed in the following experiment: Liver-activated OT-I CD8 T cells were transferred into wild-type mice. The influence of T-cell priming in the liver on migration was compared to naïve and gut-activated OT-I CD8 T cells.

Naïve and liver-activated OT-I CD8 T cells mostly migrated to the secondary lymphoid organs. In contrast, gut-activated OT-I CD8 T cells migrated to the small intestine, and less recirculation to lymph nodes was observed. Activated T cells accumulated in the livers of wild-type mice, irrespective of the site of priming. Increased migration to the liver of gut-activated T cells compared to liver-activated T cells was observed (Fig. 8).

In summary, OT-I CD8 T cells activated in the gut-associated lymphoid tissues are licensed to migrate to the gut, while liver-activated OT-I CD8 T cells

are not. In contrast, liver-activated CD8 T cells retain their ability to circulate through the lymph nodes. Gut-activated CD8 T cells accumulated in the liver to a larger extent than their liver-primed counterparts.

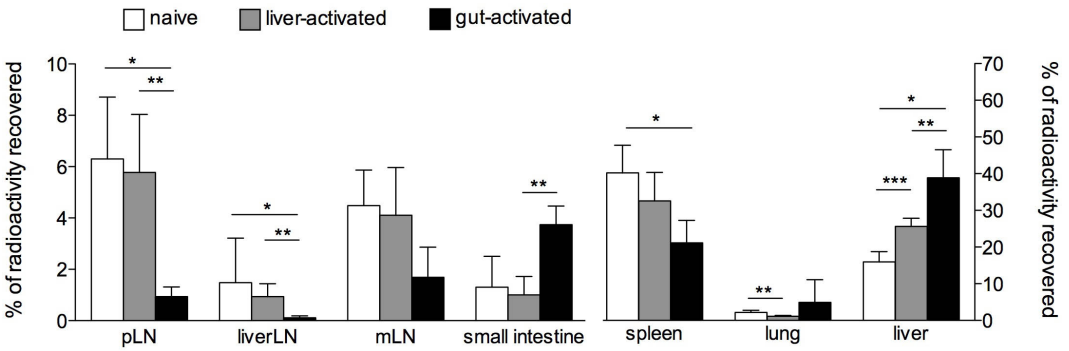

Figure 8: Migration of liver-activated OT-I CD8 T cells in wild-type mice, compared to naïve and gut-activated T cells. Naïve, liver-activated or gut-activated OT-I CD8 T cells were labeled with ^{51}Chromium and transferred into wild-type mice. Radioactivity was measured in the indicated organs 20 hours after transfer (mLN, mesenteric lymph node; pLN, peripheral lymph node). The percentage of recovered radioactivity is shown from three pooled experiments ($n \geq 5$, mean $\pm$ SD). * $p \leq 0.016$, ** $p \leq 0.003$, ** $p \leq 0.0003$; Bonferroni-corrected Mann-Whitney test. Note the different scales for large and small organs.

3.2.3 Migration of liver-activated OT-I CD8 T cells in mice expressing ovalbumin in the liver or in the small intestine

The migration patterns of liver-activated T cells in the presence of ovalbumin was investigated. Liver-activated OT-I CD8 T cells were transferred into TF-OVA mice (antigen in hepatocytes), into iFABP-OVA mice (antigen in the small intestine), and into wild-type mice to analyze whether the presence of the antigen overrides the imprinted migration pattern.

Presence of the antigen in the liver led to preferential migration to the liver, while migration to lymph nodes was slightly reduced (Fig. 9 A). Liver-activated OT-I CD8 T cells transferred into iFABP-OVA mice preferentially migrated to the mesenteric lymph nodes but did not enter the small intestine (Fig. 9 B).

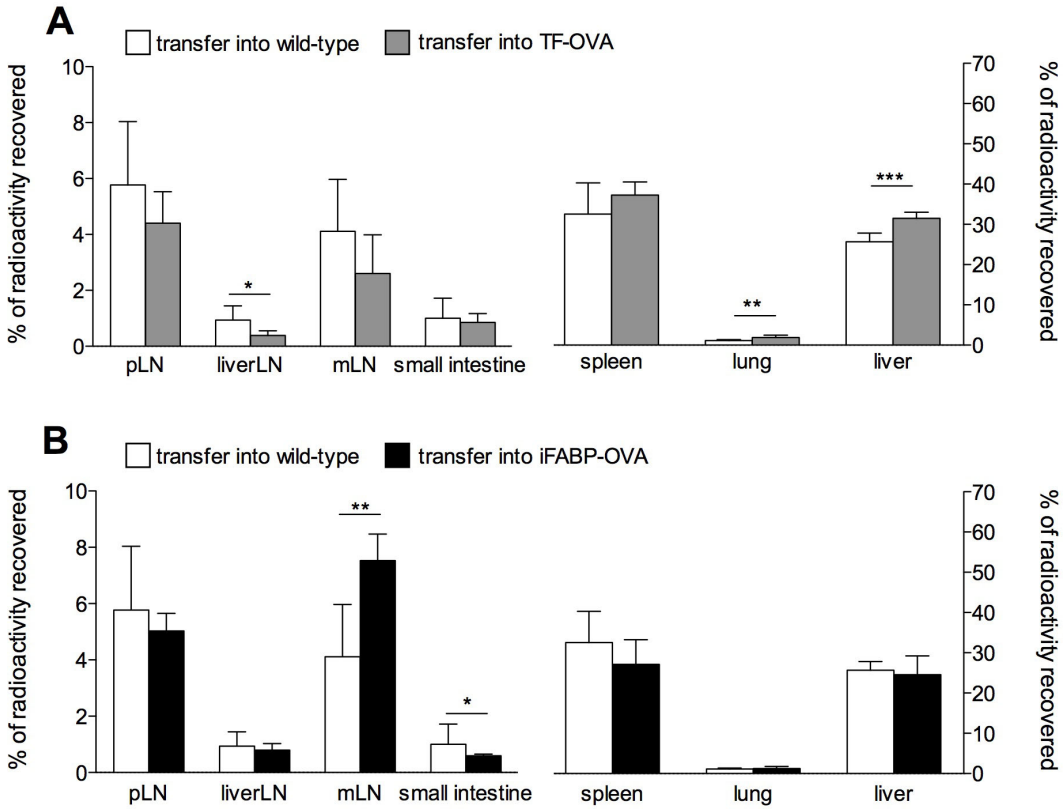

Figure 9: Migration of liver-activated OT-I CD8 T cells in mice expressing ovalbumin in the liver or in the small intestine. Liver-activated OT-I CD8 T cells were labeled with ^{51}Chromium and transferred into wild-type and TF-OVA mice (A) or into wild-type and iFABP-OVA mice (B). Radioactivity was measured in the indicated organs 20 hours after transfer (mLN, mesenteric lymph node; pLN, peripheral lymph node). The percentage of recovered radioactivity is shown from three pooled experiments ($n \geq 6$, mean $\pm$ SD). * $p \leq 0.05$, ** $p \leq 0.01$, ** $p \leq 0.001$; Mann-Whitney test. Note the different scales for large and small organs.

Thus, OT-I CD8 T cells primed in the liver displayed preferential migration towards the site of antigen expression while retaining their capacity to circulate through lymph nodes. Although activated, they were incapable of gaining access to the small intestine.

3.2.4 Migration of gut-activated OT-I CD8 T cells in mice expressing ovalbumin in the liver or in the small intestine

Finally the migration patterns of gut-activated T cells were investigated. OT-I CD8 T cells activated in the GALT were transferred into TF-OVA, iFABP-OVA, or wild-type mice.

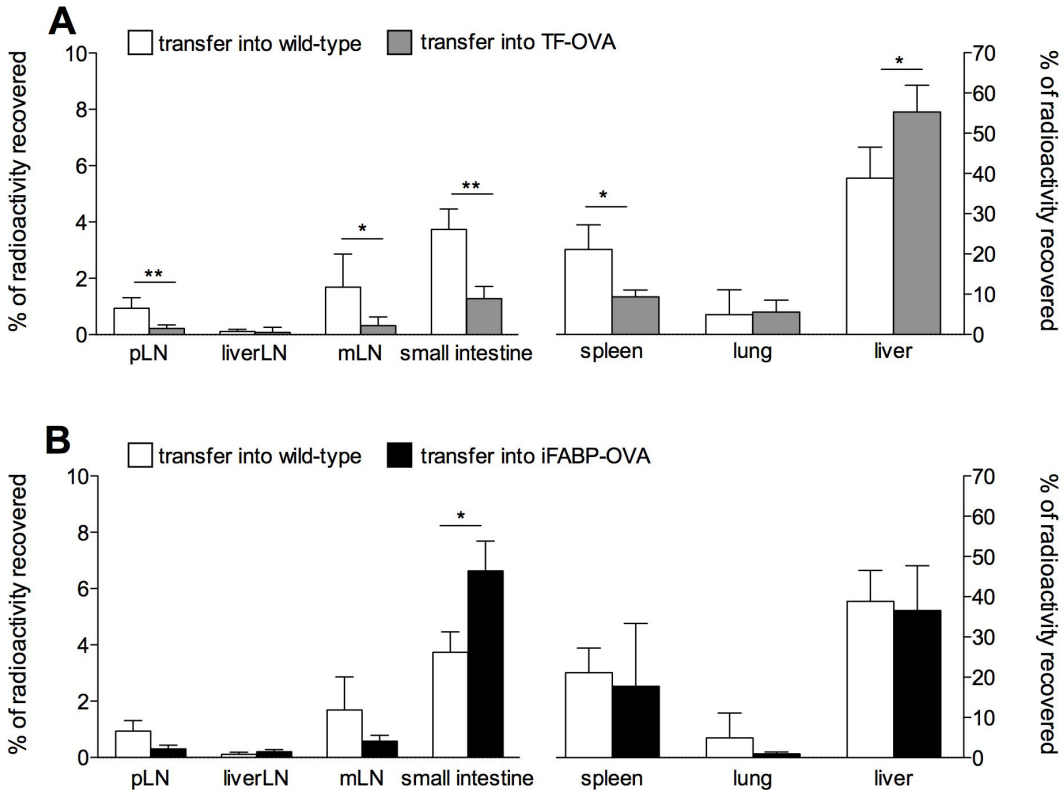

Figure 10: Migration of gut-activated CD8 T cells in mice expressing ovalbumin in the liver or in the small intestine. Gut-activated OT-I CD8 T cells were labeled with ^{51}Chromium and transferred into wild-type and TF-OVA mice (A) or into wild-type and iFABP-OVA mice (B). Radioactivity was measured in the indicated organs 20 hours after transfer (mLN, mesenteric lymph node; pLN, peripheral lymph node). The percentage of recovered radioactivity is shown from three pooled experiments ($n \geq 4$, mean $\pm$ SD). * $p \leq 0.05$, ** $p \leq 0.01$; Mann-Whitney test. Note the different scales for large and small organs.

The majority of gut-activated OT-I CD8 T cells migrated to the liver. This effect was enhanced by the presence of the antigen in the liver of TF-OVA mice. In return, decreased accumulation of gut-activated OT-I CD8 T cells in secondary lymphoid organs and in the small intestine was observed (Fig. 10 A). When the antigen was present in the small intestine of iFABP-OVA mice, increased migration to the gut was observed (Fig. 10 B).

Taken together, presence of the antigen in the liver or in the small intestine promotes the migration of gut-activated OT-I CD8 T cells towards the site of antigen expression. Further, gut-activated T cells accumulated in the livers of mice, an effect that is amplified by the expression of ovalbumin in the liver of TF-OVA mice. The gut-homing phenotype of gut-activated OT-I CD8 T cells

was overridden by the presence of the antigen in the liver (as seen in Fig. 8).

In summary, specific migration patterns are imprinted in the gut and liver, but these patterns are not stable. Licensing to the gut requires priming in the gut-associated lymphoid tissue, and liver-activated OT-I CD8 T cells are prohibited from entering the gut. Although activated, liver-primed CD8 T cells retained the ability to migrate to lymph nodes. Migration to the liver increased upon activation of CD8 T cells, and the fact that more gut-activated than liver-activated CD8 T cells accumulate in the liver suggests different stages of activation of these T-cell subsets.

3.3 Phenotype of differentially activated OT-I CD8 T cells

The migration pattern of T cells and their access to specific tissues is regulated through specific adhesion molecules and other molecules involved in trafficking. Since activation of OT-I CD8 T cells in the liver or in the gut led to differential migration patterns, the phenotype of these T cells was further characterized. Transcriptome analysis and flow cytometry were used to study the molecules that could be responsible for different migration patterns.

First, particular attention was paid to liver-activated CD8 T cells and their expression of specific molecules, which may explain the capacity to migrate through secondary lymphoid organs. Second, it was determined whether gut- and liver-activated CD8 T cells express molecular patterns that enable their migration into the opposite organ. Finally the degree of activation of liver-and gut-activated OT-I CD8 T cells was analyzed.

3.3.1 Gene expression profile of naïve, liver-activated, and gut-activated OT-I CD8 T cells

Based on the differential migration behavior of naïve, liver-activated, and gut-activated OT-I CD8 T cells, transcriptome analysis was employed to study which genes could be responsible for the different migration patterns. Gene expression profiling of naïve and activated OT-I CD8 T cells identified 10,326 differentially regulated IDs in total, as shown in figure 11 A and (Appendix Fig. 20). Each of the three circles represents one of three comparisons (7,543 IDs regulated differentially between gut-activated and naïve, 8,045 IDs regulated differentially between liver-activated and naïve and 3,226 IDs regulated differentially between gut-activated and liver-activated).

For further analysis, three groups were selected (Fig. 11 A):

- 1,081 IDs regulated differentially between all three groups
- 995 IDs regulated differentially between liver-activated and naïve T cells as well as between liver-activated and gut-activated T cells
- 528 IDs regulated differentially between gut-activated and naïve as well as between liver-activated and gut-activated T cells

This selection process resulted in a set of 2,604 differentially regulated IDs.

In this dataset of 2,604 IDs, high standard deviations of some genes from the two chips of liver-activated CD8 T cells were detected. Due to probable contamination with RNA from liver tissue, IDs were excluded (as described in methods, section 2.17.4), leaving a set of 2,537 IDs.

Hierarchical clustering of 2,537 IDs separated the samples into three main groups, discriminating naïve, liver-, and gut-activated OT-I CD8 T cells, and proved the homogeneity of biological replicates. The dendrogram shows that the relationship between naïve T cells and gut-activated is closer than the relationship between naïve and liver-activated T cells or between gut-and liver-activated T cells (Fig. 11 B).

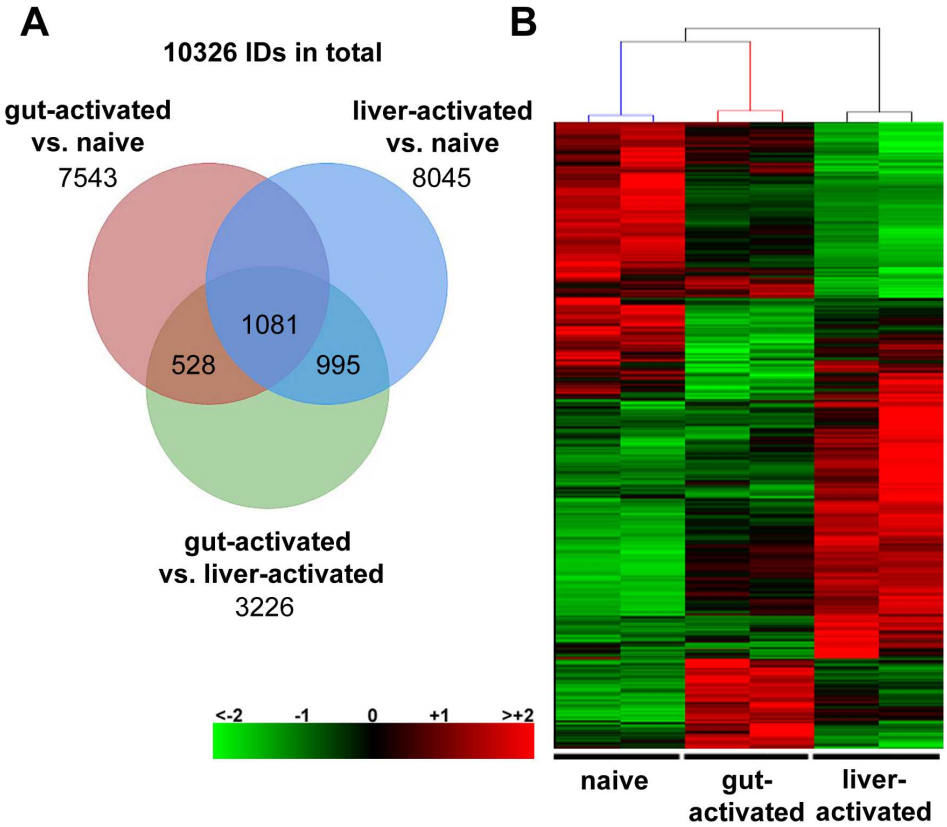

Figure 11: Gene expression profile of OT-I CD8 T cells activated in liver or gut. Gene expression profiling of purified naïve, liver-activated, and gut-activated OT-I CD8 T cells was performed in duplicates. A) Three comparisons of gut-activated T cells versus naïve T cells, liver-activated T cells versus naïve T cells and gut-activated T cells versus liver-activated T cells are visualized in a Venn diagram. B) Hierarchical clustering was performed with 2537 IDs containing the three groups, characterized in the Venn diagram, using Genes@Work.

3.3.2 Function-related groups

Based on an interest in candidate genes responsible for specific immunological processes and given a multitude of IDs, function-related gene groups were generated with a set of 2,537 IDs.

Four function-related groups of interest were selected (Fig. 12 A–D; Appendix Tab. 5, 6, 7, 8):

- 144 IDs containing genes involved in migration, adhesion molecules, and integrins
- 53 IDs containing genes involved in cytokines, chemokines and their receptors
- 87 IDs containing genes involved in T-cell activation
- 122 IDs containing genes involved in apoptosis

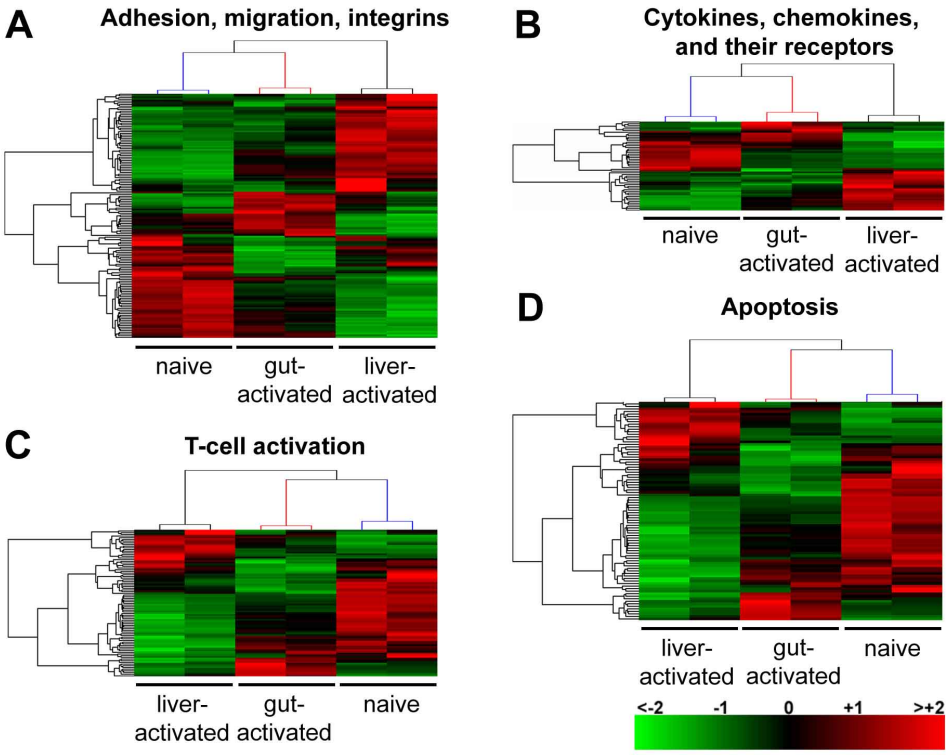

Figure 12: Hierarchical cluster analysis of function-related groups. Four functional groups were generated using the Database for Annotation, Visualization and Integrated Discovery (DAVID). Heat maps generated using Genes@Work display four functional groups: (A) Adhesion, migration and integrins, (B) Cytokines, chemokines and their receptors, (C) T-cell activation, and (D) Apoptosis.

The gene expression signature among naïve and differentially activated OT-I CD8 T cells remained different when grouped in function-related groups and restricted the number of candidate genes to a set of 406 IDs.

3.3.3 Selection of genes for protein analysis

An additional selection of specific IDs from these four function-related groups was performed according to the following criteria: a known gene product, availability of reagents to test for expression at protein level, and high probability of the gene product to be related to the function assigned to the group.

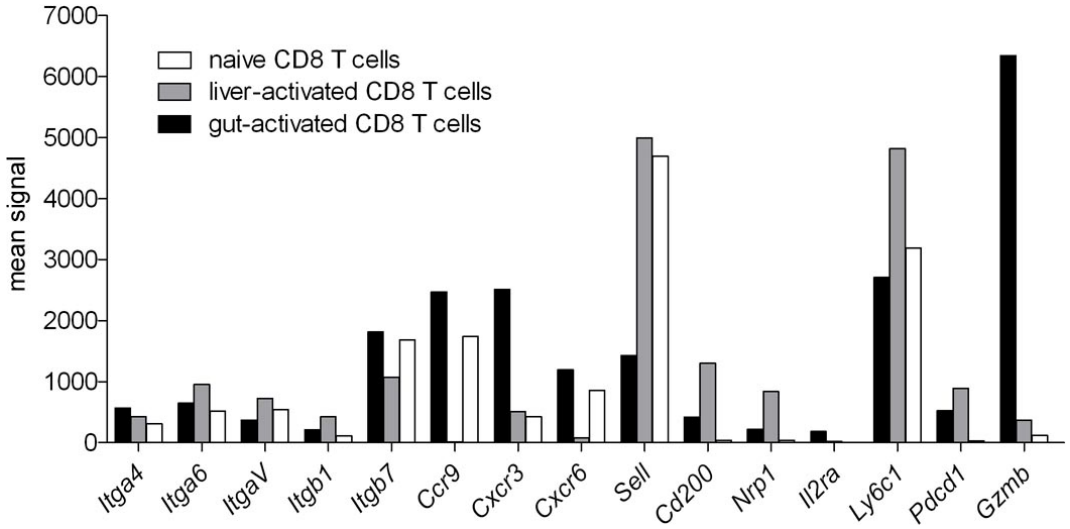

Figure 13: Selection of genes for protein analysis. IDs from the four function-related clusters were selected for further analysis at protein-level. Mean signals of specific genes are depicted, calculated by pooling multiple IDs of the same genes.

Figure 13 shows mean signals calculated for selected genes. Expression of the genes encoding granzyme B (*Gzmb*), the chemokine receptors CCR9, CXCR3, and CXCR6, as well as integrin α4 (*Itga4*) were upregulated in gut-activated T cells compared to liver-activated T cells and naïve OT-I CD8 T cells. In comparison with gut-activated and naïve OT-I CD8 T cells, liver-activated T cells displayed increased expression of the genes encoding Ly6C, integrins αV (*ItgaV*), α6 (*Itga6*), and β1(*Itgb1*), as well as PD-1, CD200, and Nrp-1.

Both liver-activated and naïve OT-I CD8 T cells showed increased expression of *Sell* (encoding CD62L) compared to gut-activated T cells, while the genes

encoding CCR9 and integrin β7 (*Itgb7*) were downregulated on liver-activated compared to gut-activated and naïve CD8 T cells.

3.3.4 Liver-activated OT-I CD8 T cells express the integrins α4β1 and α6β1

To validate selected genes at protein-level, flow cytometric analysis of naïve, liver-activated and gut-activated OT-I CD8 T cells was performed.

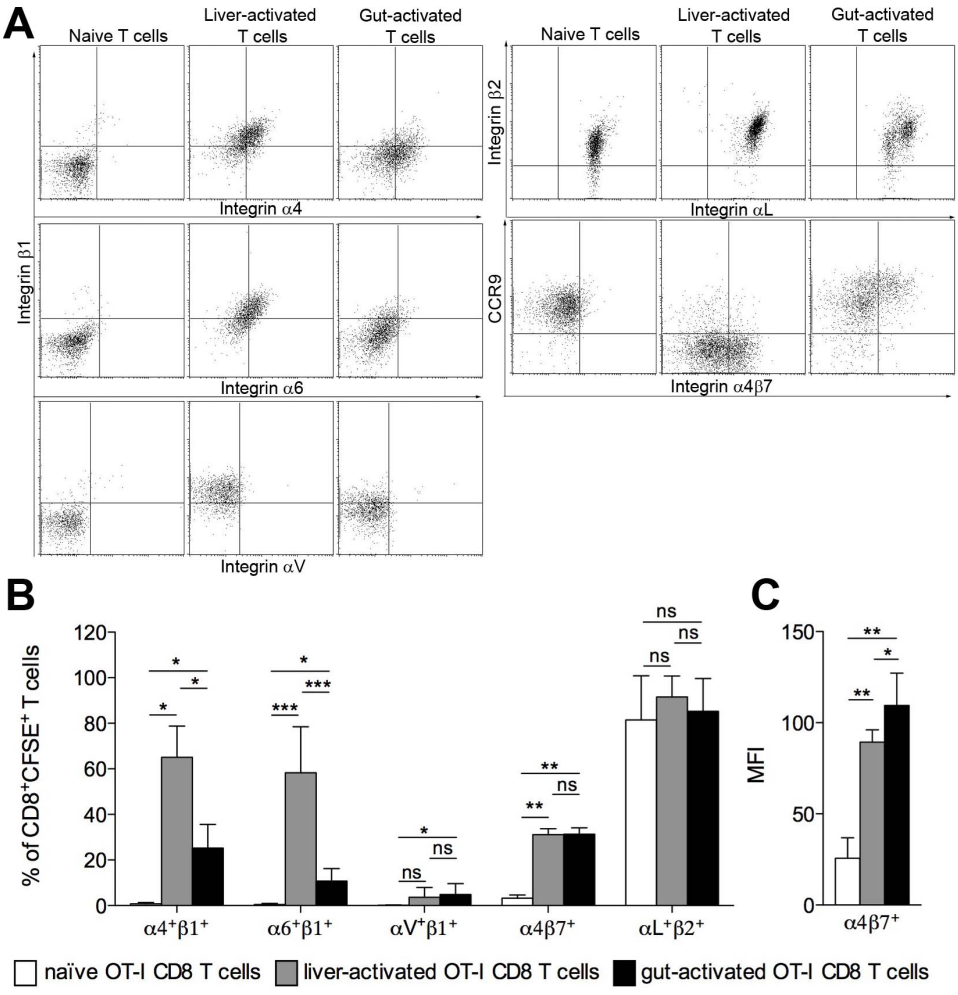

Figure 14: Expression of integrins of differentially activated OT-I CD8 T cells. Naïve, liver-activated, and gut-activated OT-I CD8 T cells were analyzed by flow cytometry regarding their expression of integrins. A) Representative dot plots of integrin-expression, gated on $CFSE^+CD8^+$ T cells, are displayed. B) Results represent the percentages of integrin-expression of OT-I CD8 T cells. C) Mean fluorescence intensity (MFI) was evaluated for α4β7. Results from at least two independent experiments are shown ($n \geq 6$, mean ± SD). * $p \leq 0.016$, ** $p \leq 0.003$, *** $p \leq 0.0003$, ns = not significant; Bonferroni-corrected Mann-Whitney test.

Increased expression of integrin β1 pairing with both α4 and α6 was observed on liver-activated OT-I CD8 T cells. All three subsets of OT-I CD8 T cells expressed the integrin αLβ2. Expression of integrin αVβ1 was negligible (Fig. 14 A, B). Although the same percentage of integrin α4β7 was detected on gut- and liver-activated OT-I CD8 T cells, only gut-activated T cells displayed increased intensity of this integrin (Fig. 14 C).

3.3.5 Liver-activated OT-I CD8 T cells do not upregulate a specific chemokine receptor

In line with the array-data (Fig. 13), the chemokine receptor CCR9 was detected on gut-activated T cells but also on naïve OT-I CD8 T cells. In contrast, CCR9 was completely downregulated upon activation in the liver (Fig. 15 A, B).

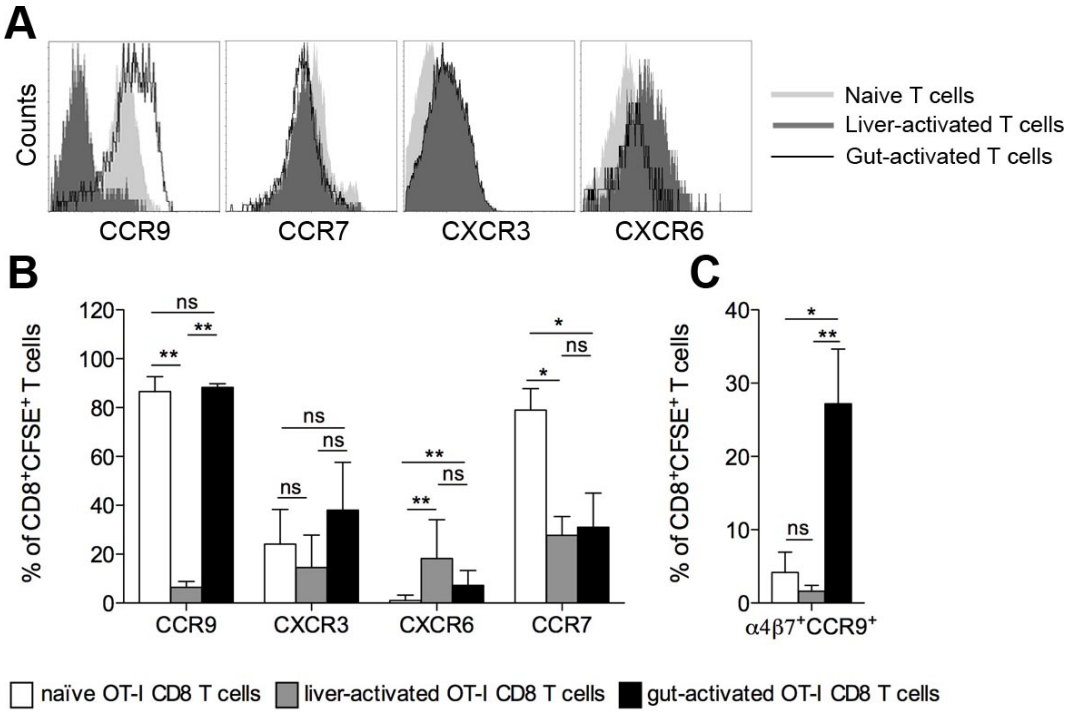

Figure 15: Expression of chemokine receptors on differentially activated OT-I CD8 T cells. Naïve, liver-activated, and gut-activated OT-I CD8 T cells were analyzed by flow cytometry regarding their expression of chemokine receptors. A) Representative histogram plots of chemokine receptor-expression, gated on $CFSE^+CD8^+$T cells, are displayed. B) depicts the percentage of T-cell subsets stained positive for chemokine receptors, and T cells stained positive for α4β7 and CCR9 at the same time (C). At least two separate experiments are shown ($n \geq 6$, mean ± SD). * $p \leq 0.016$, ** $p \leq 0.003$, ns = not significant; Bonferroni-corrected Mann-Whitney test.

Contrary to the gene array data, staining for CXCR3 was not different between the three subsets of T cells, and CXCR6 was upregulated while CCR7 was downregulated on both types of activated T cells compared to naïve OT-I CD8 T cells (Fig. 15 A, B). Co-expression of $\alpha 4\beta 7$ and CCR9 was restricted to gut-activated CD8 T cells (Fig. 15 C, Fig. 14 A).

3.3.6 Liver-activated OT-I CD8 T cells display patterns of naïve and activated T cells

As shown in Figure 16 A and B liver-activated OT-I CD8 T cells upregulated Nrp-1 compared to gut-activated and naïve T cells. Only gut-activated T cells produced granzyme B (GZMB).

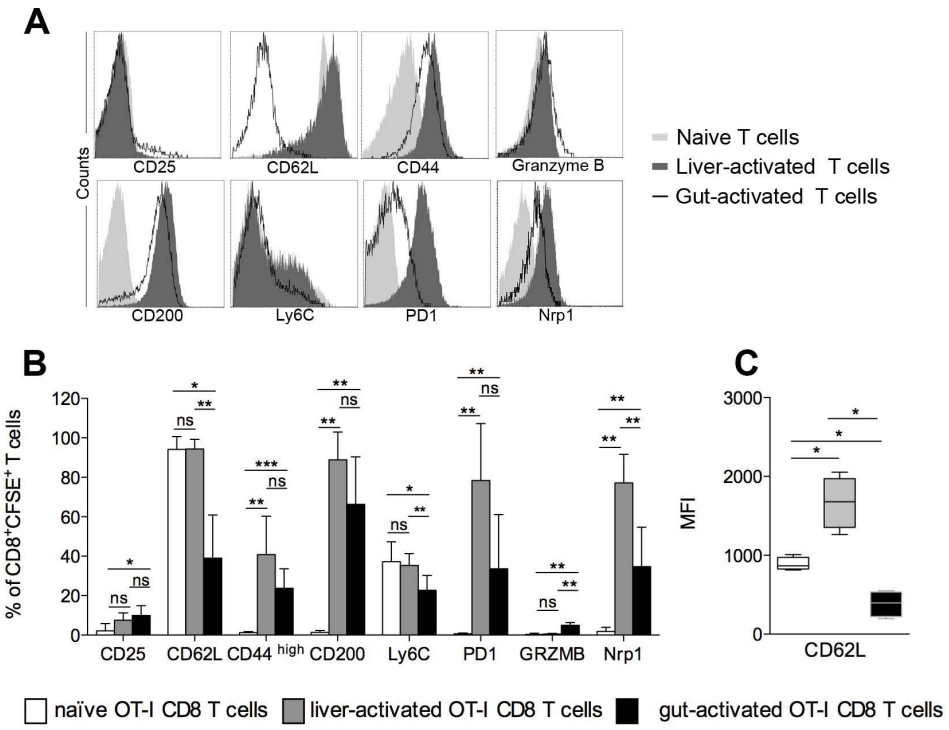

Figure 16: Expression of activation markers and inhibitory molecules. Naïve, liver-activated, and gut-activated OT-I CD8 T cells were analyzed regarding their activation status by flow cytometry. A) Representative histogram plots of activation markers and inhibitory molecules, gated on $CFSE^+CD8^+$T cells, are displayed. B) depicts the percentage of T cells positive stained for activation markers and inhibitory molecules. C) Box plot depicts the mean fluorescence intensity (MFI) evaluated for CD62L. At least two independent experiments are shown ($n \geq 6$, mean $\pm$ SD). * $p \leq 0.016$, ** $p \leq 0.003$, ** $p \leq 0.0003$ ns = not significant; Bonferroni-corrected Mann-Whitney test.

Liver-activated and gut-activated T cells expressed CD25, CD44, CD200 and PD-1 to a similar extent, while Ly6C-expression was reduced in gut-activated OT-I CD8 T cells. The most striking difference was the expression of CD62L on virtually all naïve and liver-activated OT-I CD8 T cells in contrast to its down-regulation on gut-activated OT-I CD8 T cells (Fig. 16 A, B). The mean fluorescence intensity of CD62L was significantly higher in liver-activated compared to naïve and gut-activated OT-I CD8 T cells (Fig. 16 C).

3.3.7 Liver-activated and gut-activated OT-I CD8 T cells exhibit similar effector function

Finally, it was determined whether activation in the liver or gut has an influence on the effector function of CD8 T cells. Liver-and gut-activated OT-I CD8 T cells were isolated and analyzed for their potential to produce the cytokine interferon-γ and their potential to lyse target cells.

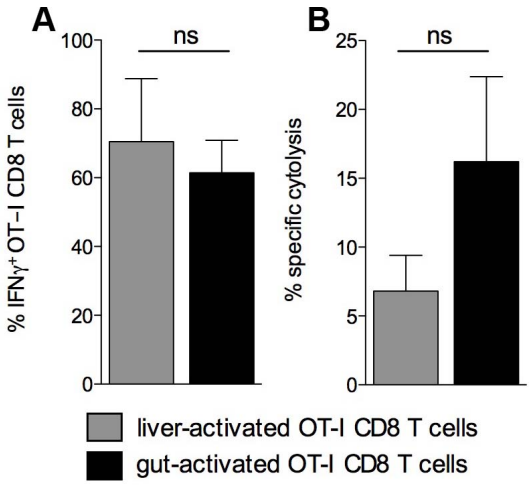

Figure 17: CD8 T cells activated in the liver and in the gut display similar effector function. Liver-activated and gut-activated OT-I CD8 T cells were sorted for CFSE-staining and analyzed *in vitro* for production of interferon-γ after stimulation with PMA/ionomycin (A) and for cytolysis of target cells (B). Percentages of IFNγ^+ T cells or specific lysis are shown from three pooled experiments (n = 3 , mean $\pm$ SD).ns = not significant; Mann-Whitney test.

Liver- and gut-activated OT-I CD8 T cells produced similar amounts of the pro-inflammatory cytokine interferon-γ after *in vitro* stimulation. They also

displayed similar potential to lyse target cells, confirming that both subsets of CD8 T cells have cytotoxic capabilities (Fig. 17).

Thus, T-cell activation in the liver and in the gut results in effector OT-I CD8 T cells.

In summary, only gut-activated OT-I CD8 T cells express both markers associated with homing to the gut, namely $\alpha 4\beta 7$ and CCR9. In contrast, liver-activated OT-I CD8 T cells express integrins $\alpha 4\beta 1$ and $\alpha 6\beta 1$, but CCR9 expression is lost upon priming in the liver. Both liver-activated and gut-activated CD8 T cells display an activated phenotype and show effector function, but liver-activated CD8 T cells retain markers of naïve cells, namely CD62L and Ly6C.

3.4 Expression of cell adhesion molecules in the inflamed liver

3.4.1 RNA levels of cell adhesion molecules

Quantitative RT-PCR analysis of normal and inflamed liver tissue was performed to determine whether inflammation leads to up-regulation of adhesion molecules. Corresponding to the integrins specifically regulated on liver- and gut-activated OT-I CD8 T cells, the following adhesion molecules were analyzed:

- ICAM-1 (intercellular adhesion molecule 1) a binding partner for αLβ2
- VCAM-1 (vascular cell adhesion molecule 1) a binding partner for α4β1
- MAdCAM-1 (mucosal addressin cell adhesion molecule 1) a binding partner for α4β7

ICAM-1 and VCAM-1 were expressed constitutively in non-inflamed livers but were strongly upregulated upon inflammation. In contrast, MAdCAM-1 was not expressed in non-inflamed livers but reached detectable levels in inflamed livers (Fig. 18 A–C).

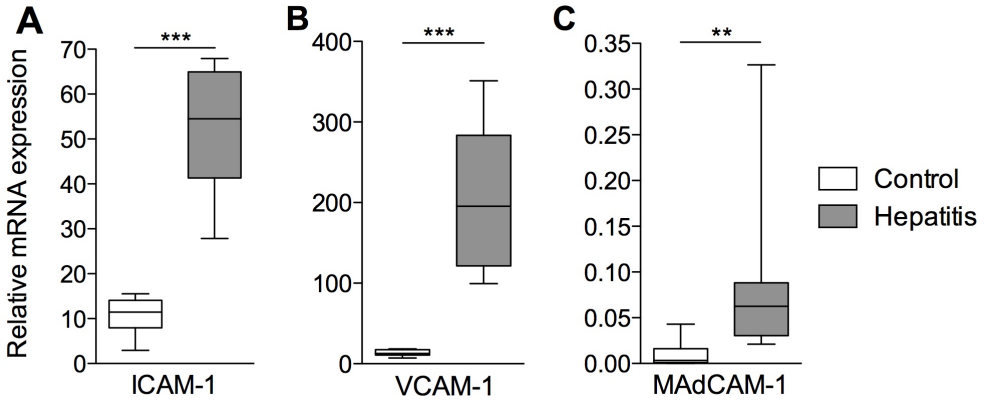

Figure 18: RNA levels of adhesion molecules in the inflamed liver. Hepatitis was induced by transfer of naïve OT-I CD8 T cells into TF-OVA mice. On day five, mRNA levels of ICAM-1 (A), VCAM-1 (B), and MAdCAM-1 (C) were analyzed in liver tissue by qRT-PCR and normalized to the housekeeping gene *RPL4*. Box plots depicted are from two independent experiments (n = 8). ** $p \leq 0.01$, *** $p \leq 0.001$; Mann-Whitney test.

3.4.2 ICAM-1, VCAM-1 and laminin are upregulated in the inflamed liver

To confirm the up-regulation of adhesion molecules at protein level, immunohistochemistry of normal and inflamed liver tissue was performed.

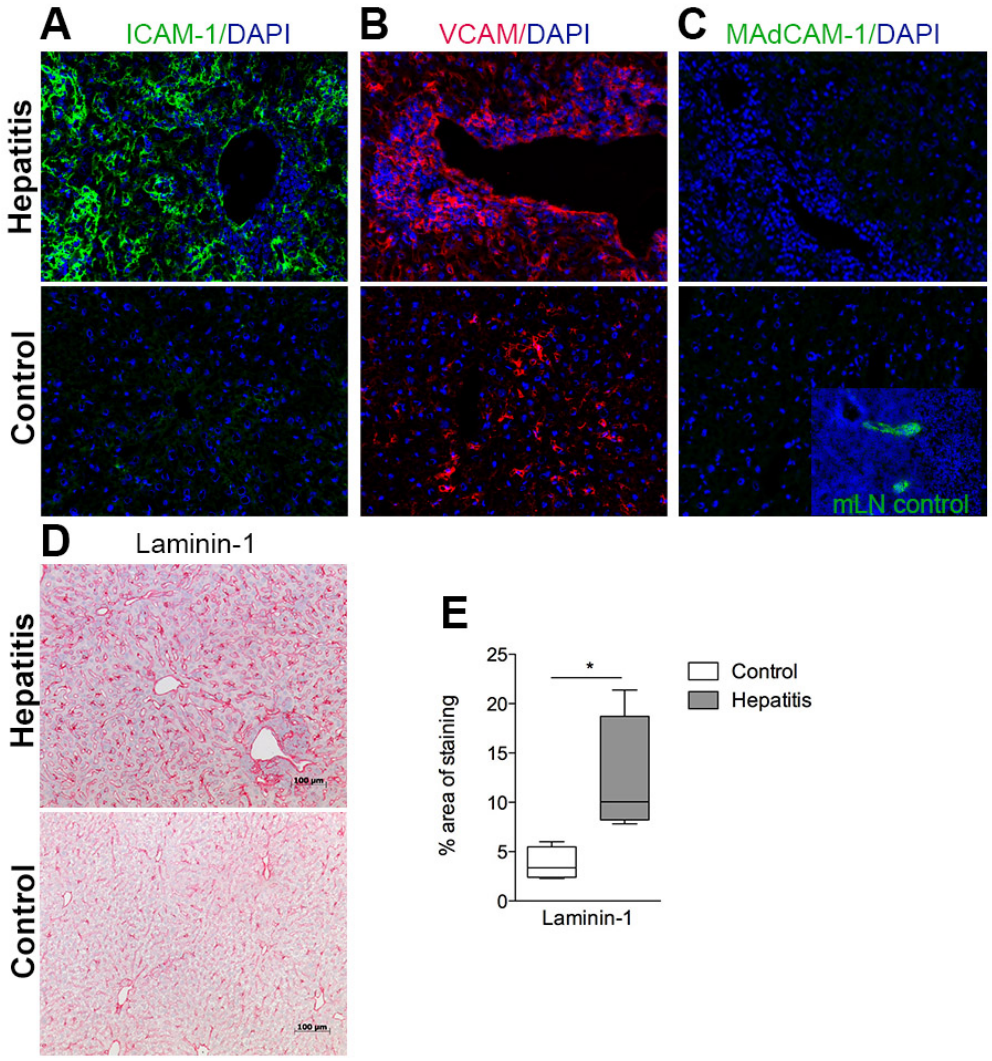

Figure 19: Adhesion molecules are upregulated in the inflamed liver. The experiment was performed as described in figure 18. On day five, livers of TF-OVA mice were sectioned and analyzed for expression of (A) ICAM-1, (B) VCAM-1, (C) MAdCAM-1 (magnification 200×), and (D) laminin (scale bar = 100µm, magnification 100×) by immunohistochemistry. Representative images of n = 4 mice are shown. The insert in (C) shows a mesenteric the lymph node as the positive control for MAdCAM-1 staining. E) Box plot depicts the percent area of staining of laminin, quantified in three visual fields (0.6 mm^2) of each liver section (n = 4).* $p \leq 0.05$; Mann-Whitney test.

ICAM-1, VCAM-1, and laminin were upregulated in inflamed livers, while MAdCAM-1 was not detected at protein level (Fig. 19 A–E).

In summary, the adhesion molecules ICAM-1, VCAM-1, and laminin are upregulated in inflamed livers and may be responsible for the binding of CD8 T cells, which express the corresponding integrins, when activated in the liver.

4 Discussion

Autoimmune liver diseases are of unknown cause and pathogenesis. It is assumed that autoreactive T cells destroy either the hepatocytes, leading to autoimmune hepatitis (AIH) or the cholangiocytes, leading to primary sclerosing cholangitis (PSC) and primary biliary cirrhosis (PBC). Untreated, these diseases lead to life-threatening conditions. Although effective therapies exist, a subgruop of patients do not respond to therapy or suffer from side effects due to long-term treatment. In addition, to date there is no available therapy for patients suffering from PSC and the only life-extending option is transplantation of the liver.

Animal models are required to study the initial immunological processes leading to autoimmune liver diseases. A mouse model, which reflects the characteristics of T cell-mediated hepatitis, was established in our laboratory. TF-OVA mice express the model antigen ovalbumin in hepatocytes and transfer of naïve antigen-specific CD8 T cells induces liver inflammation (Derkow et al., 2007).

Given the lack of knowledge about immunological processes leading to autoimmune liver diseases, this study investigated, which professional APCs are capable of activating CD8 T cells that in turn lead to liver inflammation. It is now generally accepted that CD8 T cells are activated within the liver, but knowledge about the fate of such liver-primed CD8 T cells is limited. In addition, it is assumed that extrahepatic activation of T cells, for example in the gut may contribute to autoimmune processes in the liver. Therefore, the present study compared the migratory behavior of liver-primed CD8 T cells and gut-activated CD8 T cells, and investigated their phenotype.

4.1 Hepatic APCs and their role in activating naïve CD8 T cells

Experimental models, in which antigens are presented in the liver, have demonstrated T-cell activation (Klein and Crispe, 2006; Derkow et al., 2007) or induction of apoptosis and tolerance (Liu et al., 2001; Bowen et al., 2004). Various hepatic APCs are capable of presenting antigens to naïve CD8 T cells *in vitro* (Ebrahimkhani et al., 2011; Derkow et al., 2011). In addition, non-professional APCs such as LSECs as well as hepatocytes induce tolerance or deletion rather than immunity (Bertolino et al., 2001; Limmer et al., 2000). The contribution of professional APCs to the priming self-reactive T cells in the liver remains unclear. Therefore, the present study investigated the influence of both DCs and KCs as professional APCs on CD8 T-cell activation and liver inflammation *in vivo*.

A subset of hepatic DCs contributes to the activation of naïve CD8 T cells, leading to liver inflammation

In order to investigate whether hepatic DCs contribute to the activation of antigen-specific naïve CD8 T cells in the liver and thereby induce liver inflammation, double transgenic CD11cDTRxTF-OVA mice were generated, in which the induction of hepatitis and the *in vivo* depletion of DCs are possible.

Our results show that DC-depletion reduces the number of pro-inflammatory antigen-specific CD8 T cells in the liver, indicating that priming of T cells in the liver is dependent on DCs. This result is in accordance with a study demonstrating that the depletion of a subset of CD11c^{high}MHC-II^{high}DCs impaired the activation of CD8 T cells in the liver (Plitas et al., 2008). However, Plitas *et al.* did not investigated whether hepatic DCs are capable of inducing effector CD8 T cells that mediate liver damage. Our data therefore extend these finding as they show that the absence of DCs ameliorates the hepatitis as indicated by decreased alanine aminotransferase levels (ALT), an enzyme that is released into the serum when hepatocytes are destroyed.

Although the absence of DCs reduces the severity of hepatitis, liver damage was not fully prevented. Unexpectedly, the depletion of DCs led to increased ALT levels by itself. This effect may be explained by the limitations of the CD11cDTR model, since multiple injections of diphtheria toxin are lethal (Jung et al., 2002), possibly because the diphtheria toxin receptor is expressed on radio-resistant non-hematopoietic cells (Zaft et al., 2005), and their depletion might influence the immunological homeostasis in the liver. Alternatively, elevated ALT levels results from a toxic effect on the liver.

Another possible reason why DC depletion did not fully prevents liver damage is that various other APCs exist in the liver, which are capable of activating CD8 T cells. Non-professional APCs such as LSECs as well as hepatocytes have been shown to prime CD8 T cells in the liver, but they rather induce T-cell tolerance and deletion instead of immunity (Limmer et al., 2000; Bertolino et al., 1999). These findings are consistent with data from our group. Derkow *et al.* demonstrated that hepatocytes and LSECs fail to induce effector CD8 T cells in bone marrow chimeras of TF-OVA mice, indicating that professional APCs such as DCs and KCs are essential to induce liver inflammation (Derkow et al., 2007). The data obtained in the present study therefore extend these findings and identify hepatic DCs as inducers of effector CD8 T cells and liver inflammation. Since depletion of DCs is a systemic treatment, we can not be certain whether DCs from other organs such as the spleen influence the activation of CD8 T cells in the liver. Depletion of DCs and simultaneous splenectomy could circumvent this question in an experimental setting.

DCs are professional APCs and are key activators of adaptive immunity in the lymph nodes where T-cell activation takes place. In contrast, DCs in non-lymphoid organs such as the liver are generally considered immature and thought to maintain tolerance (O'Connell et al., 2000). But tolerance is broken when diseases occur and it was shown that more immunogenic DCs are present in chronic human liver disease (Kelly et al., 2013). This might have consequences regarding autoimmune reactions in the liver. Autoantigens are constantly expressed and presented by hepatocytes, usually leading to tolerance and deletion of CD8 T cells (Bertolino et al., 2001; Wuensch et al., 2006), but DCs may take up these antigens from hepatocytes (Leiriao et al., 2005) and

induce immunity leading to activation of effector CD8 T cells and liver inflammation under inflammatory conditions. An understanding of different subsets of DCs during inflammation in the liver would be helpful to develop therapeutics based on modulation of these cells as currently tested in patients with type I diabetes (Giannoukakis et al., 2011).

In summary, our data indicate that a subtype of hepatic DCs cross-presents hepatocyte-derived antigen and generates antigen-specific effector CD8 T cells, thereby contributing to liver inflammation. However, other APCs in the liver obviously also induce the activation of CD8 T cells. Therefore, the next section addresses KCs as potential APCs.

Kupffer cells maintain tolerance in the liver

The above discussed experiments showed that hepatic DCs contribute to liver inflammation. However, other professional APCs such as KCs reside within the liver and were reported to be immunogenic (Schumann et al., 2000), whereas other studies demonstrated their tolerogenic role (Breous et al., 2009; You et al., 2008). Therefore, this study investigated whether KCs, the liver resident macrophages, generate antigen-specific effector CD8 T cells and thereby contribute to hepatitis *in vivo*. By injecting liposome-encapsulated clodronate into TF-OVA mice macrophages are effectively depleted and liver inflammation can be analyzed in the absence of KCs.

The present study demonstrates that ablation of KCs increases the severity of T cell-mediated hepatitis. This result is in line with a report, in which KC depletion in a mouse model of hepatitis B also leads to increased hepatitis (Sitia et al., 2011). Yet, there are contradictory reports showing that KC depletion resolves liver inflammation in Con A-induced hepatitis (Schumann et al., 2000). Since Con A is binding to LSECs and KCs (Knolle et al., 1996), thereby promoting the secretion of pro-inflammatory cytokines and T-cell activation (Schumann et al., 2000), the outcome of KC depletion may differ in the antigen-specific hepatitis model we used.

KC depletion enhances the severity of hepatitis in our study. It would be expected that liver inflammation is caused by increased infiltration of antigen-specific CD8 T cells into the liver, which induce hepatitis in TF-OVA

mice. In contrast, our data show that less effector CD8 T cells infiltrate the liver in the absence of KCs, whereas the numbers of CD8 T cells in the spleen remain constant. One possible reason for this observation is that besides CD8 T cells other cytotoxic cells enter the liver that contribute to liver inflammation. As shown by Sitia *et al.* KC depletion inhibits the removal of dead hepatocytes, which in turn secrete danger signals that mediate the recruitment of pro-inflammatory neutrophils that are suggested to increase the hepatitis, indicated by elevated ALT levels (Sitia et al., 2011). Histological and flow cytometric analysis in our study support this explanation, because the majority of infiltrating cells in the liver in the absence of KCs are not composed of T cells and large numbers of CD11b-positive cells, a marker primarily expressed by neutrophils and monocytes, enter the liver. Alternatively, other T cells are absent that may suppress the hepatitis. Another explanation for reduced CD8 T-cell numbers in the liver is that KC-depletion prevents the adhesion of T cells in the liver. KCs constitutively express the adhesion molecules ICAM-1 and VCAM-1, which are upregulated upon inflammation (van Oosten et al., 1995), and ICAM-1 and VCAM-1-dependent retention of naïve and activated CD8 T cells in the liver is an important mechanism of T-cell retention (Bertolino et al., 2005; Mehal et al., 1999).

However, the mechanism of tolerance-induction by KCs in the liver is still unclear. KCs are known to be effective cytokine-producers. Upon activation they secrete pro-inflammatory cytokines such as IL-18 and TNF-α (Okamura et al., 1995; Roland et al., 1994) but also anti-inflammatory cytokines such as IL-10 (Knolle et al., 1995). However, little is known about KCs and their cytokine-secretion in autoimmune liver disease and further studies are required.

In summary, KCs reduce the severity of hepatitis in our model by an unknown mechanism. They may promote adhesion and activation of naïve CD8 T cells in the liver and they induce tolerance by mechanisms that need to be further investigated.

4.2 Differential migration patterns of liver- and gut-activated CD8 T cells

Naïve T cells patrol the secondary lymphoid organs and alter their migratory phenotype upon activation, enabling them to gain access to target tissues. While migration patterns of gut-activated T cells have been well described, little is known about migration of T cells activated in the liver. Naïve and memory T cells frequently migrate through the healthy liver and activated T cells are retained preferentially (Luettig et al., 1999; Mehal et al., 1999). Activated T cells found in the liver may originate from other organs, as reported for patients suffering from the chronic liver disease PSC, in which gut-derived T cells are present in the liver (Grant et al., 2001). These gut-derived T cells may induce immune-mediated liver injury when they cause bystander hepatitis with elevated liver enzymes, as reported for influenza infection (Belz.1998) or autoimmune rheumatic diseases (Abraham et al., 2004). Since many of the mechanisms behind this interplay between gut and liver remain unknown, the migratory pattern of naïve CD8 T cells as well as liver-activated and gut-activated CD8 T cells primed by the same antigen *in vivo* was investigated.

Antigen in the liver is more accessible to naïve CD8 T cells than antigen expressed in the gut

In order to determine how presence of the antigen influences the migration of naïve antigen-specific CD8 T cells, adoptive transfer experiments were performed using recipients that express the antigen ovalbumin in the liver (TF-OVA mice) or in the small intestine (iFABP-OVA mice).

Our results show that naïve CD8 T cells migrate directly towards the antigen expressed in the liver, whereas the antigen in the small intestine does not lead to accumulation of CD8 T cells at the site of antigen presentation.

Direct migration of CD8 T cells into the liver suggests that antigen-recognition in the liver draining lymph nodes and subsequent migration into the liver is dispensable as shown by others and our group before (Bertolino et al., 2001; Derkow et al., 2007). Consistent with previous data, CD8 T cells are activated and retained within the liver (Bertolino et al., 2001; John and Crispe, 2004).

Abundance of hepatic APCs, the slow blood flow, and the unique architecture of the hepatic sinusoids, enable T cells to directly contact hepatocytes and to access the liver (Selmi et al., 2007; MacPhee et al., 1995; Warren et al., 2006).

The present study shows that expression of the antigen in the small intestine does not lead to accumulation of naïve CD8 T cells in the small intestine. The iFABP mouse model selected for this study expresses the antigen ovalbumin in the small intestine and transfer of antigen-specific CD8 T cells into these mice led to recruitment and CD8 T-cell activation in the mesenteric lymph node and subsequent migration to the small intestine (Vezys et al., 2000). Naïve T cells have to be activated in the GALT and acquire a gut-tropic phenotype before they enter the lamina propria of the small intestine (Johansson-Lindbom et al., 2005; Stenstad et al., 2007). This explains why naïve CD8 T cells are not recruited to the small intestine within twenty hours in the *in vivo* migration assay employed here.

In summary, the antigen expression in the liver leads to the accumulation of naïve CD8 T cells at this site, whereas the antigen expressed in the small intestine is not recognized.

Liver-primed T cells exhibit a distinct migratory profile compared to gut-primed T cells

Several aspects are of interest regarding the migration of T cells activated in the liver and in the gut: Liver-primed T cells may exhibit tissue-tropic migration patterns in the same way as gut-derived T cells do. They may also migrate to other organs such as the gut. Conversely, T cells initially activated in the GALT may migrate to the liver where they are retained because they are activated. To test this hypothesis liver-activated and gut-activated CD8 T cells were transferred into wild-type mice to study tissue-tropic T-cell migration independent of antigen-expression.

Both types of activated CD8 T cells accumulated in the liver, with higher numbers of gut-activated than liver-activated CD8 T cells, implicating that accumulation in the liver relates to the activation status of CD8 T cells. It has been reported that activated T cells change their migratory properties upon

activation and preferentially accumulate in the liver (Hamann et al., 2000; Luettig et al., 1999; Mehal et al., 1999).

Our data show that CD8 T cells primed in the gut have access to the small intestine, whereas CD8 T cells activated in the liver and naïve CD8 T cells do not. In agreement with earlier studies, activation by APCs in the GALT induces the gut-homing phenotype required for gaining access to the small intestine (Stenstad et al., 2007). Licensing to the small intestine requires the presence of retinoic acid in dendritic cells during priming (Iwata et al., 2004). Clearly, priming in the liver does not imprint this gut-homing phenotype on CD8 T cells despite the fact that retinoic acid is present in hepatic stellate cells. While *in vitro* experiments had suggested that none of the liver APCs are suited to induce this gut-homing phenotype in CD8 T cells (Eksteen et al., 2009), this finding was disputed by the *in vitro* finding that LSECs are capable of imprinting the gut-homing phenotype on CD4 T cells (Neumann et al., 2012). Our study demonstrates that CD8 T cells primed in the liver *in vivo* do not migrate to the intestine despite the fact that professional and non-professional APCs are present in sufficient quantity and are capable of presenting the antigen (Derkow et al., 2011).

We also observed that CD8 T cells activated in the liver display a distinct migratory profile. They preferentially migrate to liver and spleen, reflecting their activated status. However, they retain the ability to migrate through lymph nodes, whereas gut-primed CD8 T cells re-circulate through lymph nodes less frequently. Previous reports have shown that accumulation of T cells recognizing their antigen within the liver are retained and that the liver acts as a "T-cell graveyard" or as a "killing field" for activated T cells (Mehal et al., 2001; Bertolino et al., 2001; Crispe et al., 2000). The liver acting as a "T cell graveyard" implies that activated T cells undergoing programmed cell-death accumulate in the liver, whereas the "killing field" theory suggests that activated T cells are trapped and actively deleted in the liver (Crispe et al., 2000). Our data dispute these findings, since liver-activated CD8 T cells accumulate in the liver, but a large proportion of these T cells are capable of re-circulating through the lymph nodes. Regarding gut-primed CD8 T cells, which accumulated in the liver to a larger extent, it could be hypothesized that they exert bystander hepatitis upon deletion in the liver. The *in vivo*

migration-assay employed in this study is not suitable to analyze whether T cells that migrated into different organs are effector cells, undergo apoptosis or become anergic and further studies are required.

In conclusion, CD8 T cells activated by gut-derived antigen express the gut-homing phenotype and gain access to the small intestine. The activation of CD8 T cells increases their migration to the liver, independent of the site of activation. CD8 T cells activated in the liver exhibit a distinct migration behavior *in vivo*. While they show no specific liver-tropism, they have the potential to migrate into lymph nodes and are prohibited from entering the gut.

Presence of antigen in the liver and gut enhances migration of activated T cells to the respective sites

Based on findings on migration of liver- and gut-primed CD8 T cells in wild-type mice, it was important to determine additional effects of antigen-expres-sion in liver or gut on T-cell migration. CD8 T cells activated by gut-derived antigen may migrate to the liver where they encounter their cognate antigen, inducing autoimmunity. It may also re-direct liver-primed CD8 T cells into the gut.

Presence of the antigen in the liver led to more pronounced accumulation of naïve as well as liver-and gut-activated CD8 T cells in the liver. In addition, antigen-expression in the liver overrode the gut-tropism of gut-activated T cells, which accumulated in the liver in larger numbers. Expression of the antigen in the small intestine drove liver-derived CD8 T cells into the mesenteric lymph node, but they did not gain access to the small intestine.

Studies have shown that skin- and gut-tropic T cells express alternative homing receptors after re-stimulation with APCs of the reciprocal organ *in vitro* and *in vivo* (Mora et al., 2005; Oyoshi et al., 2011). In our study, liver-primed CD8 T cells displayed more pronounced migration into the mesenteric lymph nodes when the antigen was expressed in the small intestine. Thus, it is possible that they enter the small intestine at later time points after re-programming of their adhesion molecules. Conversely, presence of the antigen in the liver led to profound accumulation of gut-primed CD8 T cells in the liver and overrode gut-tropic migration. Gut-activated T cells may enter the liver

simply because they are activated, but recognizing their cognate antigen in the liver may induce re-programming of their phenotype as well.

Gut-primed CD8 T cells that recognize their antigen in the liver, may induce liver pathology in the context of inflammatory bowel disease, as proposed for patient afflicted with PSC (Grant et al., 2001; Eksteen et al., 2004). A possible explanation for their capability to migrate to the gut would be that chronic gut-inflammation induces pro-inflammatory changes in the local hepatic environment and improves the co-stimulatory capacity of APCs in the liver as recently shown by our group (Seidel et al., 2013). It is also possible that antigens originating from the inflamed intestine enter the liver (Terjung and Spengler, 2009), thereby leading to cross-reaction with gut-derived T cells.

Together, this study indicates that antigen expression enhances migration of activated CD8 T cells to the respective sites. Gut-activated CD8 T cells are re-directed to the liver and may cross-react with their cognate antigen. In contrast, liver-primed CD8 T cells have no access to the small intestine, even when the antigen is expressed there.

4.3 Comparison of the phenotype of CD8 T cells activated in the liver or in the gut

Based on the observed distinct migration patterns of liver- and gut-activated CD8 T cells, the question arises whether different homing receptors or different activation-patterns are induced. The phenotype of naïve, liver-activated, and gut-activated CD8 T cells was characterized by transcriptome analysis. The number of differentially regulated genes between the three CD8 T-cell populations was surprisingly high. Therefore, genes were selected that were relevant for the migratory behavior and the activation-status of CD8 T cells and were further analyzed at protein level.

Adhesion molecules on liver-activated and gut-activated CD8 T cells

As previously discussed, naïve CD8 T cells transferred to TF-OVA mice migrate to the lymph nodes, but also accumulate in the liver. Little is known about molecules that are responsible for the migration and adhesion of T cells to the

liver and no liver-specific adhesion molecule was reported so far.

The present study shows that liver-activated CD8 T cells upregulate the integrin β1, which is co-expressed with integrins α4 and α6, thereby forming ligands for laminin and VCAM-1. Integrins αL and β2, which dimerize to form a ligand for ICAM-1, are expressed on naïve, liver-activated, and gut-activated CD8 T cells. Apart from integrins on T cells, we also analyzed their ligands in liver tissue. ICAM-1 and VCAM-1 as well as laminin are expressed constitutively in non-inflamed livers, but are strongly upregulated upon inflammation, suggesting that these molecules promote adhesion of CD8 T cells in the liver. These results are consistent with previous reports showing that liver-primed CD8 T cells upregulate the integrins α4 and αL, and blocking of VCAM-1 and ICAM-1 reduces the adhesion of CD8 T cells to the liver (John and Crispe, 2004; Bertolino et al., 2005). Whereas there is evidence that laminin is expressed in the inflamed liver (Couvelard et al., 1993; Xu et al., 2003), upregulation of integrin α6β1 on liver-activated CD8 T cells has not been reported so far, suggesting a further mechanism for T-cell adhesion discovered in our model. While the chemokine receptors CXCR3, CXCR6, and CCR5 are expressed on T cells infiltrating the inflamed liver (Curbishley et al., 2005; Boisvert et al., 2003; Murai et al., 1999), we found no specific chemokine receptor upregulated on liver-primed CD8 T cells.

We also observed that gut-activated CD8 T cells migrate to the small intestine, whereas liver-activated and naïve CD8 T cells do not. As expected, the gut-homing markers α4β7 and CCR9 were co-expressed on gut-activated CD8 T cells only. In contrast, liver-activated CD8 T cells also expressed α4β7, but CCR9 was completely downregulated. In addition, CCR9 is constitutively expressed on naïve CD8 T cells in mice (Carramolino et al., 2001), but they do not express α4β7. These data suggest that only the co-expression of both molecules enable CD8 T cells to enter the small intestine, although CCR9-independent migration to the small intestine was reported in another model (Stenstad et al., 2007).

Finally, the present data demonstrate that CD8 T cells activated in the gut show a strong tendency to migrate to the liver, an effect that is amplified in the presence of their nominal antigen in hepatocytes. In livers of patients suffering from PSC gut-derived T cells and mucosal addressins are detected (Grant

et al., 2001; Eksteen et al., 2009). In the model studied here, gut-activated CD8 T cells express the integrin α4β7, but also αLβ2 and low amounts of α4β1. In contrast to ICAM-1 and VCAM-1, the binding partner for αLβ2 and α4β1, both expressed in the liver, MAdCAM-1, the binding partner for α4β7, was not detected in the inflamed liver by immunofluorescence although a weak signal was observed at mRNA level. The migration behavior of gut-activated T cells to the liver is likely explained by their activated phenotype per se (Mehal et al., 1999; Hamann et al., 2000) and our data also suggest that interaction of CD8 T cells with ICAM-1 and VCAM-1 may enhance accumulation of gut-primed CD8 T cells in the liver.

In summary, specific integrins are upregulated on liver-primed CD8 T cells, but no chemokine receptor was specifically induced in the liver. Based on these findings, we propose that retention of CD8 T cells in the liver is accomplished through interaction of αLβ2 with ICAM-1, α4β1 with VCAM-1, and adherence of α6β1-positive CD8 T cells to laminin. Further studies are required to elucidate whether integrin β1 – in particular when pairing with integrin α6 – mediates T-cell adhesion in the sinusoids. Adhesion of gut-activated CD8 T cells in the liver is mediated by ICAM-1 and VCAM-1, but it remains to be investigated whether there is an additional effect of the gut-homing markers α4β7 and CCR9 on migration to the liver, as proposed for patients with PSC.

Liver-primed CD8 T cells display a hybrid phenotype that mediates migration to multiple sites

We hypothesized that priming of CD8 T cells in the liver results in a distinct phenotype and analyzed various molecules on liver-primed T cells with the aim of identifying markers that distinguish them from CD8 T cells activated in other organs.

Besides the profound differences regarding expression of integrins, striking differences regarding activation markers were noted. While gut-primed CD8 T cells showed the typical hallmarks of activated T cells, liver-primed CD8 T cells displayed a hybrid phenotype. They expressed CD44, reflecting their activated status but also CD62L, resembling naïve cells, as well as Ly6C,

previously reported on memory T cells (Cerwenka et al., 1998). CD62L is expressed by the majority of naïve T cells and specific subsets of memory T cells and mediates homing to peripheral lymphoid organs (Arbones et al., 1994; Sallusto et al., 1999). Ly6C expression on CD8 T cells differentiates central from effector memory cells, supports homing to lymph nodes, and potentiates adhesion of CD8 T cells to ICAM-1 (Hänninen et al., 2011). Liver-activated CD8 T cells expressed high levels of CD44, CD62L, and Ly6C, resembling central memory cells, confirming recent data from CD8 T cells primed on LSECs (Böttcher et al., 2013). Expression of these molecules therefore explains two of the characteristics of liver-activated CD8 T cells in our model, namely circulation through lymph nodes and accumulation in the liver.

It can be argued that the distinct phenotype of liver-primed CD8 T cells results from incomplete activation in the liver. While this possibility can not be excluded, our analysis regarding the effector function of liver-primed CD8 T cells revealed their potential to produce pro-inflammatory cytokines and to lyse target cells. In contrast to gut-primed CD8 T cells, liver-activated CD8 T cells did not produce granzyme B and they may use the alternative Fas/FasL-pathway to destroy target cells (Roth and Harch.2004).

Apart from the expression of the more common markers, we detected an unusual molecule, namely Nrp-1 (Neuropilin-1), which is highly upregulated on liver-primed CD8 T cells compared to gut-activated CD8 T cells. Nrp-1, formerly known as a neuronal receptor (Kolodkin et al., 1997), is expressed on CD4 T_{regs}, conventional CD4 T cells, and CD8 T cells (Bruder et al., 2004; Yadav et al., 2012; Milpied et al., 2009). It is essential for initiation of the primary immune response (Tordjman et al., 2002) and promotes prolonged contact of CD4 T_{regs} with immature DCs (Sarris et al., 2008). Recently it was reported that Nrp-1 is expressed on CD8 T cells activated by LSECs in a bone marrow chimeric mouse model (Böttcher et al., 2013). In contrast to this model, in which CD8 T cells are exclusively primed by LSECs, CD8 T-cell activation is mediated by professional and non-professional APCs in our model (Derkow et al., 2007). Our data suggest that Nrp-1-positive CD8 T cells are not exclusively induced by LSEC and not restricted to T cells lacking effector

function. It requires further investigation whether expression of Nrp-1 on liver-primed CD8 T cells regulates their activation status or promotes adhesion within the liver. Finally, the analysis of specific markers on T cells and their ligands found in this study should be extended to human T cells and livers of patients suffering from autoimmune liver diseases.

In summary, we characterized the population of CD8 T cells generated by priming in the liver, which shows both distinct activation status and migratory behavior *in vivo*. We demonstrate that CD8 T cells activated in the liver exhibit effector function. While accumulating in the liver they also retain their ability to circulate through lymph nodes, explained by a hybrid phenotype, with aspects of naïve, effector, and also central memory CD8 T cells.

4.4 Conclusion

The present study provides evidence that hepatic DCs are effective APCs, which induce functional effector CD8 T cells in the liver and contribute to liver inflammation in our mouse model. In contrast, KCs ameliorate inflammation in the liver. Thus, whereas hepatocytes, LSECs, and KCs play a tolerogenic role, hepatic DCs may contribute to the pathogenesis of T cell-mediated liver diseases.

T-cell priming in the liver *in vivo* induces effector CD8 T cells that have a distinct phenotype and differ from that of CD8 T cells primed in the gut. Liver-primed CD8 T cells express an unusual molecule, namely Nrp-1 and the integrins αLβ2, α4β1, and α6β1. The corresponding ligands ICAM-1, VCAM-1, and laminin are upregulated in the inflamed liver, suggesting that adhesion of T cells in the liver is accomplished through these molecules. Therefore, these interactions are a possible target for blocking and may provide an opportunity to inhibit T cell-mediated pathology in the liver.

Activation of CD8 T cells in the liver also induces a specific migration behavior. Liver-primed CD8 T cells accumulate in the liver, but also migrate to lymph nodes, explained by their hybrid phenotype, which reflects aspects of naïve, effector, but also central memory CD8 T cells. They may interact with APCs and other immune cells in the lymph nodes, possibly influencing immune homeostasis.

Whereas liver-activated CD8 T cells have no access to the gut, gut-primed CD8 T cells migrate into the small intestine, depending on the regulation of gut-specific homing molecules. In addition, gut-primed CD8 T cells preferentially accumulate in the liver, an effect that is amplified in the presence of their nominal antigen in hepatocytes. Thus, migration of activated CD8 T cells is leading from the gut to the liver, but not from the liver to the gut. Therefore, it is possible that extrahepatic activation of CD8 T cells contributes to the development of liver pathology. But it is unlikely that CD8 T cells primed in the liver directly influence the mucosal immune system.

Bibliography

Abdel-Misih, S. R. Z. and Bloomston, M. (2010). Liver anatomy. The Surgical Clinics of North America *90*, 643–653.

Abraham, S., Begum, S. and Isenberg, D. (2004). Hepatic manifestations of autoimmune rheumatic diseases. Annals of the rheumatic diseases *63*, 123–129.

Abshagen, K., Eipel, C., Kalff, J. C., Menger, M. D. and Vollmar, B. (2008). Kupffer cells are mandatory for adequate liver regeneration by mediating hyperperfusion via modulation of vasoactive proteins. Microcirculation *15*, 37–47.

Alabraba, E., Nightingale, P., Gunson, B., Hubscher, S., Olliff, S., Mirza, D. and Neuberger, J. (2009). A re-evaluation of the risk factors for the recurrence of primary sclerosing cholangitis in liver allografts. Liver Transplantation *15*, 330–340.

Arbones, M. L., Ord, D. C., Ley, K., Ratech, H., Maynard-Curry, C., Otten, G., Capon, D. J. and Tedder, T. F. (1994). Lymphocyte homing and leukocyte rolling and migration are impaired in L-selectin-deficient mice. Immunity *1*, 247–260.

Bamboat, Z. M., Stableford, J. A., Plitas, G., Burt, B. M., Nguyen, H. M., Welles, A. P., Gonen, M., Young, J. W. and DeMatteo, R. P. (2009). Human liver dendritic cells promote T cell hyporesponsiveness. Journal of Immunology *182*, 1901–1911.

Bargatze, R. F., Jutila, M. A. and Butcher, E. C. (1995). Distinct roles of L-selectin and integrins alpha 4 beta 7 and LFA-1 in lymphocyte homing to Peyer's patch-HEV in situ: the multistep model confirmed and refined. Immunity *3*, 99–108.

Benseler, V., Warren, A., Vo, M., Holz, L. E., Tay, S. S., Le Couteur, D. G., Breen, E., Allison, A. C., van Rooijen, N., McGuffog, C., Schlitt, H. J., Bowen, D. G., McCaughan, G. W. and Bertolino, P. (2011). Hepatocyte entry leads to degradation of autoreactive CD8 T cells. Proc. Natl. Acad. Sci. U.S.A. *108*, 16735–16740.

Berlin, C., Berg, E. L., Briskin, M. J., Andrew, D. P., Kilshaw, P. J., Holzmann, B., Weissman, I. L., Hamann, A. and Butcher, E. C. (1993). Alpha 4 beta 7 integrin mediates lymphocyte binding to the mucosal vascular addressin MAdCAM-1. Cell *74*, 185–195.

Bertolino, P., Bowen, D. G., McCaughan, G. W. and Fazekas de St Groth, B. (2001). Antigen-specific primary activation of CD8+ T cells within the liver. Journal of Immunology *166*, 5430–5438.

Bertolino, P., Schrage, A., Bowen, D. G., Klugewitz, K., Ghani, S., Eulenburg, K., Holz, L., Hogg, N., McCaughan, G. W. and Hamann, A. (2005). Early intrahepatic antigen-specific retention of naïve CD8+ T cells is predominantly ICAM-1/LFA-1 dependent in mice. Hepatology *42*, 1063–1071.

Bertolino, P., Trescol-Biémont, M. C., Thomas, J., Fazekas de St Groth, B., Pihlgren, M., Marvel, J. and Rabourdin-Combe, C. (1999). Death by neglect as a deletional mechanism of peripheral tolerance. International Immunology *11*, 1225–1238.

Bevan, M. J. (1976). Cross-priming for a secondary cytotoxic response to minor H antigens with H-2 congenic cells which do not cross-react in the cytotoxic assay. The Journal of Experimental Medicine *143*, 1283–1288.

Bogdanos, D. P., Smyk, D. S., Rigopoulou, E. I., Mytilinaiou, M. G., Heneghan, M. A., Selmi, C. and Gershwin, M. E. (2012). Twin studies in autoimmune disease: genetics, gender and environment. Journal of Autoimmunity *38*, J156–69.

Boisvert, J., Kunkel, E. J., Campbell, J. J., Keeffe, E. B., Butcher, E. C. and Greenberg, H. B. (2003). Liver-infiltrating lymphocytes in end-stage hepatitis

C virus: subsets, activation status, and chemokine receptor phenotypes. Journal of Hepatology *38*, 67–75.

Böttcher, J. P., Schanz, O., Wohlleber, D., Abdullah, Z., Debey-Pascher, S., Staratschek-Jox, A., Hochst, B., Hegenbarth, S., Grell, J., Limmer, A., Atreya, I., Neurath, M. F., Busch, D. H., Schmitt, E., van Endert, P., Kolanus, W., Kurts, C., Schultze, J. L., Diehl, L. and Knolle, P. A. (2013). Liver-Primed Memory T Cells Generated under Noninflammatory Conditions Provide Anti-infectious Immunity. Cell Reports *3*, 779–795.

Bowen, D. G., Zen, M., Holz, L., Davis, T., McCaughan, G. W. and Bertolino, P. (2004). The site of primary T cell activation is a determinant of the balance between intrahepatic tolerance and immunity. The Journal of Clinical Investigation *114*, 701–712.

Breous, E., Somanathan, S., Vandenberghe, L. H. and Wilson, J. M. (2009). Hepatic regulatory T cells and Kupffer cells are crucial mediators of systemic T cell tolerance to antigens targeting murine liver. Hepatology *50*, 612–621.

Briskin, M., Winsor-Hines, D., Shyjan, A., Cochran, N., Bloom, S., Wilson, J., McEvoy, L. M., Butcher, E. C., Kassam, N., Mackay, C. R., Newman, W. and Ringler, D. J. (1997). Human mucosal addressin cell adhesion molecule-1 is preferentially expressed in intestinal tract and associated lymphoid tissue. The American Journal of Pathology *151*, 97–110.

Broomé, U. and Bergquist, A. (2006). Primary sclerosing cholangitis, inflammatory bowel disease, and colon cancer. Seminars in Liver Disease *26*, 31–41.

Bruder, D., Probst-Kepper, M., Westendorf, A. M., Geffers, R., Beissert, S., Loser, K., Boehmer, H. v., Buer, J. and Hansen, W. (2004). Neuropilin-1: a surface marker of regulatory T cells. European Journal of Immunology *34*, 623–630.

Butcher, E. C. (1991). Leukocyte-endothelial cell recognition: three (or more) steps to specificity and diversity. Cell *67*, 1033–1036.

Buxbaum, J., Qian, P., Allen, P. M. and Peters, M. G. (2008). Hepatitis resulting from liver-specific expression and recognition of self-antigen. Journal of autoimmunity *31*, 208–215.

Calne, R. Y., Sells, R. A., Pena, J. R., Davis, D. R., Millard, P. R., Herbertson, B. M., Binns, R. M. and Davies, D. A. (1969). Induction of immunological tolerance by porcine liver allografts. Nature *223*, 472–476.

Campbell, J. J., Haraldsen, G., Pan, J., Rottman, J., Qin, S., Ponath, P., Andrew, D. P., Warnke, R., Ruffing, N., Kassam, N., Wu, L. and Butcher, E. C. (1999). The chemokine receptor CCR4 in vascular recognition by cutaneous but not intestinal memory T cells. Nature *400*, 776–780.

Carramolino, L., Zaballos, A., Kremer, L., Villares, R., Martin, P., Ardavin, C., Martinez-A, C. and Marquez, G. (2001). Expression of CCR9 beta-chemokine receptor is modulated in thymocyte differentiation and is selectively maintained in CD8(+) T cells from secondary lymphoid organs. Blood *97*, 850–857.

Cernuda-Morollon, E., Gharbi, S. and Millan, J. (2010). Discriminating between the paracellular and transcellular routes of diapedesis. Methods in Molecular Biology *616*, 69–82.

Cerwenka, A., Carter, L. L., Reome, J. B., Swain, S. L. and Dutton, R. W. (1998). In vivo persistence of CD8 polarized T cell subsets producing type 1 or type 2 cytokines. Journal of Immunology *161*, 97–105.

Chapman, R. W., Arborgh, B. A., Rhodes, J. M., Summerfield, J. A., Dick, R., Scheuer, P. J. and Sherlock, S. (1980). Primary sclerosing cholangitis: a review of its clinical features, cholangiography, and hepatic histology. Gut *21*, 870–877.

Chen, L. (2004). Co-inhibitory molecules of the B7-CD28 family in the control of T-cell immunity. Nature Reviews Immunology *4*, 336–347.

Chen, Y., Jiang, G., Yang, H.-R., Gu, X., Wang, L., Hsieh, C.-C., Chou, H.-S., Fung, J. J., Qian, S. and Lu, L. (2009). Distinct response of liver myeloid

dendritic cells to endotoxin is mediated by IL-27. Journal of Hepatology *51*, 510–519.

Cooper, G. S., Miller, F. W. and Pandey, J. P. (1999). The role of genetic factors in autoimmune disease: implications for environmental research. Environmental Health Perspectives *107 Suppl 5*, 693–700.

Cornall, R. J., Goodnow, C. C. and Cyster, J. G. (1995). The regulation of self-reactive B cells. Current Opinion in Immunology *7*, 804–811.

Couvelard, A., Scoazec, J. Y. and Feldmann, G. (1993). Expression of cell-cell and cell-matrix adhesion proteins by sinusoidal endothelial cells in the normal and cirrhotic human liver. The American Journal of Pathology *143*, 738–752.

Crispe, I. N., Dao, T., Klugewitz, K., Mehal, W. Z. and Metz, D. P. (2000). The liver as a site of T-cell apoptosis: graveyard, or killing field? Immunological Reviews *174*, 47–62.

Curbishley, S. M., Eksteen, B., Gladue, R. P., Lalor, P. and Adams, D. H. (2005). CXCR 3 activation promotes lymphocyte transendothelial migration across human hepatic endothelium under fluid flow. The American Journal of Pathology *167*, 887–899.

Cyster, J. G. (1999). Chemokines and cell migration in secondary lymphoid organs. Science *286*, 2098–2102.

Dao, T., Mehal, W. Z. and Crispe, I. N. (1998). IL-18 augments perforin-dependent cytotoxicity of liver NK-T cells. Journal of Immunology *161*, 2217–2222.

Derkow, K., Loddenkemper, C., Mintern, J., Kruse, N., Klugewitz, K., Berg, T., Wiedenmann, B., Ploegh, H. L. and Schott, E. (2007). Differential priming of CD8 and CD4 T-cells in animal models of autoimmune hepatitis and cholangitis. Hepatology *46*, 1155–1165.

Derkow, K., Müller, A., Eickmeier, I., Seidel, D., Rust Moreira, M. V., Kruse, N., Klugewitz, K., Mintern, J., Wiedenmann, B. and Schott, E. (2011).

Failure of CD4 T-cells to respond to liver-derived antigen and to provide help to CD8 T-cells. PloS One *6*, e21847.

Diehl, L., Schurich, A., Grochtmann, R., Hegenbarth, S., Chen, L. and Knolle, P. A. (2008). Tolerogenic maturation of liver sinusoidal endothelial cells promotes B7-homolog 1-dependent CD8+ T cell tolerance. Hepatology *47*, 296–305.

Dunham, R. M., Thapa, M., Velazquez, V. M., Elrod, E. J., Denning, T. L., Pulendran, B. and Grakoui, A. (2013). Hepatic stellate cells preferentially induce Foxp3+ regulatory T cells by production of retinoic acid. Journal of Immunology *190*, 2009–2016.

Ebrahimkhani, M. R., Mohar, I. and Crispe, I. N. (2011). Cross-presentation of antigen by diverse subsets of murine liver cells. Hepatology *54*, 1379–1387.

Efe, C., Wahlin, S., Ozaslan, E., Berlot, A. H., Purnak, T., Muratori, L., Quarneti, C., Yuksel, O., Thiefin, G. and Muratori, P. (2012). Autoimmune hepatitis/primary biliary cirrhosis overlap syndrome and associated extrahepatic autoimmune diseases. European Journal of Gastroenterology & Hepatology *24*, 531–534.

Eipel, C., Hirschmann, M., Abshagen, K., Menger, M. D. and Vollmar, B. (2007). Local interaction of apoptotic hepatocytes and Kupffer cells in a rat model of systemic endotoxemia. Hepatology Research *37*, 863–871.

Eksteen, B., Grant, A. J., Miles, A., Curbishley, S. M., Lalor, P. F., Hübscher, S. G., Briskin, M., Salmon, M. and Adams, D. H. (2004). Hepatic endothelial CCL25 mediates the recruitment of CCR9+ gut-homing lymphocytes to the liver in primary sclerosing cholangitis. The Journal of Experimental Medicine *200*, 1511–1517.

Eksteen, B., Mora, J. R., Haughton, E. L., Henderson, N. C., Lee-Turner, L., Villablanca, E. J., Curbishley, S. M., Aspinall, A. I., Andrian, U. H. v. and Adams, D. H. (2009). Gut homing receptors on CD8 T cells are retinoic acid dependent and not maintained by liver dendritic or stellate cells. Gastroenterology *137*, 320–329.

Eri, R., Jonsson, J. R., Pandeya, N., Purdie, D. M., Clouston, A. D., Martin, N., Duffy, D., Powell, E. E., Fawcett, J., Florin, T. H. J. and Radford-Smith, G. L. (2004). CCR5-Delta32 mutation is strongly associated with primary sclerosing cholangitis. Genes and Immunity *5*, 444–450.

Fausa, O., Schrumpf, E. and Elgjo, K. (1991). Relationship of inflammatory bowel disease and primary sclerosing cholangitis. Seminars in Liver Disease *11*, 31–39.

Förster, R., Davalos-Misslitz, A. C. and Rot, A. (2008). CCR7 and its ligands: balancing immunity and tolerance. Nature Reviews Immunology *8*, 362–371.

Franco, A., Barnaba, V., Natali, P., Balsano, C., Musca, A. and Balsano, F. (1988). Expression of class I and class II major histocompatibility complex antigens on human hepatocytes. Hepatology *8*, 449–454.

Frith, J. C., Mönkkönen, J., Blackburn, G. M., Russell, R. G. and Rogers, M. J. (1997). Clodronate and liposome-encapsulated clodronate are metabolized to a toxic ATP analog, adenosine 5'-(beta, gamma-dichloromethylene) triphosphate, by mammalian cells in vitro. Journal of Bone and Mineral Research *12*, 1358–1367.

Fussey, S. P., Ali, S. T., Guest, J. R., James, O. F., Bassendine, M. F. and Yeaman, S. J. (1990). Reactivity of primary biliary cirrhosis sera with Escherichia coli dihydrolipoamide acetyltransferase (E2p): characterization of the main immunogenic region. Proc. Natl. Acad. Sci. U.S.A. *87*, 3987–3991.

Fussey, S. P., Guest, J. R., James, O. F., Bassendine, M. F. and Yeaman, S. J. (1988). Identification and analysis of the major M2 autoantigens in primary biliary cirrhosis. Proc. Natl. Acad. Sci. U.S.A. *85*, 8654–8658.

Gallegos, A. M. and Bevan, M. J. (2006). Central tolerance: good but imperfect. Immunological Reviews *209*, 290–296.

Giannoukakis, N., Phillips, B., Finegold, D., Harnaha, J. and Trucco, M. (2011). Phase I (safety) study of autologous tolerogenic dendritic cells in type 1 diabetic patients. Diabetes care *34*, 2026–2032.

Goddard, S., Youster, J., Morgan, E. and Adams, D. H. (2004). Interleukin-10 secretion differentiates dendritic cells from human liver and skin. The American Journal of Pathology *164*, 511–519.

Gossard, A. A. and Lindor, K. D. (2012). Autoimmune hepatitis: a review. Journal of Gastroenterology *47*, 498–503.

Goubier, A., Dubois, B., Gheit, H., Joubert, G., Villard-Truc, F., Asselin-Paturel, C., Trinchieri, G. and Kaiserlian, D. (2008). Plasmacytoid dendritic cells mediate oral tolerance. Immunity *29*, 464–475.

Grant, A. J., Lalor, P. F., Hübscher, S. G., Briskin, M. and Adams, D. H. (2001). MAdCAM-1 expressed in chronic inflammatory liver disease supports mucosal lymphocyte adhesion to hepatic endothelium (MAdCAM-1 in chronic inflammatory liver disease). Hepatology *33*, 1065–1072.

Gressner, A. M. and Weiskirchen, R. (2006). Modern pathogenetic concepts of liver fibrosis suggest stellate cells and TGF-beta as major players and therapeutic targets. Journal of Cellular and Molecular Medicine *10*, 76–99.

Gupta, A., Kumar, C. A., Ningappa, M., Sun, Q., Higgs, B. W., Snyder, S., Zeevi, A., Thomson, A. W., Mazariegos, G. V. and Sindhi, R. (2009). Elevated myeloid: plasmacytoid dendritic cell ratio associates with late, but not early, liver rejection in children induced with rabbit anti-human thymocyte globulin. Transplantation *88*, 589–594.

Hamann, A., Klugewitz, K., Austrup, F. and Jablonski-Westrich, D. (2000). Activation induces rapid and profound alterations in the trafficking of T cells. European Journal of Immunology *30*, 3207–3218.

Hänninen, A., Maksimow, M., Alam, C., Morgan, D. J. and Jalkanen, S. (2011). Ly6C supports preferential homing of central memory CD8+ T cells into lymph nodes. European Journal of Immunology *41*, 634–644.

Herkel, J., Jagemann, B., Wiegard, C., Lazaro, J. F. G., Lueth, S., Kanzler, S., Blessing, M., Schmitt, E. and Lohse, A. W. (2003). MHC class II-expressing hepatocytes function as antigen-presenting cells and activate specific CD4 T lymphocytes. Hepatology *37*, 1079–1085.

Heydtmann, M., Lalor, P. F., Eksteen, J. A., Hubscher, S. G., Briskin, M. and Adams, D. H. (2005). CXC chemokine ligand 16 promotes integrin-mediated adhesion of liver-infiltrating lymphocytes to cholangiocytes and hepatocytes within the inflamed human liver. Journal of Immunology *174*, 1055–1062.

Hillan, K. J., Hagler, K. E., MacSween, R. N., Ryan, A. M., Renz, M. E., Chiu, H. H., Ferrier, R. K., Bird, G. L., Dhillon, A. P., Ferrell, L. D. and Fong, S. (1999). Expression of the mucosal vascular addressin, MAdCAM-1, in inflammatory liver disease. Liver International *19*, 509–518.

Hirakata, Y., Tomono, K., Tateda, K., Matsumoto, T., Furuya, N., Shimoguchi, K., Kaku, M. and Yamaguchi, K. (1991). Role of bacterial association with Kupffer cells in occurrence of endogenous systemic bacteremia. Infection and Immunity *59*, 289–294.

Hirschfield, G. M. and Gershwin, M. E. (2011). Primary biliary cirrhosis: one disease with many faces. The Israel Medical Association Journal *13*, 55–59.

Hirschfield, G. M., Liu, X., Xu, C., Lu, Y., Xie, G., Lu, Y., Gu, X., Walker, E. J., Jing, K., Juran, B. D., Mason, A. L., Myers, R. P., Peltekian, K. M., Ghent, C. N., Coltescu, C., Atkinson, E. J., Heathcote, E. J., Lazaridis, K. N., Amos, C. I. and Siminovitch, K. A. (2009). Primary biliary cirrhosis associated with HLA, IL12A, and IL12RB2 variants. The New England Journal of Medicine *360*, 2544–2555.

Hogquist, K. A., Jameson, S. C., Heath, W. R., Howard, J. L., Bevan, M. J. and Carbone, F. R. (1994). T cell receptor antagonist peptides induce positive selection. Cell *76*, 17–27.

Holdener, M., Hintermann, E., Bayer, M., Rhode, A., Rodrigo, E., Hintereder, G., Johnson, E. F., Gonzalez, F. J., Pfeilschifter, J., Manns, M. P., Herrath, M. v. G. and Christen, U. (2008). Breaking tolerance to the natural human liver autoantigen cytochrome P450 2D6 by virus infection. The Journal of Experimental Medicine *205*, 1409–1422.

Holz, L. E., Benseler, V., Bowen, D. G., Bouillet, P., Strasser, A., O'Reilly, L., d'Avigdor, W. M. H., Bishop, A. G., McCaughan, G. W. and Bertolino, P.

(2008). Intrahepatic murine CD8 T-cell activation associates with a distinct phenotype leading to Bim-dependent death. Gastroenterology *135*, 989–997.

Homey, B., Alenius, H., Müller, A., Soto, H., Bowman, E. P., Yuan, W., McEvoy, L., Lauerma, A. I., Assmann, T., Bünemann, E., Lehto, M., Wolff, H., Yen, D., Marxhausen, H., To, W., Sedgwick, J., Ruzicka, T., Lehmann, P. and Zlotnik, A. (2002). CCL27-CCR10 interactions regulate T cell-mediated skin inflammation. Nature Medicine *8*, 157–165.

Houssin, D., Gigou, M., Franco, D., Bismuth, H., Charpentier, B., Lang, P. and Martin, E. (1980). Specific transplantation tolerance induced by spontaneously tolerated liver allograft in inbred strains of rats. Transplantation *29*, 418–419.

Hov, J. R., Keitel, V., Laerdahl, J. K., Spomer, L., Ellinghaus, E., ElSharawy, A., Melum, E., Boberg, K. M., Manke, T., Balschun, T., Schramm, C., Bergquist, A., Weismuller, T., Gotthardt, D., Rust, C., Henckaerts, L., Onnie, C. M., Weersma, R. K., Sterneck, M., Teufel, A., Runz, H., Stiehl, A., Ponsioen, C. Y., Wijmenga, C., Vatn, M. H., Stokkers, P. C. F., Vermeire, S., Mathew, C. G., Lie, B. A., Beuers, U., Manns, M. P., Schreiber, S., Schrumpf, E., Haussinger, D., Franke, A. and Karlsen, T. H. (2010). Mutational characterization of the bile acid receptor TGR5 in primary sclerosing cholangitis. PloS One *5*, e12403.

Huang, D. W., Sherman, B. T. and Lempicki, R. A. (2009). Systematic and integrative analysis of large gene lists using DAVID bioinformatics resources. Nature Protocols *4*, 44–57.

Ichikawa, S., Mucida, D., Tyznik, A. J., Kronenberg, M. and Cheroutre, H. (2011). Hepatic stellate cells function as regulatory bystanders. Journal of Immunology *186*, 5549–5555.

Ishibashi, H., Komori, A., Shimoda, S., Ambrosini, Y. M., Gershwin, M. E. and Nakamura, M. (2011). Risk factors and prediction of long-term outcome in primary biliary cirrhosis. Internal Medicine (Tokyo, Japan) *50*, 1–10.

Iwata, M., Hirakiyama, A., Eshima, Y., Kagechika, H., Kato, C. and Song, S.-Y. (2004). Retinoic acid imprints gut-homing specificity on T cells. Immunity *21*, 527–538.

Jiang, G., Yang, H.-R., Wang, L., Wildey, G. M., Fung, J., Qian, S. and Lu, L. (2008). Hepatic stellate cells preferentially expand allogeneic CD4+ CD25+ FoxP3+ regulatory T cells in an IL-2-dependent manner. Transplantation *86*, 1492–1502.

Jiang, Z., Chen, Y., Feng, X., Jiang, J., Chen, T., Xie, H., Zhou, L. and Zheng, S. (2013). Hepatic stellate cells promote immunotolerance following orthotopic liver transplantation in rats via induction of T cell apoptosis and regulation of Th2/Th3-like cell cytokine production. Experimental and Therapeutic Medicine *5*, 165–169.

Johansson-Lindbom, B., Svensson, M., Pabst, O., Palmqvist, C., Marquez, G., Förster, R. and Agace, W. W. (2005). Functional specialization of gut CD103+ dendritic cells in the regulation of tissue-selective T cell homing. The Journal of Experimental Medicine *202*, 1063–1073.

John, B. and Crispe, I. N. (2004). Passive and active mechanisms trap activated CD8+ T cells in the liver. Journal of Immunology *172*, 5222–5229.

Jung, S., Unutmaz, D., Wong, P., Sano, G.-I., los Santos, K. d., Sparwasser, T., Wu, S., Vuthoori, S., Ko, K., Zavala, F., Pamer, E. G., Littman, D. R. and Lang, R. A. (2002). In vivo depletion of CD11c+ dendritic cells abrogates priming of CD8+ T cells by exogenous cell-associated antigens. Immunity *17*, 211–220.

Kakimi, K., Lane, T. E., Chisari, F. V. and Guidotti, L. G. (2001). Cutting edge: Inhibition of hepatitis B virus replication by activated NK T cells does not require inflammatory cell recruitment to the liver. Journal of Immunology *167*, 6701–6705.

Kamada, N., Davies, H. S. and Roser, B. (1981). Reversal of transplantation immunity by liver grafting. Nature *292*, 840–842.

Kaneko, Y., Harada, M., Kawano, T., Yamashita, M., Shibata, Y., Gejyo, F., Nakayama, T. and Taniguchi, M. (2000). Augmentation of Valpha14 NKT cell-mediated cytotoxicity by interleukin 4 in an autocrine mechanism resulting in the development of concanavalin A-induced hepatitis. The Journal of Experimental Medicine *191*, 105–114.

Kantele, A., Zivny, J., Häkkinen, M., Elson, C. O. and Mestecky, J. (1999). Differential homing commitments of antigen-specific T cells after oral or parenteral immunization in humans. Journal of Immunology *162*, 5173–5177.

Karlsen, T. H., Schrumpf, E. and Boberg, K. M. (2010). Update on primary sclerosing cholangitis. Digestive and Liver Disease *42*, 390–400.

Katz, S. C., Pillarisetty, V. G., Bleier, J. I., Shah, A. B. and DeMatteo, R. P. (2004). Liver sinusoidal endothelial cells are insufficient to activate T cells. Journal of Immunology *173*, 230–235.

Kelly, A., Fahey, R., Fletcher, J. M., Keogh, C., Carroll, A. G., Siddachari, R., Geoghegan, J., Hegarty, J. E., Ryan, E. J. and O'Farrelly, C. (2013). CD141 myeloid dendritic cells are enriched in healthy human liver. Journal of Hepatology *in press*.

Kerkar, N., Choudhuri, K., Ma, Y., Mahmoud, A., Bogdanos, D. P., Muratori, L., Bianchi, F., Williams, R., Mieli-Vergani, G. and Vergani, D. (2003). Cytochrome P4502D6(193-212): a new immunodominant epitope and target of virus/self cross-reactivity in liver kidney microsomal autoantibody type 1-positive liver disease. Journal of Immunology *170*, 1481–1489.

Kingham, T. P., Chaudhry, U. I., Plitas, G., Katz, S. C., Raab, J. and DeMatteo, R. P. (2007). Murine liver plasmacytoid dendritic cells become potent immunostimulatory cells after Flt-3 ligand expansion. Hepatology *45*, 445–454.

Kinoshita, M., Uchida, T., Sato, A., Nakashima, M., Nakashima, H., Shono, S., Habu, Y., Miyazaki, H., Hiroi, S. and Seki, S. (2010). Characterization of

two F4/80-positive Kupffer cell subsets by their function and phenotype in mice. Journal of Hepatology *53*, 903–910.

Kita, H., Lian, Z.-X., van de Water, J., He, X.-S., Matsumura, S., Kaplan, M., Luketic, V., Coppel, R. L., Ansari, A. A. and Gershwin, M. E. (2002). Identification of HLA-A2-restricted CD8(+) cytotoxic T cell responses in primary biliary cirrhosis: T cell activation is augmented by immune complexes cross-presented by dendritic cells. The Journal of Experimental Medicine *195*, 113–123.

Klein, I. and Crispe, I. N. (2006). Complete differentiation of CD8+ T cells activated locally within the transplanted liver. The Journal of Experimental Medicine *203*, 437–447.

Knolle, P., Schlaak, J., Uhrig, A., Kempf, P., Zum Meyer Buschenfelde, K. H. and Gerken, G. (1995). Human Kupffer cells secrete IL-10 in response to lipopolysaccharide (LPS) challenge. Journal of Hepatology *22*, 226–229.

Knolle, P. A., Gerken, G., Loser, E., Dienes, H. P., Gantner, F., Tiegs, G., Zum Meyer Buschenfelde, K. H. and Lohse, A. W. (1996). Role of sinusoidal endothelial cells of the liver in concanavalin A-induced hepatic injury in mice. Hepatology *24*, 824–829.

Knolle, P. A., Germann, T., Treichel, U., Uhrig, A., Schmitt, E., Hegenbarth, S., Lohse, A. W. and Gerken, G. (1999). Endotoxin down-regulates T cell activation by antigen-presenting liver sinusoidal endothelial cells. Journal of Immunology *162*, 1401–1407.

Knolle, P. A., Uhrig, A., Hegenbarth, S., Loser, E., Schmitt, E., Gerken, G. and Lohse, A. W. (1998). IL-10 down-regulates T cell activation by antigen-presenting liver sinusoidal endothelial cells through decreased antigen uptake via the mannose receptor and lowered surface expression of accessory molecules. Clinical and Experimental Immunology *114*, 427–433.

Kolodkin, A. L., Levengood, D. V., Rowe, E. G., Tai, Y. T., Giger, R. J. and Ginty, D. D. (1997). Neuropilin is a semaphorin III receptor. Cell *90*, 753–762.

Kotzin, B. L. (1996). Systemic lupus erythematosus. Cell *85*, 303–306.

Krawitt, E. L. (2006). Autoimmune hepatitis. The New England Journal of Medicine *354*, 54–66.

Kruse, N., Neumann, K., Schrage, A., Derkow, K., Schott, E., Erben, U., Kuhl, A., Loddenkemper, C., Zeitz, M., Hamann, A. and Klugewitz, K. (2009). Priming of CD4+ T cells by liver sinusoidal endothelial cells induces CD25low forkhead box protein 3- regulatory T cells suppressing autoimmune hepatitis. Hepatology *50*, 1904–1913.

Kunkel, E. J., Campbell, J. J., Haraldsen, G., Pan, J., Boisvert, J., Roberts, A. I., Ebert, E. C., Vierra, M. A., Goodman, S. B., Genovese, M. C., Wardlaw, A. J., Greenberg, H. B., Parker, C. M., Butcher, E. C., Andrew, D. P. and Agace, W. W. (2000). Lymphocyte CC chemokine receptor 9 and epithelial thymus-expressed chemokine (TECK) expression distinguish the small intestinal immune compartment: Epithelial expression of tissue-specific chemokines as an organizing principle in regional immunity. The Journal of Experimental Medicine *192*, 761–768.

Kurts, C., Cannarile, M., Klebba, I. and Brocker, T. (2001). Dendritic cells are sufficient to cross-present self-antigens to CD8 T cells in vivo. Journal of Immunology *166*, 1439–1442.

Küsters, S., Gantner, F., Kunstle, G. and Tiegs, G. (1996). Interferon gamma plays a critical role in T cell-dependent liver injury in mice initiated by concanavalin A. Gastroenterology *111*, 462–471.

Lang, M., Kahl, A., Bechstein, W. O., Neumann, U., Settmacher, U., Frei, U. and Neuhaus, P. (1998). Combined liver-kidney transplantation: long-term follow-up in 18 patients. Transplantation Proceedings *30*, 1865–1867.

Larrubia, J.-R., Calvino, M., Benito, S., Sanz-de Villalobos, E., Perna, C., Perez-Hornedo, J., Gonzalez-Mateos, F., Garcia-Garzon, S., Bienvenido, A. and Parra, T. (2007). The role of CCR5/CXCR3 expressing CD8+ cells in liver damage and viral control during persistent hepatitis C virus infection. Journal of Hepatology *47*, 632–641.

LaRusso, N. F., Shneider, B. L., Black, D., Gores, G. J., James, S. P., Doo, E. and Hoofnagle, J. H. (2006). Primary sclerosing cholangitis: summary of a workshop. Hepatology *44*, 746–764.

Lehenkari, P. P., Kellinsalmi, M., Näpänkangas, J. P., Ylitalo, K. V., Mönkkönen, J., Rogers, M. J., Azhayev, A., Väänänen, H. K. and Hassinen, I. E. (2002). Further insight into mechanism of action of clodronate: inhibition of mitochondrial ADP/ATP translocase by a nonhydrolyzable, adenine-containing metabolite. Molecular Pharmacology *61*, 1255–1262.

Leiriao, P., Mota, M. M. and Rodriguez, A. (2005). Apoptotic Plasmodium-infected hepatocytes provide antigens to liver dendritic cells. The Journal of infectious diseases *191*, 1576–1581.

Lepre, J., Rice, J. J., Tu, Y. and Stolovitzky, G. (2004). Genes@Work: an efficient algorithm for pattern discovery and multivariate feature selection in gene expression data. Bioinformatics *20*, 1033–1044.

Ley, K. and Kansas, G. S. (2004). Selectins in T-cell recruitment to non-lymphoid tissues and sites of inflammation. Nature Reviews Immunology *4*, 325–335.

Li, D. and Friedman, S. L. (1999). Liver fibrogenesis and the role of hepatic stellate cells: new insights and prospects for therapy. Journal of Gastroenterology *14*, 618–633.

Lian, Z.-X., Okada, T., He, X.-S., Kita, H., Liu, Y.-J., Ansari, A. A., Kikuchi, K., Ikehara, S. and Gershwin, M. E. (2003). Heterogeneity of dendritic cells in the mouse liver: identification and characterization of four distinct populations. Journal of Immunology *170*, 2323–2330.

Liaskou, E., Karikoski, M., Reynolds, G. M., Lalor, P. F., Weston, C. J., Pullen, N., Salmi, M., Jalkanen, S. and Adams, D. H. (2011). Regulation of mucosal addressin cell adhesion molecule 1 expression in human and mice by vascular adhesion protein 1 amine oxidase activity. Hepatology *53*, 661–672.

Lichtman, S. N., Wang, J. and Lemasters, J. J. (1998). Lipopolysaccharide-stimulated TNF-alpha release from cultured rat Kupffer cells: sequence of intracellular signaling pathways. Journal of Leukocyte Biology *64*, 368–372.

Limmer, A., Ohl, J., Kurts, C., Ljunggren, H. G., Reiss, Y., Groettrup, M., Momburg, F., Arnold, B. and Knolle, P. A. (2000). Efficient presentation of exogenous antigen by liver endothelial cells to CD8+ T cells results in antigen-specific T-cell tolerance. Nature Medicine *6*, 1348–1354.

Limmer, A., Sacher, T., Alferink, J., Kretschmar, M., Schonrich, G., Nichterlein, T., Arnold, B. and Hammerling, G. J. (1998). Failure to induce organ-specific autoimmunity by breaking of tolerance: importance of the microenvironment. European Journal of Immunology *28*, 2395–2406.

Liu, G. Y., Fairchild, P. J., Smith, R. M., Prowle, J. R., Kioussis, D. and Wraith, D. C. (1995). Low avidity recognition of self-antigen by T cells permits escape from central tolerance. Immunity *3*, 407–415.

Liu, Z. X., Govindarajan, S., Okamoto, S. and Dennert, G. (2001). Fas-mediated apoptosis causes elimination of virus-specific cytotoxic T cells in the virus-infected liver. Journal of Immunology *166*, 3035–3041.

Lloyd, C. M., Phillips, A. R. J., Cooper, G. J. S. and Dunbar, P. R. (2008). Three-colour fluorescence immunohistochemistry reveals the diversity of cells staining for macrophage markers in murine spleen and liver. Journal of Immunological Methods *334*, 70–81.

Loftus, E. V., Harewood, G. C., Loftus, C. G., Tremaine, W. J., Harmsen, W. S., Zinsmeister, A. R., Jewell, D. A. and Sandborn, W. J. (2005). PSC-IBD: a unique form of inflammatory bowel disease associated with primary sclerosing cholangitis. Gut *54*, 91–96.

Lohse, A. W., Dinkelmann, M., Kimmig, M., Herkel, J. and Zum Meyer Büschenfelde, K. H. (1996). Estimation of the frequency of self-reactive T cells in health and inflammatory diseases by limiting dilution analysis and single cell cloning. Journal of Autoimmunity *9*, 667–675.

Luckheeram, R. V., Zhou, R., Verma, A. D. and Xia, B. (2012). CD4(+)T cells: differentiation and functions. Clinical & Developmental Immunology *2012*, 925135.

Luettig, B., Pape, L., Bode, U., Bell, E. B., Sparshott, S. M., Wagner, S. and Westermann, J. (1999). Naive and memory T lymphocytes migrate in comparable numbers through normal rat liver: activated T cells accumulate in the periportal field. Journal of Immunology *163*, 4300–4307.

Luo, B.-H., Carman, C. V. and Springer, T. A. (2007). Structural basis of integrin regulation and signaling. Annual Review of Immunology *25*, 619–647.

MacPhee, P. J., Schmidt, E. E. and Groom, A. C. (1995). Intermittence of blood flow in liver sinusoids, studied by high-resolution in vivo microscopy. The American Journal of Physiology *269*, G692–8.

Manns, M. P., Griffin, K. J., Sullivan, K. F. and Johnson, E. F. (1991). LKM-1 autoantibodies recognize a short linear sequence in P450IID6, a cytochrome P-450 monooxygenase. The Journal of Clinical Investigation *88*, 1370–1378.

Manns, M. P. and Vergani, D. (2009). Autoimmune hepatitis. Seminars in Liver Disease *29*, 239–240.

Matta, B. M., Raimondi, G., Rosborough, B. R., Sumpter, T. L. and Thomson, A. W. (2012). IL-27 production and STAT3-dependent upregulation of B7-H1 mediate immune regulatory functions of liver plasmacytoid dendritic cells. Journal of Immunology *188*, 5227–5237.

Mehal, W. Z., Azzaroli, F. and Crispe, I. N. (2001). Antigen presentation by liver cells controls intrahepatic T cell trapping, whereas bone marrow-derived cells preferentially promote intrahepatic T cell apoptosis. Journal of Immunology *167*, 667–673.

Mehal, W. Z., Juedes, A. E. and Crispe, I. N. (1999). Selective retention of activated CD8+ T cells by the normal liver. Journal of Immunology *163*, 3202–3210.

Menssen, A., Edinger, G., Grün, J. R., Haase, U., Baumgrass, R., Grützkau, A., Radbruch, A., Burmester, G.-R. and Häupl, T. (2009). SiPaGene: A new repository for instant online retrieval, sharing and meta-analyses of GeneChip expression data. BMC Genomics *10*, 98.

Michaels, A. and Levy, C. (2008). Endoscopic and surgical management of primary sclerosing cholangitis. Medscape Journal of Medicine *10*, 242.

Miller, J. F., Kurts, C., Allison, J., Kosaka, H., Carbone, F. and Heath, W. R. (1998). Induction of peripheral CD8+ T-cell tolerance by cross-presentation of self antigens. Immunological Reviews *165*, 267–277.

Milpied, P., Renand, A., Bruneau, J., Mendes-da Cruz, D. A., Jacquelin, S., Asnafi, V., Rubio, M.-T., MacIntyre, E., Lepelletier, Y. and Hermine, O. (2009). Neuropilin-1 is not a marker of human Foxp3+ Treg. European Journal of Immunology *39*, 1466–1471.

Mondino, A., Khoruts, A. and Jenkins, M. K. (1996). The anatomy of T-cell activation and tolerance. Proc. Natl. Acad. Sci. U.S.A. *93*, 2245–2252.

Mora, J. R., Cheng, G., Picarella, D., Briskin, M., Buchanan, N. and Andrian, U. H. v. (2005). Reciprocal and dynamic control of CD8 T cell homing by dendritic cells from skin- and gut-associated lymphoid tissues. The Journal of Experimental Medicine *201*, 303–316.

Moreno, C., Gustot, T., Nicaise, C., Quertinmont, E., Nagy, N., Parmentier, M., Le Moine, O., Deviere, J. and Louis, H. (2005). CCR5 deficiency exacerbates T-cell-mediated hepatitis in mice. Hepatology *42*, 854–862.

Mori, Y., Mori, T., Ueda, S., Yoshida, H., Iesato, K., Wakashin, Y., Wakashin, M. and Okuda, K. (1985). Study of cellular immunity in experimental autoimmune hepatitis in mice: transfer of spleen cells sensitized with liver proteins. Clinical and Experimental Immunology *61*, 577–584.

Murai, M., Yoneyama, H., Harada, A., Yi, Z., Vestergaard, C., Guo, B., Suzuki, K., Asakura, H. and Matsushima, K. (1999). Active participation of CCR5(+)CD8(+) T lymphocytes in the pathogenesis of liver injury in graft-versus-host disease. The Journal of Clinical Investigation *104*, 49–57.

Narumi, S., Tominaga, Y., Tamaru, M., Shimai, S., Okumura, H., Nishioji, K., Itoh, Y. and Okanoue, T. (1997). Expression of IFN-inducible protein-10 in chronic hepatitis. Journal of Immunology *158*, 5536–5544.

Neefjes, J., Jongsma, M. L. M., Paul, P. and Bakke, O. (2011). Towards a systems understanding of MHC class I and MHC class II antigen presentation. Nature Reviews Immunology *11*, 823–836.

Neumann, K., Kruse, N., Szilagyi, B., Erben, U., Rudolph, C., Flach, A., Zeitz, M., Hamann, A. and Klugewitz, K. (2012). Connecting liver and gut: murine liver sinusoidal endothelium induces gut tropism of CD4+ T cells via retinoic acid. Hepatology *55*, 1976–1984.

Nimmerjahn, F., Milosevic, S., Behrends, U., Jaffee, E. M., Pardoll, D. M., Bornkamm, G. W. and Mautner, J. (2003). Major histocompatibility complex class II-restricted presentation of a cytosolic antigen by autophagy. European Journal of Immunology *33*, 1250–1259.

Norris, S., Collins, C., Doherty, D. G., Smith, F., McEntee, G., Traynor, O., Nolan, N., Hegarty, J. and O'Farrelly, C. (1998). Resident human hepatic lymphocytes are phenotypically different from circulating lymphocytes. Journal of Hepatology *28*, 84–90.

O'Connell, P. J., Morelli, A. E., Logar, A. J. and Thomson, A. W. (2000). Phenotypic and functional characterization of mouse hepatic CD8 alpha+ lymphoid-related dendritic cells. Journal of Immunology *165*, 795–803.

O'Connell, P. J., Son, Y.-I., Giermasz, A., Wang, Z., Logar, A. J., Thomson, A. W. and Kalinski, P. (2003). Type-1 polarized nature of mouse liver CD8alpha- and CD8alpha+ dendritic cells: tissue-dependent differences offset CD8alpha-related dendritic cell heterogeneity. European Journal of Immunology *33*, 2007–2013.

Okamura, H., Tsutsi, H., Komatsu, T., Yutsudo, M., Hakura, A., Tanimoto, T., Torigoe, K., Okura, T., Nukada, Y. and Hattori, K. (1995). Cloning of a new cytokine that induces IFN-gamma production by T cells. Nature *378*, 88–91.

Oppen, N. v., Schurich, A., Hegenbarth, S., Stabenow, D., Tolba, R., Weiskirchen, R., Geerts, A., Kolanus, W., Knolle, P. and Diehl, L. (2009). Systemic antigen cross-presented by liver sinusoidal endothelial cells induces liver-specific CD8 T-cell retention and tolerization. Hepatology *49*, 1664–1672.

Oyoshi, M. K., Elkhal, A., Scott, J. E., Wurbel, M.-A., Hornick, J. L., Campbell, J. J. and Geha, R. S. (2011). Epicutaneous challenge of orally immunized mice redirects antigen-specific gut-homing T cells to the skin. The Journal of Clinical Investigation *121*, 2210–2220.

Papadakis, K. A., Prehn, J., Nelson, V., Cheng, L., Binder, S. W., Ponath, P. D., Andrew, D. P. and Targan, S. R. (2000). The role of thymus-expressed chemokine and its receptor CCR9 on lymphocytes in the regional specialization of the mucosal immune system. Journal of Immunology *165*, 5069–5076.

Picker, L. J., Kishimoto, T. K., Smith, C. W., Warnock, R. A. and Butcher, E. C. (1991). ELAM-1 is an adhesion molecule for skin-homing T cells. Nature *349*, 796–799.

Pillarisetty, V. G., Katz, S. C., Bleier, J. I., Shah, A. B. and DeMatteo, R. P. (2005). Natural killer dendritic cells have both antigen presenting and lytic function and in response to CpG produce IFN-gamma via autocrine IL-12. Journal of Immunology *174*, 2612–2618.

Plitas, G., Burt, B. M., Stableford, J. A., Nguyen, H. M., Welles, A. P. and DeMatteo, R. P. (2008). Dendritic cells are required for effective cross-presentation in the murine liver. Hepatology *47*, 1343–1351.

Probst, H. C., McCoy, K., Okazaki, T., Honjo, T. and van den Broek, M. (2005). Resting dendritic cells induce peripheral CD8+ T cell tolerance through PD-1 and CTLA-4. Nature Immunology *6*, 280–286.

Racanelli, V. and Rehermann, B. (2006). The liver as an immunological organ. Hepatology *43*, S54–62.

Rasmussen, A., Davies, H. F., Jamieson, N. V., Evans, D. B. and Calne, R. Y. (1995). Combined transplantation of liver and kidney from the same

donor protects the kidney from rejection and improves kidney graft survival. Transplantation *59*, 919–921.

Roland, C. R., Walp, L., Stack, R. M. and Flye, M. W. (1994). Outcome of Kupffer cell antigen presentation to a cloned murine Th1 lymphocyte depends on the inducibility of nitric oxide synthase by IFN-gamma. Journal of Immunology *153*, 5453–5464.

Rust, C. and Beuers, U. (2008). Overlap syndromes among autoimmune liver diseases. World Journal of Gastroenterology *14*, 3368–3373.

Sacher, T., Knolle, P., Nichterlein, T., Arnold, B., Hammerling, G. J. and Limmer, A. (2002). CpG-ODN-induced inflammation is sufficient to cause T-cell-mediated autoaggression against hepatocytes. European Journal of Immunology *32*, 3628–3637.

Saich, R. and Chapman, R. (2008). Primary sclerosing cholangitis, autoimmune hepatitis and overlap syndromes in inflammatory bowel disease. World Journal of Gastroenterology *14*, 331–337.

Sakaguchi, S., Ono, M., Setoguchi, R., Yagi, H., Hori, S., Fehervari, Z., Shimizu, J., Takahashi, T. and Nomura, T. (2006). Foxp3+ CD25+ CD4+ natural regulatory T cells in dominant self-tolerance and autoimmune disease. Immunological Reviews *212*, 8–27.

Sallusto, F., Lenig, D., Forster, R., Lipp, M. and Lanzavecchia, A. (1999). Two subsets of memory T lymphocytes with distinct homing potentials and effector functions. Nature *401*, 708–712.

Sarris, M., Andersen, K. G., Randow, F., Mayr, L. and Betz, A. G. (2008). Neuropilin-1 expression on regulatory T cells enhances their interactions with dendritic cells during antigen recognition. Immunity *28*, 402–413.

Sato, T., Habtezion, A., Beilhack, A., Schulz, S., Butcher, E. and Thorlacius, H. (2006). Short-term homing assay reveals a critical role for lymphocyte function-associated antigen-1 in the hepatic recruitment of lymphocytes in graft-versus-host disease. Journal of Hepatology *44*, 1132–1140.

Sato, T., Thorlacius, H., Johnston, B., Staton, T. L., Xiang, W., Littman, D. R. and Butcher, E. C. (2005). Role for CXCR6 in recruitment of activated CD8+ lymphocytes to inflamed liver. Journal of Immunology *174*, 277–283.

Schildberg, F. A., Hegenbarth, S. I., Schumak, B., Scholz, K., Limmer, A. and Knolle, P. A. (2008). Liver sinusoidal endothelial cells veto CD8 T cell activation by antigen-presenting dendritic cells. European Journal of Immunology *38*, 957–967.

Schmid, D., Pypaert, M. and Munz, C. (2007). Antigen-loading compartments for major histocompatibility complex class II molecules continuously receive input from autophagosomes. Immunity *26*, 79–92.

Schumann, J., Wolf, D., Pahl, A., Brune, K., Papadopoulos, T., van Rooijen, N. and Tiegs, G. (2000). Importance of Kupffer cells for T-cell-dependent liver injury in mice. The American Journal of Pathology *157*, 1671–1683.

Seidel, D., Eickmeier, I., Kühl, A. A., Hamann, A., Loddenkemper, C. and Schott, E. (2013). CD8 T cells primed in the gut-associated lymphoid tissue induce immune-mediated cholangitis in mice. Hepatology *doi: 10.1002/hep.26702*.

Selmi, C., Balkwill, D. L., Invernizzi, P., Ansari, A. A., Coppel, R. L., Podda, M., Leung, P. S., Kenny, T. P., van de Water, J., Nantz, M. H., Kurth, M. J. and Gershwin, M. E. (2003). Patients with primary biliary cirrhosis react against a ubiquitous xenobiotic-metabolizing bacterium. Hepatology *38*, 1250–1257.

Selmi, C., Mackay, I. R. and Gershwin, M. E. (2007). The immunological milieu of the liver. Seminars in Liver Disease *27*, 129–139.

Shevach, E. M. (2009). Mechanisms of foxp3+ T regulatory cell-mediated suppression. Immunity *30*, 636–645.

Shields, P. L., Morland, C. M., Salmon, M., Qin, S., Hubscher, S. G. and Adams, D. H. (1999). Chemokine and chemokine receptor interactions provide a mechanism for selective T cell recruitment to specific liver compartments within hepatitis C-infected liver. Journal of Immunology *163*, 6236–6243.

Shimoda, S., van de Water, J., Ansari, A., Nakamura, M., Ishibashi, H., Coppel, R. L., Lake, J., Keeffe, E. B., Roche, T. E. and Gershwin, M. E. (1998). Identification and precursor frequency analysis of a common T cell epitope motif in mitochondrial autoantigens in primary biliary cirrhosis. The Journal of Clinical Investigation *102*, 1831–1840.

Shlomchik, M. J. (2009). Activating systemic autoimmunity: B's, T's, and tolls. Current Opinion in Immunology *21*, 626–633.

Siegmund, K. and Hamann, A. (2006). Use of Labeled Lymphocytes to Analyze Trafficking In Vivo. In Leukocyte Trafficking pp. 497–508. Wiley-VCH Verlag GmbH & Co. KGaA.

Sigmundsdottir, H., Pan, J., Debes, G. F., Alt, C., Habtezion, A., Soler, D. and Butcher, E. C. (2007). DCs metabolize sunlight-induced vitamin D3 to 'program' T cell attraction to the epidermal chemokine CCL27. Nature Immunology *8*, 285–293.

Simmonds, M. J. and Gough, S. C. L. (2004). Genetic insights into disease mechanisms of autoimmunity. British Medical Bulletin *71*, 93–113.

Sitia, G., Iannacone, M., Aiolfi, R., Isogawa, M., van Rooijen, N., Scozzesi, C., Bianchi, M. E., Andrian, U. H. v., Chisari, F. V. and Guidotti, L. G. (2011). Kupffer cells hasten resolution of liver immunopathology in mouse models of viral hepatitis. PLoS Pathogens *7*, e1002061.

Smedsrod, B., Pertoft, H., Gustafson, S. and Laurent, T. C. (1990). Scavenger functions of the liver endothelial cell. The Biochemical Journal *266*, 313–327.

Smyk, D. S., Rigopoulou, E. I., Pares, A., Billinis, C., Burroughs, A. K., Muratori, L., Invernizzi, P. and Bogdanos, D. P. (2012). Sex differences associated with primary biliary cirrhosis. Clinical & Developmental Immunology *2012*, 610504.

Stagg, A. J., Kamm, M. A. and Knight, S. C. (2002). Intestinal dendritic cells increase T cell expression of alpha4beta7 integrin. European Journal of Immunology *32*, 1445–1454.

Steinhoff, G., Behrend, M., Schrader, B., Duijvestijn, A. M. and Wonigeit, K. (1993). Expression patterns of leukocyte adhesion ligand molecules on human liver endothelia. Lack of ELAM-1 and CD62 inducibility on sinusoidal endothelia and distinct distribution of VCAM-1, ICAM-1, ICAM-2, and LFA-3. The American Journal of Pathology *142*, 481–488.

Stenstad, H., Svensson, M., Cucak, H., Kotarsky, K. and Agace, W. W. (2007). Differential homing mechanisms regulate regionalized effector CD8alphabeta+ T cell accumulation within the small intestine. Proc. Natl. Acad. Sci. U.S.A. *104*, 10122–10127.

Sugioka, A., Morita, M., Fujita, J., Hasumi, A. and Shiroishi, T. (2001). Graft acceptance and tolerance induction in mouse liver transplantation using wild mice. Transplantation Proceedings *33*, 137–139.

Tang, J., Zhou, C., Zhang, Z.-J. and Zheng, S.-S. (2012). Association of polymorphisms in non-classic MHC genes with susceptibility to autoimmune hepatitis. Hepatobiliary & Pancreatic Diseases International *11*, 125–131.

Terjung, B. and Spengler, U. (2009). Atypical p-ANCA in PSC and AIH: a hint toward a "leaky gut"? Clinical reviews in allergy & immunology *36*, 40–51.

Thorsby, E. and Lie, B. A. (2005). HLA associated genetic predisposition to autoimmune diseases: Genes involved and possible mechanisms. Transplant Immunology *14*, 175–182.

Tiegs, G., Hentschel, J. and Wendel, A. (1992). A T cell-dependent experimental liver injury in mice inducible by concanavalin A. The Journal of Clinical Investigation *90*, 196–203.

Tordjman, R., Lepelletier, Y., Lemarchandel, V., Cambot, M., Gaulard, P., Hermine, O. and Romeo, P.-H. (2002). A neuronal receptor, neuropilin-1, is essential for the initiation of the primary immune response. Nature Immunology *3*, 477–482.

Tu, Z., Bozorgzadeh, A., Crispe, I. N. and Orloff, M. S. (2007). The activation state of human intrahepatic lymphocytes. Clinical and Experimental Immunology *149*, 186–193.

van Oosten, M., van de Bilt, E., Vries, H. E. d., van Berkel, T. J. and Kuiper, J. (1995). Vascular adhesion molecule-1 and intercellular adhesion molecule-1 expression on rat liver cells after lipopolysaccharide administration in vivo. Hepatology *22*, 1538–1546.

van Rooijen, N., Bakker, J. and Sanders, A. (1997). Transient suppression of macrophage functions by liposome-encapsulated drugs. Trends in Biotechnology *15*, 178–185.

van Rooijen, N. and Sanders, A. (1994). Liposome mediated depletion of macrophages: mechanism of action, preparation of liposomes and applications. Journal of Immunological Methods *174*, 83–93.

Vergani, D. and Mieli-Vergani, G. (2008). Aetiopathogenesis of autoimmune hepatitis. World Journal of Gastroenterology *14*, 3306–3312.

Vezys, V., Olson, S. and Lefrançois, L. (2000). Expression of intestine-specific antigen reveals novel pathways of CD8 T cell tolerance induction. Immunity *12*, 505–514.

Vinas, O., Bataller, R., Sancho-Bru, P., Gines, P., Berenguer, C., Enrich, C., Nicolas, J. M., Ercilla, G., Gallart, T., Vives, J., Arroyo, V. and Rodes, J. (2003). Human hepatic stellate cells show features of antigen-presenting cells and stimulate lymphocyte proliferation. Hepatology *38*, 919–929.

Voehringer, D., Blaser, C., Grawitz, A. B., Chisari, F. V., Buerki, K. and Pircher, H. (2000). Break of T cell ignorance to a viral antigen in the liver induces hepatitis. Journal of Immunology *165*, 2415–2422.

Wang, C., Sun, J., Li, L., Wang, L., Dolan, P. and Sheil, A. G. (1998). Conversion of pancreas allograft rejection to acceptance by liver transplantation. Transplantation *65*, 188–192.

Warren, A., Le Couteur, D. G., Fraser, R., Bowen, D. G., McCaughan, G. W. and Bertolino, P. (2006). T lymphocytes interact with hepatocytes through fenestrations in murine liver sinusoidal endothelial cells. Hepatology *44*, 1182–1190.

Watanabe, T., Katsukura, H., Chiba, T., Kita, T. and Wakatsuki, Y. (2007). Periportal and sinusoidal liver dendritic cells suppressing T helper type 1-mediated hepatitis. Gut *56*, 1445–1451.

Wiegard, C., Frenzel, C., Herkel, J., Kallen, K.-J., Schmitt, E. and Lohse, A. W. (2005). Murine liver antigen presenting cells control suppressor activity of CD4+CD25+ regulatory T cells. Hepatology *42*, 193–199.

Winau, F., Hegasy, G., Weiskirchen, R., Weber, S., Cassan, C., Sieling, P. A., Modlin, R. L., Liblau, R. S., Gressner, A. M. and Kaufmann, S. H. E. (2007). Ito cells are liver-resident antigen-presenting cells for activating T cell responses. Immunity *26*, 117–129.

Wisse, E., Braet, F., Luo, D., Zanger, R. d., Jans, D., Crabbé, E. and Vermoesen, A. (1996). Structure and function of sinusoidal lining cells in the liver. Toxicologic Pathology *24*, 100–111.

Wong, J., Johnston, B., Lee, S. S., Bullard, D. C., Smith, C. W., Beaudet, A. L. and Kubes, P. (1997). A minimal role for selectins in the recruitment of leukocytes into the inflamed liver microvasculature. The Journal of Clinical Investigation *99*, 2782–2790.

Wu, T.-J., Wang, Y.-C., Wu, T.-H., Lee, C.-F., Chan, K.-M. and Lee, W.-C. (2012). Inhibition of allogenic T-cell cytotoxicity by hepatic stellate cell via CD4(+) CD25(+) Foxp3(+) regulatory T cells in vitro. Transplantation Proceedings *44*, 1055–1059.

Wucherpfennig, K. W. (2001). Mechanisms for the induction of autoimmunity by infectious agents. The Journal of Clinical Investigation *108*, 1097–1104.

Wucherpfennig, K. W. and Strominger, J. L. (1995). Molecular mimicry in T cell-mediated autoimmunity: viral peptides activate human T cell clones specific for myelin basic protein. Cell *80*, 695–705.

Wuensch, S. A., Pierce, R. H. and Crispe, I. N. (2006). Local intrahepatic CD8+ T cell activation by a non-self-antigen results in full functional differentiation. Journal of Immunology *177*, 1689–1697.

Wuensch, S. A., Spahn, J. and Crispe, I. N. (2010). Direct, help-independent priming of CD8+ T cells by adeno-associated virus-transduced hepatocytes. Hepatology *52*, 1068–1077.

Wurbel, M.-A., McIntire, M. G., Dwyer, P. and Fiebiger, E. (2011). CCL25/CCR9 interactions regulate large intestinal inflammation in a murine model of acute colitis. PloS One *6*, e16442.

Wurbel, M. A., Philippe, J. M., Nguyen, C., Victorero, G., Freeman, T., Wooding, P., Miazek, A., Mattei, M. G., Malissen, M., Jordan, B. R., Malissen, B., Carrier, A. and Naquet, P. (2000). The chemokine TECK is expressed by thymic and intestinal epithelial cells and attracts double- and single-positive thymocytes expressing the TECK receptor CCR9. European Journal of Immunology *30*, 262–271.

Xu, B., Broome, U., Uzunel, M., Nava, S., Ge, X., Kumagai-Braesch, M., Hultenby, K., Christensson, B., Ericzon, B.-G., Holgersson, J. and Sumitran-Holgersson, S. (2003). Capillarization of hepatic sinusoid by liver endothelial cell-reactive autoantibodies in patients with cirrhosis and chronic hepatitis. The American Journal of Pathology *163*, 1275–1289.

Yadav, M., Louvet, C., Davini, D., Gardner, J. M., Martinez-Llordella, M., Bailey-Bucktrout, S., Anthony, B. A., Sverdrup, F. M., Head, R., Kuster, D. J., Ruminski, P., Weiss, D., Schack, D. v. and Bluestone, J. A. (2012). Neuropilin-1 distinguishes natural and inducible regulatory T cells among regulatory T cell subsets in vivo. The Journal of Experimental Medicine *209*, 1713–22, S1–19.

You, Q., Cheng, L., Kedl, R. M. and Ju, C. (2008). Mechanism of T cell tolerance induction by murine hepatic Kupffer cells. Hepatology *48*, 978–990.

Zaft, T., Sapoznikov, A., Krauthgamer, R., Littman, D. R. and Jung, S. (2005). CD11chigh dendritic cell ablation impairs lymphopenia-driven proliferation of naive and memory CD8+ T cells. Journal of Immunology *175*, 6428–6435.

Zhang, N. and Bevan, M. J. (2011). CD8(+) T cells: foot soldiers of the immune system. Immunity *35*, 161–168.

Zhang, W., Fei, Y., Gao, J., Liu, B. and Zhang, F. (2011). The role of CXCR3 in the induction of primary biliary cirrhosis. Clinical & Developmental Immunology *2011*, 564062.

Zhu, J. and Paul, W. E. (2010). Heterogeneity and plasticity of T helper cells. Cell Research *20*, 4–12.

Zhu, J., Yamane, H. and Paul, W. E. (2010). Differentiation of effector CD4 T cell populations. Annual Review of Immunology *28*, 445–489.

Zierden, M., Kuhnen, E., Odenthal, M. and Dienes, H.-P. (2010). Effects and regulation of autoreactive CD8+ T cells in a transgenic mouse model of autoimmune hepatitis. Gastroenterology *139*, 975–86, 986.e1–3.

Appendix

Supplementary data

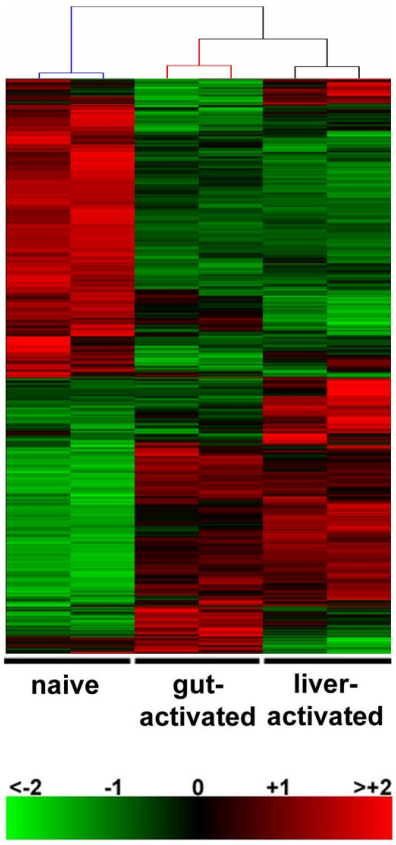

Figure 20: Gene expression profile of 10,326 IDs, differentially regulated between naïve, liver-activated, and gut-activated CD8 T cells. Gene expression profiling of purified OT-I CD8 T cells was performed in duplicates. Hierarchical clustering was performed with 10,326 IDs containing the three groups of CD8 T-cell subtypes using Genes@Work.

Table 5: Genes involved in adhesion, migration and integrins. The function related group of 144 IDs was generated using the Database for Annotation, Visualization and Integrated Discovery (DAVID) and used for Figure 12 A.

Affy Number	Gene Symbol	gut-activated		liver-activated		naive	
1415821_at	Nptn	2262.8	2154.8	1757.4	1519.6	1343.3	1321.3
1416034_at	Cd24a	51	132.8	236.2	434.7	920.8	189.1
1416271_at	Perp	76.7	55.1	111.4	106.7	0.6	2.6
1417122_at	Vav3	110.9	166.4	177	184.6	59.6	59.6
1417171_at	Itk	965	876.4	606.1	643.8	1636.4	1845.1
1417391_a_at	Il16	1187.8	1061.8	920.6	923	1346.9	1436.1
1417523_at	Plek	186.1	137.6	271.5	230.1	17.4	3.6
1417756_a_at	Lsp1	3143.8	2704.3	2732.9	2006.8	1846.7	2199.8
1417976_at	Ada	186.7	157.7	62.9	51.8	126.5	115.6
1418014_a_at	B4galt1	750	718.8	487.5	358.8	906.1	918.4
1418084_at	Nrp1	166.5	313.1	1016.4	778	28.2	27.5
1418126_at	Ccl5	404.9	310.2	191.5	64.1	2536.9	1695.7
1418230_a_at	Lims1	989.2	696.6	1281.9	1205.3	621.5	630
1418340_at	Fcer1g	34	94	322.9	151.6	130.5	68.7
1418465_at	Ncf4	379.3	272	256.6	182	458.9	487.1
1418741_at	Itgb7	1940.7	1694.6	1191.8	955	1549.4	1816.4
1418770_at	Cd2	1855.7	1605.3	916	494.7	2515.1	2588.7
1418831_at	Pkp3	579.4	548	438	317.1	264.9	321
1418925_at	Celsr1	124.4	136.7	92.5	60.2	198.1	208.2
1419128_at	Itgax	153.2	79.6	33.1	23.1	46.4	20.3
1419226_at	Cd96	1276.3	1139	599.9	495.1	968.7	1013.7
1419394_s_at	S100a8	29.1	195.2	1563.9	697.4	2084.1	654.5
1419412_at	Xcl1	1121.1	1476.8	1883.9	2299.2	33.9	60.9
1419480_at	Sell	1149.6	1477.3	5108.3	4362.2	4555	4635.4
1419481_at	Sell	1442.9	1647	5508.9	5000.9	4898.3	4684.4
1419561_at	Ccl3	95.4	127.6	189.7	149.1	10.9	8.9
1419768_at	Cd22	121.9	248.4	73.2	48.8	173.6	56.2
1420699_at	Clec7a	22.4	70.8	170.8	79.4	41.2	28.1
1420996_at	Plxna3	23.2	38.7	64	76.2	30.1	34.4
1421194_at	Itga4	245.9	285.1	158.1	140.8	94.7	71.5
1421420_at	Ccr10	25.4	8.8	90.4	77.2	24.4	5.4
1421614_at	Zan	1.9	2.9	52.3	70.7	1	1.7
1421861_at	Clstn1	93.2	82.8	60.6	62.1	103.2	108.3
1421919_a_at	Ccr9	708.7	629	6.6	0.6	323.1	351.3
1421920_a_at	Ccr9	1933	1641.8	12.8	3.9	1022.6	1259.6
1421926_at	Mapk11	68.7	88.2	142.5	167.2	44	79.7
1422445_at	Itga6	595.3	700.3	1052.2	852.8	487.9	551.3
1422818_at	Nedd9	578.8	596.5	481.5	416.6	854	909.3
1422875_at	Cd84	432.2	519.5	659.5	517.5	370.6	422.2
1422938_at	Bcl2	71.4	63.6	127.6	133.7	150.4	149.4
1422992_s_at	Pik3cd	408.5	407.9	203.7	136.3	528.5	418.7
1423135_at	Thy1	3698.3	3396.8	1904.7	1698.3	2777.1	3446.3
1423325_at	Pnn	81.1	48.5	123.6	99.6	40.1	26.1
1423584_at	Igfbp7	13.7	18	240.4	236.2	15	14.8
1423885_at	Lamc1	53.2	40.5	21.2	16.7	20.1	14
1424027_at	Pxn	194.7	190	114.8	117	172.7	234.5
1424067_at	Icam1	278.8	257.6	167	120.6	674.6	807.1

continued on next page ...

...Table 5 continued I

Affy Number	Gene Symbol	gut-activated		liver-activated		naive	
1424139_at	Rap1a	4288.8	4763.3	5749.8	5293.2	3633.2	4226
1424485_at	Angptl3	1.2	1.2	18.1	58.3	0.5	0.7
1425515_at	Pik3r1	136.6	158.5	117.5	92.7	289.8	221.3
1425518_at	Rapgef4	74.3	81.7	45.1	24.1	368.1	389
1426300_at	Alcam	253.6	274.6	519.8	497.8	34.8	15.7
1426301_at	Alcam	186.7	209.2	349.5	386.3	24.4	10.3
1426794_at	Ptprs	224.5	202.7	490.2	566.3	134.1	90.5
1426918_at	Itgb1	200.5	187.3	635.8	261	128.2	100.7
1427064_a_at	Scrib	124.5	143.7	190.6	213.6	156.1	160.7
1427419_x_at	Ccr9	5297.2	4627.2	10.7	15.5	3535.2	3956.3
1427442_a_at	App	15	70.9	121.8	45.3	242.6	180.5
1427615_at	Itga4	19.4	23.7	43.3	75.4	4	5.7
1428471_at	Sorbs1	157.3	190	267.2	272.7	208.3	203.6
1428585_at	Actn1	1975.8	1969.3	972.6	630.3	3237	3854.5
1428850_x_at	Cd99	437.3	374.7	529.1	553	115	140
1429882_at	6820431F20Rik	141	130.2	204.3	262.7	274	269.4
1430514_a_at	Cd99	229.6	210.5	287	282.5	75	57.8
1431355_s_at	Trpm7	65.5	53.9	117.8	164.4	98.3	81.6
1433963_a_at	Fermt3	679.9	747.1	502.9	525.5	810.9	907.2
1434674_at	Lyst	207.6	291.4	399.3	378.1	789	839.9
1434980_at	Pik3r5	339.5	239.8	243.3	141.5	576.2	605.8
1435149_at	Plcg1	1014.4	951.9	733.3	717.8	825.4	918.8
1435349_at	Nrp2	60.8	64	20.7	23.2	87.9	90.7
1435448_at	Bcl2l11	1326.7	1380.8	1052.9	792.7	628.6	590.2
1435518_at	Rap1b	3700.3	3397.5	2945.9	2497.4	4032.7	3542.9
1435519_at	Rap1b	5486.4	6358.5	4905.5	4514.1	7074	7107
1435807_at	Cdc42	166.6	166.1	204.6	169.8	118.5	104.2
1436037_at	Itga4	1613	1506.7	1334.5	994	888.9	785.8
1436173_at	Dlc1	9	1.3	46.8	59.2	0.5	3.5
1436398_at	—	129.5	97.7	171.7	293	267.9	280.7
1436740_at	LOC100041567	217.2	237	299.3	387.4	460.4	414
1436778_at	Cybb	46.4	163.1	214.1	92.1	225.9	95.7
1437122_at	Bcl2	124.7	133.2	175.9	261.3	427.7	476.4
1437132_x_at	Nedd9	696.6	748.7	413.3	509.5	1164.7	1516.9
1437466_at	Alcam	71.5	80.4	217.4	194.5	11.4	4.9
1437467_at	Alcam	174.6	176	352.3	383.2	10.8	11.9
1437502_x_at	Cd24a	41	108	216.4	305.2	1033.4	366.9
1437717_x_at	LOC100041567	343.6	315.6	458.1	570.5	679.3	633.2
1438279_at	Dpp4	76.7	72.7	126.9	157.7	176.5	131.5
1438682_at	Pik3r1	668.9	698.4	514.7	426.3	1396.3	1426.1
1440708_at	Myh9	81.9	53	100.5	140.5	63.1	56.7
1440760_at	—	19.2	34.2	32.4	51.3	97.8	119.2
1440770_at	Bcl2	81.8	68.3	131	225.1	166.8	157.5
1441411_at	Lims1	66.1	55.7	107.3	101.3	60.4	45.5
1443086_at	Alcam	31.3	21.9	85.3	79.1	6.5	1
1443837_x_at	Bcl2	76.2	59	138.4	176	131.6	156.3
1445395_at	—	17.7	3.5	44.9	88.3	22.7	9.7

continued on next page ...

...Table 5 continued II

Affy Number	Gene Symbol	gut-activated		liver-activated		naive	
1446720_at	Alcam	22.4	19.2	46.7	73.6	7.2	12.4
1447541_s_at	Itgae	1282.2	648.3	14.9	9.2	1483	1807.7
1448123_s_at	Tgfbi	14.4	58.5	195.7	58.4	79.8	40.7
1448182_a_at	Cd24a	128.8	292.5	585	889.7	2182.7	607.2
1448234_at	Dnajb6	2233.3	2416.8	1901.6	1752.9	1766	1638.4
1448327_at	Actn2	163.6	112.3	24.3	31.7	478.3	555.5
1448371_at	Mylpf	151.8	114.1	176.5	193.7	89.7	89.6
1448380_at	Lgals3bp	849.7	786.5	215	127	973	1027.1
1448600_s_at	Vav3	92.4	128.2	239.3	191.1	62.4	72.6
1448620_at	Fcgr3	26.7	63.6	138.4	50.2	41.9	15.1
1448710_at	Cxcr4	204.4	324.6	499.5	638.1	606.7	538.3
1448749_at	Plek	498.7	466.7	735	611.2	51.6	23.5
1448756_at	S100a9	23.3	87.1	1098.7	551	1290.8	412.5
1448943_at	Nrp1	294.6	498.1	1731	1444.3	75.3	79.9
1448944_at	Nrp1	114.2	244.7	729.4	549.9	7.4	17.7
1448996_at	Rom1	187.2	204.3	105.8	52	97.7	100.4
1449127_at	Selplg	2595.8	2823	1819.1	1344.9	2771.8	3217.4
1449156_at	Ly9	736.7	765.7	589.8	602.4	765.1	811.4
1449216_at	Itgae	454.4	227.3	10.1	11.2	452	538.6
1449399_a_at	Il1b	29	65.2	181.4	148.8	49.9	37.7
1449507_a_at	Cd47	3456.9	3426	2879.5	2135.2	2750.6	2305.6
1449846_at	Ear2 /// Ear3	1.8	13.2	114.2	63.2	43.4	22
1450029_s_at	Itga9	1	19.4	58.4	76.1	5.8	9.5
1450850_at	Ezr	3064.5	3058.6	2582.2	2214	3287.3	3724.3
1450945_at	Prkca	148.7	142.9	226.2	282.7	47.9	34.8
1451225_at	Ptpn11	673.8	863.4	1255.4	1240.9	574.6	608.4
1451767_at	Ncf1	160	211.1	28.1	7.5	124.2	83.3
1451910_a_at	Cd6	977	773.6	572.9	537.5	946.4	1169.5
1452209_at	Pkp4	705.9	709.8	548.9	577.9	1040.7	1163.7
1452545_a_at	Itgb1	248.2	211	529.1	280.8	120.8	83.3
1452784_at	Itgav	360.5	385.8	685.1	766.8	502.9	583.9
1452997_at	6820431F20Rik	722.6	591.5	745	889.4	670.1	585.1
1453016_at	2900042B11Rik	341.2	345.5	235	235	459.2	555
1453281_at	Pik3cd	1411.5	1273.7	734.8	649.6	1694.2	1922.9
1453788_at	—	91.5	179.1	282.9	302.6	50.8	93.9
1454268_a_at	Cyba	3274.5	3029.1	2121.9	1743.9	2345.5	2567.1
1455257_at	Itgb3	132.4	180.2	56.6	66.9	127.9	129.2
1455349_at	LOC100048397	1148.6	1192.2	932.6	798.3	1444.8	1491.4
1456005_a_at	Bcl2l11	2585.5	2669.2	2133.7	1591.6	1110.3	1018.9
1456135_s_at	Pxn	1076.5	976.1	852.8	740.7	1158.2	1278
1456250_x_at	Tgfbi	7.6	45.8	217.8	70.3	74.4	36.6
1456498_at	Itga4	597.5	265	469.7	167.5	468.3	173
1456772_at	Ncf1	498.7	635.8	145	52.1	399.8	340
1457120_at	Itk	192.4	155.5	65.4	91.8	217.4	285.9
1457198_at	Nrp1	42.5	54.3	218.9	244.2	17.6	12.8
1457687_at	Bcl2	403.7	400.4	698	818.9	1003.8	1083.6
1460235_at	Scarb2	548	497.3	422.2	343.4	686.1	768.7
1460253_at	Cmtm7	1517.8	1119.2	1913.9	2176.1	599.7	503.4
1460285_at	Itga9	15.6	27.7	69.3	75.1	12.4	18
1460419_a_at	Prkcb1	1099.7	1225.6	948.9	830.2	1599.4	1793.6

Table 6: Genes involved in cytokines, chemokines, and their receptors. The function related group of 53 IDs was generated using the Database for Annotation, Visualization and Integrated Discovery (DAVID) and used for Figure 12 B.

Affy Number	Gene Symbol	gut-activated		liver-activated		naive	
1418126_AT	Ccl5	404.9	310.2	191.5	64.1	2536.9	1695.7
1418652_AT	Cxcl9	1.7	18.2	62.5	45.9	28.9	14.4
1418803_A_AT	Tnfsf6	56.7	47.6	88.4	107.4	10.5	2.8
1419083_AT	Tnfsf11	101	129.9	188.5	202.2	2	11.6
1419135_AT	Ltb	5252.6	5019.3	4050.9	3090.9	6472.6	6305.3
1419307_AT	Tnfrsf13c	200.4	209.9	132.6	106.8	111.8	68.5
1419412_AT	Xcl1	1121.1	1476.8	1883.9	2299.2	33.9	60.9
1419455_AT	Il10rb	734.5	649.3	461.2	331.9	752.8	781.8
1419561_AT	Ccl3	95.4	127.6	189.7	149.1	10.9	8.9
1419872_AT	Csf1r	30.1	212.5	925.8	416.6	212.4	65.7
1419873_S_AT	Csf1r	19.4	58	202.1	109.9	49.9	4.4
1420678_A_AT	Il17rb	21.2	4.5	59.6	87.8	21.9	30.6
1420691_AT	Il2ra	143.4	80.7	22.1	24.7	16.9	14.5
1420692_AT	Il2ra	227.5	140.2	12.9	28.8	7.5	4.5
1420703_AT	Csf2ra	34.9	36.3	44.3	67.4	36.3	31.6
1420895_AT	Tgfbr1	286.2	247.8	213.6	203.6	548.9	684.2
1420895_AT	Tgfbr1	286.2	247.8	213.6	203.6	548.9	684.2
1421034_A_AT	Il4ra	212.4	189.2	133	112.9	473.1	562.5
1421207_AT	Lif	28.5	51.4	99.4	67.8	1.5	8.2
1421291_AT	Il18rap	54.9	84.6	141.5	116.7	51.2	28.1
1421420_AT	Gpr2	25.4	8.8	90.4	77.2	24.4	5.4
1421628_AT	Il18r1	651.2	319.9	4396.4	4401.9	628.3	434
1421919_A_AT	Ccr9	708.7	629	6.6	0.6	323.1	351.3
1421920_A_AT	Ccr9	1933	1641.8	12.8	3.9	1022.6	1259.6
1422003_AT	Blr1	67.9	92.5	58	41	83.9	58.8
1422231_A_AT	Tnfrsf25	56.3	40.2	7.7	1.1	134.4	154.4
1422812_AT	Cxcr6	1261.5	920.7	68.5	59.4	832.5	981.7
1422924_AT	Tnfsf9	59.3	49.6	103	127.3	28.1	20.9
1424727_AT	Ccr5	198.8	135.8	112.1	74.2	93.3	51.3
1425145_AT	Il1rl1	55.9	87.2	151.6	182.6	73.4	23.9
1425832_A_AT	Cxcr6	1394.3	1196.7	95.7	100.5	837.1	771.8
1426397_AT	Tgfbr2	1166.7	1176.2	854.9	637.8	2921.5	3129.4
1427419_X_AT	Ccr9	5297.2	4627.2	10.7	15.5	3535.2	3956.3
1433795_AT	Tgfbr3	92.2	93.8	6.2	3	213.5	235
1434279_AT	Xbp1	96.8	62.6	126	153.2	59.6	37.6
1434310_AT	Bmpr2	50.6	59.3	100.3	105.4	63.8	66.1
1437270_A_AT	Bsf3	235.9	191.7	164.6	115	655.5	694.7
1448575_AT	Il7r	835.8	596.2	175.6	107	4476.4	4477.2
1448576_AT	Il7r	209.3	141.2	41.3	23.7	1630.8	1664.7
1448710_AT	Cxcr4	204.4	324.6	499.5	638.1	606.7	538.3
1448731_AT	Il10ra	71.3	71.6	55.8	43.7	92.3	75.6
1449026_AT	Ifnar1	338.8	317.9	254.8	201	368.4	313.1
1449925_AT	Cxcr3	2627.7	2398.4	689.7	326.9	454.6	392.9
1450272_AT	Tnfsf8	78.1	60.7	149.5	133.9	108.9	87.9
1450298_AT	Tnfsf14	118.6	119.8	209	181.6	51.7	50.6
1450357_A_AT	Ccr6	102.1	155.4	52.4	47.4	43.7	37.1

continued on next page ...

...Table 6 continued

Affy Number	Gene Symbol	gut-activated		liver-activated		naive	
1451462_A_AT	Ifnar2	431.4	483.8	636.4	612.2	384.1	309.7
1451944_A_AT	Tnfsf11	13.4	19.5	43	47.2	1.6	3.8
1452416_AT	Il6ra	91.1	120.8	71.1	39.6	1096.2	1436
1453572_A_AT	Plp2	1991.2	2103.7	2898.7	2966.2	637.8	679.9
1455660_AT	Csf2rb1	18.6	49.7	116.3	67.2	150.5	108.4
1460220_A_AT	Csf1	2.6	14.2	74.1	92.3	9.6	1.9
1460251_AT	Tnfrsf6	100.2	105	69.5	51.2	166.3	217.8

Table 7: Genes involved in T-cell activation. The function related group of 87 IDs was generated using the Database for Annotation, Visualization and Integrated Discovery (DAVID) and used for Figure 12 C.

Affy Number	Gene Symbol	gut-activated		liver-activated		naive	
1415743_AT	Hdac5	128.6	143.2	189	210.2	196.6	175.4
1415907_AT	Ccnd3	855.9	711.2	328.8	288.1	830.6	1034.1
1416007_AT	Satb1	2887.6	3059.7	1136.4	802.5	5042.7	5763.4
1416008_AT	Satb1	2222.7	2347.6	923.4	621.1	3390.6	3507.6
1416034_AT	Cd24a	51	132.8	236.2	434.7	920.8	189.1
1417976_AT	Ada	186.7	157.7	62.9	51.8	126.5	115.6
1418133_AT	Bcl3	209.3	201	94.9	67.1	279.7	419.4
1418340_AT	Fcer1g	34	94	322.9	151.6	130.5	68.7
1419128_AT	Itgax	153.2	79.6	33.1	23.1	46.4	20.3
1419631_AT	Was	1152.8	1134.5	1021.6	883.5	1228.9	1391.7
1419853_A_AT	Dnajb9	288.1	164.3	21.8	19.4	63.9	44.6
1420813_AT	Hdac7a	562.3	561.8	922.5	1067.8	587.6	653.4
1421140_A_AT	Foxp1	443.3	618.3	558.6	726.9	1098	1305
1421141_A_AT	Foxp1	527.4	667.9	893.4	958.5	1324.2	1305.7
1421142_S_AT	Foxp1	401.5	477.9	607.5	639.2	829.5	953.2
1421173_AT	Irf4	538.3	668.2	847.8	771.5	64.5	34.5
1421618_AT	Myo1f	407.9	324.5	93.8	11.7	101.6	114.8
1422103_A_AT	Stat5b	519.1	505.5	361	310.1	652.5	715.9
1422938_AT	Bcl2	71.4	63.6	127.6	133.7	150.4	149.4
1422992_S_AT	Pik3cd	408.5	407.9	203.7	136.3	528.5	418.7
1423226_AT	Ms4a1	150.6	389.8	68.3	28.2	426.9	243.1
1425335_AT	Cd8a	3903.3	3616.8	2422.7	1851.7	2691.8	3023.6
1425396_A_AT	Lck	5346.4	5523.5	4715.2	4158.5	5355.8	5865.8
1425515_AT	Pik3r1	136.6	158.5	117.5	92.7	289.8	221.3
1425869_A_AT	Psen2	432.2	608.9	1125.5	1155	358.1	357.4
1426001_AT	Eomes	148.2	217.4	196.5	297.9	576.5	477.4
1426397_AT	Tgfbr2	1166.7	1176.2	854.9	637.8	2921.5	3129.4
1426538_A_AT	Trp53	107.8	66.2	150.2	175.2	39.2	38.1
1427301_AT	Cd48	5227.5	4994.6	3405.5	2756.1	2875.9	2826.5
1427739_A_AT	Trp53	167	131.9	177.2	195.1	98.5	96
1429477_AT	D15Ertd785e	129	114.1	156.9	164.1	118.1	99.2

continued on next page ...

...Table 7 continued I

Affy Number	Gene Symbol	gut-activated		liver-activated		naive	
1429524_AT	Myo1f	984.9	874.4	227.2	84.9	249.4	205.4
1429525_S_AT	Myo1f	975.2	813.7	242.2	87.5	275	253
1432459_A_AT	Rog	451.3	392.7	1269.5	922.4	3.8	23.3
1434279_AT	Xbp1	96.8	62.6	126	153.2	59.6	37.6
1435222_AT	Foxp1	930.6	1086.7	1314.6	1403.4	2064.8	2329.9
1435227_AT	Bcl11b	1555.7	1481	964	868.6	3201.8	3264.7
1435272_AT	Itpkb	350.7	277.7	438	357.3	507.2	583.1
1435477_S_AT	Fcgr2b	25.9	83.3	200.6	66.7	96.2	17.2
1436182_AT	Satb1	624.1	775.4	265.8	153.4	1355.8	1417
1436423_AT	Themis	772.2	753.8	207.6	236.4	1223.9	1351.9
1437122_AT	Bcl2	124.7	133.2	175.9	261.3	427.7	476.4
1437270_A_AT	Bsf3	235.9	191.7	164.6	115	655.5	694.7
1437304_AT	Cblb	375.1	488.1	1096.8	920.1	289.1	318
1437502_X_AT	Cd24a	41	108	216.4	305.2	1033.4	366.9
1437504_AT	Sla2	178.9	181.8	93.5	81.6	270.2	320.9
1438682_AT	Pik3r1	668.9	698.4	514.7	426.3	1396.3	1426.1
1438784_AT	Bcl11b	373.1	309.7	220.6	227	695.5	560.8
1438802_AT	Foxp1	87.3	81.9	119.4	185.3	161.6	142.4
1439449_AT	Satb1	71.7	57.9	47.4	37.3	117.4	121.3
1439719_AT	Themis	273.7	222.8	34.9	61.5	249.1	263.7
1439787_AT	Dnajb9	524.6	359.9	31.2	34.5	115.6	124.2
1440708_AT	Myh9	81.9	53	100.5	140.5	63.1	56.7
1440770_AT	Bcl2	81.8	68.3	131	225.1	166.8	157.5
1440811_X_AT	Cd8a	958.3	875.6	612.7	472.9	847.3	941
1441058_AT	Itpkb	65.2	77.3	141.2	259.3	135	132.3
1442022_AT	Themis	126.3	122	46.2	34.5	100.1	100.8
1442233_AT	Fyb	114.1	111.8	169.4	196.7	216	169.7
1443284_AT	Satb1	75	66.3	34.9	29	109.6	88.1
1443837_X_AT	Bcl2	76.2	59	138.4	176	131.6	156.3
1444078_AT	Cd8a	2823.2	2780.2	2090.4	1336.8	3455.1	4011.8
1447209_AT	Foxp1	28.3	39.9	47.5	79	143.7	118.9
1448182_A_AT	Cd24a	128.8	292.5	585	889.7	2182.7	607.2
1448436_A_AT	Irf1	1102.3	945.9	714.1	503.5	1921.2	2177
1448575_AT	Il7r	835.8	596.2	175.6	107	4476.4	4477.2
1448576_AT	Il7r	209.3	141.2	41.3	23.7	1630.8	1664.7
1448620_AT	Fcgr3	26.7	63.6	138.4	50.2	41.9	15.1
1448710_AT	Cxcr4	204.4	324.6	499.5	638.1	606.7	538.3
1449026_AT	Ifnar1	338.8	317.9	254.8	201	368.4	313.1
1449131_S_AT	Cd1d1	263.7	271.6	207.5	157.6	428	466.9
1450339_A_AT	Bcl11b	953.6	805.7	584.3	544.2	1742.7	2162.6
1450495_A_AT	Klrk1	850.9	671	2134.4	1681.5	71.3	45.2
1450912_AT	Ms4a1	45.8	136.2	23.6	8.6	270.7	135.2
1451492_AT	Sla2	286.3	264.1	197.1	141.7	321.1	390.6
1451673_AT	Cd8a	3619.9	3028.6	2508.6	1996.1	1663.1	1583.3
1451780_AT	Blnk	18.1	82.3	20.1	6	147.7	45.1
1452966_AT	Bcl11b	420.1	341.1	259.6	178.8	727.7	840.1
1453281_AT	Pik3cd	1411.5	1273.7	734.8	649.6	1694.2	1922.9
1453361_AT	Hells	66.3	45.9	120.1	118.2	17.7	17.7
1453851_A_AT	Gadd45g	156.9	158.2	52.1	53.7	130.7	193.5

continued on next page ...

...Table 7 continued II

Affy Number	Gene Symbol	gut-activated		liver-activated		naive	
1454960_AT	Madh3	356.9	296.5	184.3	174.8	486.2	475.1
1455082_AT	Cblb	649	765.4	1420	1322.6	582.7	586.1
1456174_X_AT	Ndr1	116.3	158	69.1	56	104.7	147.5
1456429_AT	Malt1	155.8	161.7	201.4	218.1	263.3	202.1
1457687_AT	Bcl2	403.7	400.4	698	818.9	1003.8	1083.6
1458469_AT	Cblb	199.2	193	595.1	976.1	203.6	188
1460651_AT	Lat	3021.9	2870.5	1894.3	1893.5	3196.1	3755.2

Table 8: Genes involved in apoptosis. The function related group of 122 IDs was generated using the Database for Annotation, Visualization and Integrated Discovery (DAVID) and used for Figure 12 D.

Affy Number	Gene Symbol	gut-activated		liver-activated		naive	
1415910_S_AT	Ciapin1	372.7	395.4	525.7	524	206.1	192.2
1416000_A_AT	Prdx1	4614.6	4935.6	3865.1	3916.9	3296.1	3668.6
1416034_AT	Cd24a	51	132.8	236.2	434.7	920.8	189.1
1416271_AT	Perp	76.7	55.1	111.4	106.7	0.6	2.6
1416303_AT	Litaf	311.9	439	827.4	694	143.3	116.2
1416304_AT	Litaf	156.2	162.4	340.7	338.6	37.2	23.9
1416406_AT	Pea15	123.5	94.6	66.3	40.1	140.8	191.5
1416407_AT	Pea15	166.8	196.1	115.3	112.9	269	280.8
1416505_AT	Nr4a1	192.7	326.8	479.4	681.1	146.6	167.6
1416813_AT	Tia1	261.4	228	294.7	350.8	203.2	155.4
1416950_AT	Tnfaip8	913.5	945.2	1223.3	1281.3	1127.5	1335.1
1416961_AT	Bub1b	584.9	568.5	702.5	766.2	78	31.8
1417346_AT	Asc	2984.5	3116	2471.8	2206.8	1812.7	2180.6
1417756_A_AT	Lsp1	3143.8	2704.3	2732.9	2006.8	1846.7	2199.8
1417898_A_AT	Gzma	9778.7	8379.4	261.4	41.9	953.4	409.9
1418110_A_AT	Inpp5d	386.5	348.3	240.4	316	433.4	527.1
1418133_AT	Bcl3	209.3	201	94.9	67.1	279.7	419.4
1418203_AT	Pmaip1	302.9	250.5	390.6	512.7	163.2	160
1418626_A_AT	Clu	1.9	9.6	44.9	157.9	15.6	6.3
1418649_AT	Egln3	106.5	112.7	26.5	27.6	35.7	71.7
1418803_A_AT	Tnfsf6	56.7	47.6	88.4	107.4	10.5	2.8
1418840_AT	Pdcd4	2411.5	2588.3	1872.3	1810.7	3450.3	3876.3
1419060_AT	Gzmb	7617.9	5069.6	451.6	291	154.8	87
1419135_AT	Ltb	5252.6	5019.3	4050.9	3090.9	6472.6	6305.3
1420499_AT	Gch	170.9	191.5	348.4	338.4	169.7	206.4
1420691_AT	Il2ra	143.4	80.7	22.1	24.7	16.9	14.5
1420692_AT	Il2ra	227.5	140.2	12.9	28.8	7.5	4.5

continued on next page ...

...Table 8 continued I

Affy Number	Gene Symbol	gut-activated		liver-activated		naive	
1420895_AT	Tgfbr1	286.2	247.8	213.6	203.6	548.9	684.2
1420932_AT	Mapk8	116.7	101.9	157.3	163.7	84.2	90.5
1421027_A_AT	Mef2c	22.3	59	8.3	11.5	101.4	31.6
1421066_AT	Jak2	643.3	627.9	498.1	425.9	652.7	672.8
1422005_AT	Prkr	269.6	335.1	109.2	77.7	256.4	173.6
1422006_AT	Prkr	197.6	191.7	97.6	88.1	100	79.5
1422631_AT	Ahr	79.6	71.2	33	23.8	45.2	49.4
1422938_AT	Bcl2	71.4	63.6	127.6	133.7	150.4	149.4
1423790_AT	Dap	777.1	762.2	1017.1	1034.3	671.7	635.1
1423986_A_AT	Scotin	4801.7	4946.4	4250	3724.3	4960.4	5243.4
1424850_AT	Map3k1	249.9	265.7	410.8	367.7	435.5	467.7
1425396_A_AT	Lck	5346.4	5523.5	4715.2	4158.5	5355.8	5865.8
1425419_A_AT	Raf1	1059.8	1222.1	939.4	822.5	804.2	754.3
1425869_A_AT	Psen2	432.2	608.9	1125.5	1155	358.1	357.4
1426165_A_AT	Casp3	293.3	217.6	506.2	428.8	67.8	27.8
1426184_A_AT	Pdcd6ip	82.5	70.2	54.7	37	187.5	170.2
1426313_AT	Bre	337.9	315.2	474.5	406.1	227.9	164.8
1426538_A_AT	Trp53	107.8	66.2	150.2	175.2	39.2	38.1
1427064_A_AT	AI118201	124.5	143.7	190.6	213.6	156.1	160.7
1427442_A_AT	App	15	70.9	121.8	45.3	242.6	180.5
1423790_AT	Dap	777.1	762.2	1017.1	1034.3	671.7	635.1
1423986_A_AT	Scotin	4801.7	4946.4	4250	3724.3	4960.4	5243.4
1424850_AT	Map3k1	249.9	265.7	410.8	367.7	435.5	467.7
1425396_A_AT	Lck	5346.4	5523.5	4715.2	4158.5	5355.8	5865.8
1425419_A_AT	Raf1	1059.8	1222.1	939.4	822.5	804.2	754.3
1425869_A_AT	Psen2	432.2	608.9	1125.5	1155	358.1	357.4
1426165_A_AT	Casp3	293.3	217.6	506.2	428.8	67.8	27.8
1426184_A_AT	Pdcd6ip	82.5	70.2	54.7	37	187.5	170.2
1426313_AT	Bre	337.9	315.2	474.5	406.1	227.9	164.8
1426538_A_AT	Trp53	107.8	66.2	150.2	175.2	39.2	38.1
1427064_A_AT	AI118201	124.5	143.7	190.6	213.6	156.1	160.7
1427442_A_AT	App	15	70.9	121.8	45.3	242.6	180.5
1427739_A_AT	Trp53	167	131.9	177.2	195.1	98.5	96
1428433_AT	Hipk2	116.4	164.9	79.7	82.4	448	366.1
1428842_A_AT	Ngfrap1	718.1	698.6	932.6	760.9	459.1	413.7
1429734_AT	4632434I11Rik	68.4	59.4	113.7	106.6	30.9	12.6
1430165_AT	Stk17b	490	405.2	673	850.1	742.8	721.2
1430192_AT	Casp3	47.5	35	80.9	77.3	23.8	9
1430705_AT	Puf60	53.8	37.1	75.4	99.1	57.2	42.3
1431708_A_AT	Tia1	94.3	106.8	147.8	176.6	163.1	127.2
1432466_A_AT	Apoe	34.6	143.9	208.9	584.4	62.2	75.4
1433428_X_AT	Tgm2	5.1	27.2	281.1	85.3	77.1	24.8
1433699_AT	Tnfaip3	253.2	281.9	389.3	525.6	489.6	484.9
1433757_A_AT	Nisch	190.8	154.5	234.2	260.4	489	420
1433758_AT	Nisch	137.1	115.6	171.2	181.8	263.5	255.2
1434279_AT	Xbp1	96.8	62.6	126	153.2	59.6	37.6

continued on next page ...

...Table 8 continued II

Affy Number	Gene Symbol	gut-activated		liver-activated		naive	
1434557_AT	Hip1	89.2	80.4	51.9	37.4	14.6	2.8
1434699_AT	G2e3	196.1	172.1	257.3	263.9	141.2	125.3
1434700_AT	G2e3	195.1	182.8	256.9	271.3	131.4	151
1435448_AT	Bcl2l11	1326.7	1380.8	1052.9	792.7	628.6	590.2
1437122_AT	Bcl2	124.7	133.2	175.9	261.3	427.7	476.4
1437277_X_AT	Tgm2	9.3	44.8	210	67.4	59.3	30.3
1437393_AT	AI875142	206.2	255.3	461.1	447	294.8	255.4
1437502_X_AT	Cd24a	41	108	216.4	305.2	1033.4	366.9
1437532_AT	Rnf216	113.8	84.5	142.7	164.9	55	40.2
1437594_X_AT	Pigt	175.3	164.6	128.9	116.2	216.3	244.3
1437689_X_AT	Clu	0.2	1.2	76.1	275.5	2.1	2.2
1437862_AT	Rbm25	483.6	397.2	766.9	901.1	647	545.3
1438069_A_AT	Rbm5	98.1	69.7	130.5	133.2	198.8	142.3
1438553_X_AT	4930453N24Rik	109.4	156.1	67.6	67	174.2	298.6
1440275_AT	Runx3	1091.9	987.7	697.3	535.2	810.2	1033.7
1440533_AT	Bfar	43.2	35.4	54	66.2	99.5	73.7
1440770_AT	Bcl2	81.8	68.3	131	225.1	166.8	157.5
1440866_AT	EIF2AK2	243.5	232.2	99.3	75	150.6	139.5
1441943_X_AT	Ciapin1	169.4	128.4	189.2	202.8	129	155.7
1443540_AT	Map3k1	42.8	32.9	91.7	65.2	35.7	23.1
1443698_AT	Xaf-1	1349.9	1377.4	630.4	280.5	918.4	870.3
1443837_X_AT	Bcl2	76.2	59	138.4	176	131.6	156.3
1443856_AT	Nup88	96.1	111.6	125.8	125.6	104.4	116.9
1445395_AT	Prkca	17.7	3.5	44.9	88.3	22.7	9.7
1445452_AT	Traf1	423.1	384.6	536.3	631.4	355.1	245.1
1447363_S_AT	Bub1b	732.6	715.5	884.4	992.4	75.7	42.6
1448140_AT	Ciapin1	167.2	157.7	176.6	211.4	105.7	101.4
1448155_AT	Pdcd6ip	367.5	416.2	325.4	271.5	762.7	757.2
1448182_A_AT	Cd24a	128.8	292.5	585	889.7	2182.7	607.2
1448620_AT	Fcgr3	26.7	63.6	138.4	50.2	41.9	15.1
1449193_AT	Cd5l	13.2	61	882.5	371.6	31.8	15.7
1449235_AT	Tnfsf6	143.8	116.1	190.8	229	21.8	14.4
1449317_AT	Cflar	152.2	122.1	186.6	190.9	101	96.3
1449523_AT	Bcl7c	209.3	184.3	269.8	330.7	188.4	178.5
1449674_S_AT	Pdcd6ip	675.1	653.8	451.8	471.2	1023.8	1298.5
1449773_S_AT	Gadd45b	98.2	112.6	50.5	46.8	117.4	124.1
1449835_AT	Pdcd1	419.8	628.7	824.2	961	23.8	31.4
1449839_AT	Casp3	1386.9	1407.4	2168.8	2061.2	354.7	238.2
1450112_A_AT	Gas2	70.3	94.1	138.8	151.8	19.3	12.8
1450945_AT	Prkca	148.7	142.9	226.2	282.7	47.9	34.8
1450971_AT	Gadd45b	267.1	219.8	40.3	48.8	203.7	173.2
1451112_S_AT	Dap	1944.3	1877.9	2328	2390.3	1706.3	1696.9
1451485_AT	Luc7l3	1546.8	1199.6	1841.6	1786.5	1315.9	1287.7
1451767_AT	Ncf1	160	211.1	28.1	7.5	124.2	83.3
1452070_AT	Dedd2	297.7	323.8	178.4	215.7	272.4	223.7
1453568_AT	Dapl1	1896.4	1684.4	4713.7	3561.7	3541.9	2991.6
1453851_A_AT	Gadd45g	156.9	158.2	52.1	53.7	130.7	193.5

continued on next page ...

...Table 8 continued III

Affy Number	**Gene Symbol**	**gut-activated**		**liver-activated**		**naive**	
1454733_AT	Card4	238.9	203.9	129	82.2	367.1	351.3
1455355_AT	G2e3	129	126.4	179.7	245.6	38	33.6
1455900_X_AT	Tgm2	15.2	39.4	172.8	64.7	64.7	32.2
1456005_A_AT	Bcl2l11	2585.5	2669.2	2133.7	1591.6	1110.3	1018.9
1456022_AT	Hipk2	115.6	108.5	71.9	41.2	289.3	265.7
1456071_A_AT	Cycs	7125.2	7475.3	6065.8	5960	5244.6	5305.3
1456262_AT	Rbm5	149.1	121.1	168.9	275.1	202.5	186.1
1456429_AT	Malt1	155.8	161.7	201.4	218.1	263.3	202.1
1456772_AT	Ncf1	498.7	635.8	145	52.1	399.8	340
1456950_AT	Alms1	46.1	35.8	73.1	69.5	41.8	19
1457687_AT	Bcl2	403.7	400.4	698	818.9	1003.8	1083.6
1460251_AT	Tnfrsf6	100.2	105	69.5	51.2	166.3	217.8
1460710_AT	Adora2a	205.1	236.4	268.8	333.6	135.5	105.1
1460718_S_AT	Mtch1	431.2	427.6	299.5	299	204.2	203.5

Danksagung

Ich möchte mich bei allen bedanken, die mich bei der Erstellung dieser Arbeit unterstützt haben.
Mein besonderer Dank gilt meinem Doktorvater Prof. Dr. Eckart Schott, der mir die Möglichkeit gab in die immunologische Forschung zu gehen. Ich danke Ihm für seine Diskussionsbereitschaft, seine spannenden Anregungen und die fortwährende Unterstützung. Bei Prof. Dr. Alf Hamann bedanke ich mich für die unkomplizierte Übernahme der Begutachtung dieser Arbeit sowie für die Unterstützung, auch in seinem Labor tätig sein zu dürfen. Außerdem danke ich Dr. Michal Or-Guil, als Gutachterin sowie Prof. Dr. Thomas Sommer und Prof. Dr. Bernhard Grimm für die Zusage zur Prüfungskommission von Seiten der Humboldt-Universität zu Berlin.
Beim gesamten Team der Forschung der Abteilung Hepatologie und Gastroenterologie bedanke ich mich für die angenehme Atmosphäre. Insbesondere bei Daniel Seidel für die vielen Diskussionen, Ideen und Ratschläge. Ein ganz besonderes Dankeschön geht an Dr. Katja Derkow und Dr. Daniela Paclik, die mich von Anfang bis zum Ende dieser Arbeit begleitet und immer wieder ermuntert haben.
Dr. Anja Kühl, Prof. Dr. Loddenkemper und Simone Spieckermann danke ich für die Hilfe bei den histologischen Färbungen und bei Dr. Joachim Grün bedanke ich mich für die Hilfe bei der Microarray-Analyse.
Schließlich möchte ich mich herzlich bei meiner Familie und allen Freunden bedanken. Anthony, Katja, Daniela und Jan – vielen Dank für das Korrekturlesen der Arbeit. Mein größter Dank gilt zweifelsohne Jan für seinen Rückhalt, seine Geduld und jegliche Art von Unterstützung. Ohne euch wäre diese Arbeit nicht möglich gewesen.

Eidesstattliche Erklärung

Hiermit erkläre ich, dass die vorliegende Dissertation selbständig und nur unter Verwendung der angegebenen Hilfen und Hilfsmittel angefertigt worden ist.
Ich habe mich anderweitig nicht um einen Doktorgrad beworben und besitze keinen entsprechenden Doktorgrad.
Ich erkläre die Kenntnisnahme der dem Verfahren zugrunde liegenden Promotionsordnung der Mathematisch-Naturwissenschaftlichen Fakultät I der Humboldt-Universität zu Berlin.

Ira Eickmeier